METHODOLOGY FOR CAPACITY AND SAFETY ANALYSIS FOR A FLOW CORRIDOR WITH DYNAMIC WAKE SEPARATION

by

Azin Zare Noghabi
A Dissertation
Submitted to the
Graduate Faculty
of
George Mason University
in Partial Fulfillment of
The Requirements for the Degree
of
Doctor of Philosophy
Systems Engineering and Operations Research

Committee:

_____ Dr. John F. Shortle, Dissertation Director

_____ Dr. George Donohue, Committee Member

_____ Dr. Lance Sherry, Committee Member

_____ Dr. Anand Vidyashankar, Committee Member

_____ Dr. John Shortle, Department Chair

_____ Dr. Kenneth S. Ball, Dean, Volgenau School of Engineering

Date:_____ Fall Semester 2019
George Mason University
Fairfax, VA

Methodology for Capacity and Safety Analysis for a Flow Corridor with Dynamic Wake Separation

A Dissertation submitted in partial fulfillment of the requirements for the degree of Doctor of Philosophy at George Mason University

by

Azin Zare Noghabi
Master of Science
Sharif University of Technology, 2013
Bachelor of Science
Sharif University of Technology, 2010

Director: John Shortle, Professor
Department of Systems Engineering and Operations Research

Fall Semester 2019
George Mason University
Fairfax, VA

DEDICATION

To my wonderful parents Hassan and Batool and my loving husband Arsalan.

ACKNOWLEDGEMENTS

My PhD would not have been possible without the guidance, help, and support I received from my mentors, friends, and my family.

I would like to thank my advisor Prof. John Shortle for all the help and support he provided during my PhD. This dissertation would not have been complete without his patience and encouragement.

I would like to thank my committee members, Dr. Sherry, Dr. Donohue and Dr. Vidyashankar, who with their feedbacks, advices and questions guided the enhancement of this research.

To my husband and my best friend Arsalan, thank you for supporting me all the way through this journey and encouraging me to continue. I love you.

To my friends, thank you for always being there for me, thank you for listening to me, and supporting me through this entire process. Special thanks to my friends Arsalan, Elaheh, Shadi, Hamed, Sahar, Armita, Reza, Sajjad, Sahar, Bahman, Parinaz, Sareh, and Soroush, you are the best friends someone can ask for.

I would also like to thank my friends at Center for Air Transportation Systems Research, Seungwon and Sasha.

Most importantly, I want to thank my parents and my siblings Arghavan and Elyas for their endless support and unconditional love. I owe all of my achievements to you.

TABLE OF CONTENTS

Page

LIST OF TABLES

LIST OF FIGURES

ABSTRACT

METHODOLOGY FOR CAPACITY AND SAFETY ANALYSIS FOR A FLOW CORRIDOR WITH DYNAMIC WAKE SEPARATION

Azin Zare Noghabi, Ph.D.

George Mason University, 2019

Dissertation Director: Dr. John Shortle

This dissertation presents a simulation framework to investigate the capacity benefits and safety analysis for employing a proposed *dynamic wake separation* policy in a single lane *flow corridor*. The flow corridor concept is proposed as a Next Generation Transportation System (NextGen) route structure in en-route airspace to increase capacity in response to growing demand of air travel. To increase throughput, aircraft in flow corridors may fly closer to each other and have lower in-trail separations. But such aircraft must be safely separated with respect to wake vortices. Wake vortices are circular patterns of rotating air left behind a wing as it generates lift and can impose a significant hazard to other aircraft. Vortex trails, depending on atmospheric conditions, can persist for several minutes and many miles behind the generating aircraft in cruise altitudes.

In this research, we consider a dynamic wake separation concept that uses information about actual weight and airspeed of aircraft and meteorological conditions to determine the minimum required wake separation between aircraft in a flow corridor.

Aircraft characteristics and weather data are inputs to a fast-time wake prediction model that calculates the separation distances. These distances are updated periodically. To generate aircraft trajectories that are similar to real trajectories of aircraft in cruise, historical ADS-B flight track data are collected and analyzed. Trailing pairs in cruise altitudes are identified, and distributions for average and standard deviation of separation distance and ground speed, and standard deviation of altitude in level flight are obtained. Using these distributions, a simulation framework is developed to generate the trajectories of aircraft in a flow corridor. The simulation results demonstrate capacity benefits compared to current static separation standards.

To demonstrate the safety of flow corridor operations, a rare event splitting methodology is used to estimate the probability of a potential wake encounter for a pair of trailing aircraft in cruise altitudes. Results of this simulation show that for aircraft trailing each other at the same altitude, occurrence of a potential wake encounter is very rare. Sensitivity analysis shows that altitude conformance is the most important parameter in determining the probability of the potential wake encounters. This analysis is extended to the flow corridor where every two consecutive aircraft can be considered as a trailing pair. Safety analysis is performed considering the worst-case scenarios that could happen in determining the dynamic separation, which demonstrate the safety of flow corridor in terms of wake vortex hazard.

CHAPTER 1: INTRODUCTION

1.1 Background

According to the Federal Aviation Administration (FAA) baseline forecast (FAA, 2018), the number of enplanements will grow from 840.4 million passengers in 2017 to 1.05 billion passengers in 2028 and to 1.28 billion passengers in 2038. A 1.9% annual growth in the number of passengers is forecasted for 2018-2038. In addition, aircraft handled at en-route centers are forecast to increase at an average rate of 1.4 percent each year, reaching 59.37 million in 2038 compared to 44.7 million in 2018. According to the FAA, activity at en-route centers is predicted to grow faster than activity at towered airports, because more of the activity at en-route centers is from the faster growing commercial sector and high-end general aviation flying (FAA 2018). This significant increase in demand for air travel will result in congestion and more delays. According to a Eurocontrol report for calendar year 2018 (Pan-European ANS Performance Data Portal), en-route ATFM (Air Traffic Flow Management) delays increased for the fifth consecutive year in 2018, with a 3.8% in air traffic over 2017; total en-route ATFM delays more than doubled in 2018 (+104%) and reached 19 million minutes.

One of the factors that causes an increase in delays is controller workload. In fact, controller workload is a key limiting factor to increasing capacity for air traffic operations. The en-route airspace over the continental U.S. is divided into 20 regions

known as Air Route Traffic Control Centers (ARTCCs), which are further divided into smaller regions of airspace known as sectors. To ensure safe and efficient flow of traffic through these sectors, a Monitor Alert Parameter (MAP) value is calculated for each sector from the average sector flight time and the average time to provide service, which is a surrogate metric for workload (Marr and Lindsay, 2015). The MAP value is an indicator of capacity for each air sector and is the maximum number of aircraft that can be safely managed. If future traffic volume for a sector is predicted to be more than its MAP value in any 1-minute period, a monitor alert function of the Traffic Flow Management System (TFMS) notifies the traffic manager to reroute aircraft or to redistribute the traffic in space or time (Roychoudhury et al., 2018). With increasing demand, more sectors will have a demand above their MAP value, and this will lead to significant en-route delays.

Considering the projected growth in demand and resulting delays, the flow corridor concept was proposed as a Next Generation Transportation System (NextGen) route structure in en-route airspace, with the main goals of reducing the airspace complexity and increasing the capacity (JPDO, 2012). According to the definition provided in JPDO (2012), a corridor is "a long tube of airspace that encloses groups of flights flying along the same path in one direction. It is airspace procedurally separated from surrounding traffic and special use airspace, and it is reserved for aircraft in that group." Flow corridors accommodate aircraft that are capable of self-separation, equipped with ADS- B and onboard conflict detection and alerting (JPDO, 2011). This en-route structure has the potential to increase the airspace capacity by reducing the

controller workload required to manage aircraft outside the corridor and by reducing separation of aircraft within corridor (Zhang, 2014). Reduction in controller workload also results in higher MAP values for the sectors.

The shift of responsibility for separation from controller to the pilot and auto separation is enabled by new surveillance technology, Automatic Dependent Surveillance-Broadcast (ADS-B), which allows an aircraft to receive its own position and airspeed via GPS. Using ADS-B out and ADS-B in, an aircraft can broadcast its own information and can receive information from surrounding aircraft.

To increase throughput, aircraft in flow corridors may fly closer to each other and have lower in-trail separations. For example, the FAA is looking at 3 nautical mile (NM) separation in en-route operations. Before implementing any of these procedures, however, they should be assessed regarding their effect on safety. Zhang (2014) investigated the safety of flow corridors *with respect to collision risk* using a hybrid risk analysis methodology combining Monte Carlo simulation with dynamic event tree analysis.

In addition to collision risk, there is another important hazard when aircraft get very close together – namely, *wake vortex encounter risk*. Wake vortices are circular patterns of rotating air left behind a wing as it generates lift. Wake induced turbulence can happen when an aircraft encounters the wake vortex of another aircraft. This turbulence usually happens without any warning – because these vortices are normally invisible – and can impose a significant threat on the encountering aircraft by inducing an un-commanded roll which in the worst case can lead to a total loss of control. The

probable recovery from encountering strong wake vortices depends on altitude, pilot skill, maneuverability, and the power of the trailing aircraft.

The wake vortex phenomenon is well known and well-studied in the terminal area where it is easier to collect data on wake vortices near the ground using ground-based laser imaging detection and ranging (LIDAR) equipment. Furthermore, the probability of wake encounters is higher due to the proximity of landing or departing aircraft and the probability of recovery is lower since an aircraft has less altitude to recover in the event of an un-commanded roll. To avoid catastrophic consequences in the terminal area, separation rules for determining the spacing between aircraft have been developed, which ensure safety in many meteorological conditions, but diminish the capacity of the airports.

The topic of this study is *en-route* wake vortex encounters for aircraft in a flow corridor. The potential for en-route wake vortex encounters leads to an increased risk of injury for the flight crew and passengers who might not be seated or wearing a seatbelt. Since vortex trails, depending on atmospheric conditions, can persist for several minutes and many miles behind the generating aircraft in cruise altitudes, it is important to study the en-route wake vortex hazard before proceeding with the proposed concept of a flow corridor. The question is, will such procedures generate a wake vortex encounter risk?

1.2 Motivation

Why should we be concerned about wake vortices in cruise? The answer is safety. To the best of our knowledge, no fatal accidents have been attributed to wake vortex encounters at cruise altitudes, but numerous wake upsets have been reported with minor

or serious injuries. A recent incident (Jan 7, 2017) happened when a Challenger 604 at flight level FL340 operating from Male-Abu Dhabi passed an A380 opposite direction at FL350, one thousand feet above, over the Arabian Sea. The aircraft encountered wake vortices sending the aircraft into an uncontrolled roll, turning the aircraft around at least 3 times. Both engines flamed out, and the aircraft lost about 10,000 feet of altitude until the crew was able to recover control of the aircraft. In this incident, the aircraft received damage beyond repair due and was written off. Two passengers were seriously injured, and two other passengers and a flight attendant received minor injuries (Flight Safety Foundation, 2017).

Studies by Rossow and James (2000) and Nelson (2006) indicate that the strength of wake vortices generated in cruise is comparable to the ones generated during take-off and landing. Furthermore, the wake vortex induced roll moment at cruise altitudes is comparable to that during take-off or landing for a generating aircraft with the same weight when the wake has the same age. Ambient turbulence level in cruise altitudes is usually very low which contributes to slower decay of the vortices, and the clean configuration of the aircraft in cruise is another factor in generation of stronger wake vortices compared to when the gear and flaps are deployed.

With the purpose of providing a better understanding of wake encounters in cruise, Hoogstraten et al. (2015) developed a simulation framework using historical surveillance data and a wake vortex model to generate the probable trajectories of aircraft and their wakes. Their simulation predicts that a severe wake-vortex encounter occurs approximately once every 38 days in European airspace. They also identify encounter

geometry as an important factor – aircraft that are climbing or descending behind a heavy aircraft, or aircraft which are flying behind a climbing or descending heavy aircraft, have an increased risk of encountering wake vortices.

Increasing demand for air travel, reduced vertical separation minimums (RVSM), and the greater disparity in the size of aircraft in airspace after introducing super heavy aircraft and very light narrow body jets to airspace, all reinforce the need for further studies on potential wake encounters during cruise.

1.3 Wake Separation Standards

1.3.1 History of Wake Separation Standards

Before 1969 and the introduction of the Boeing-747 and military Lockheed C-5A, the problem of encountering wake vortices was not considered to be important. With the introduction of these new large aircraft, with maximum takeoff weights around 300,000 pounds, an interim standard was introduced in January 1970, which required all aircraft behind a Boeing 747 or Lockheed C5-A, within 60 degrees either side and 2,000 feet below, to be at least 10 miles behind. Furthermore, the first wake vortex separation standards for other aircraft using the Heavy, Large, Small weight categories were introduced in 1970 (Thompson, 1997).

In May 1972, a DC-9 two miles behind a DC-10 crashed at Dallas Fort Worth on final approach due to a wake vortex encounter. The standards were revised again in 1975 because they were conservative for commercial aircraft but a concern for small aircraft (Hallock, 2005).

In 1986, the 3 nautical mile radar and wake vortex separation minimums were reduced to 2.5 nautical miles between certain aircraft at certain airports. Wake separation standards were revised again in 1994 when the B-757 was put in a new category that required a 4 nautical mile spacing behind it for all aircraft (Thompson, 1997).

1.3.2 ICAO Wake Vortex Separation Standards

The majority of wake separation standards are for avoiding encounters during take-off or landing, where lower aircraft speeds lead to stronger vortices, and the closer proximity of aircraft increases the chances of an encounter. ICAO mandates separation minima that are based on the size and weight of the generating aircraft and the following aircraft. The weight categories are *light* (aircraft types with Maximum Take-Off Weight (MTOW) less than 15,500 lbs), *medium* (aircraft types with MTOW less than 300,000 lbs and more than 15,500 lbs), and *heavy* (aircraft types with MTOW more than 300,000 lbs). Another category, *super*, was added after the introduction of the A380. Table 1 summarizes the existing separation minima for approach. Empty fields indicate minimum radar separation, which is 3 NM, or 2.5 NM when certain requirements are met.

Table 1 ICAO Separation Standards for Landing

Leading Aircraft	Following Aircraft			
	Super	Heavy	Medium	Light
Super		6.0 NM	7.0 NM	8.0 NM
Heavy		4.0 NM	5.0 NM	6.0 NM
Medium				5.0 NM
Light				

The conservative nature of these separation minima means over separation in many cases and has a negative impact on capacity. Many countries have developed their individual variations from the ICAO standards.

1.3.3 RECAT

Wake Turbulence Recategorization, or Wake RECAT, is the safe decrease in separation standards between certain aircraft. RECAT is designed as a three-phased approach, with the ultimate goal of achieving dynamic pairwise separation (Cheng et al., 2016).

The existing ICAO wake vortex separation rules are based solely upon aircraft weight. While these rules ensure safety, they are based on the worst-case combinations of aircraft within each category, and thus can be overly conservative. As an example, both the Boeing 747 and the Boeing 767 are "Heavy" aircraft by the ICAO definition, so the traditional separation distance for them is 4 NM. This is appropriate when the lighter 767 is following the heavier 747. However, when the 747 is following the 767, the separation requirement is overly conservative. This adversely effects airport capacity, increasing traffic delays, costs, fuel burn, and emissions.

RECAT I: In RECAT Phase I, six new wake categories were created and aircraft were assigned to the new categories. The new categories were designed to decrease the discrepancy between the largest and smallest aircraft within each category. To derive theses new categories, Maximum Certificated Gross Takeoff Weight (MCGTOW) and Maximum Landing Weight (MLW) were coupled with approach speed and wingspan

to more accurately represent the wake severity of a generating aircraft as well as the vulnerability of a trailing aircraft to a potential wake encounter (Cheng et al., 2016).

On November 1, 2012, the Federal Aviation Administration (FAA) implemented RECAT Phase I in United States, starting with Memphis. It was operational at 23 airports as of September 2016. Increases in capacity and fuel saving have been reported at some airports.

RECAT II: In RECAT Phase II, there is a transition from six static categories to a pairwise separation matrix based on *individual* aircraft types. The aircraft list for RECAT Phase II includes 123 ICAO type designator aircraft. These aircraft comprise more than 99% of the U.S. commercial traffic from 32 U.S. airports and also include new aircraft that are currently flying that are expected to grow in numbers over time, but are not yet included in the 99% traffic mix. In RECAT Phase II, each TRACON has its own categorization matrix that is derived from the 123 x 123 pairwise matrix and is optimized for the fleet mix of the TRACON.

RECAT III: RECAT Phase III is still in the early concept exploration and development phase. RECAT III envisions dynamic pairwise separation, using Phase II pair-wise static separations as a base, and applying real meteorological data from ground and airborne sensors to dynamically change the separations. Progress in this phase is reliant on systems and products to provide wind and weather data. There will be increased availability of wind/weather dependent solutions, and access to decay driven solutions. There are also plans to apply RECAT Phase III to en-route wake mitigation operations and help transition to en-route “3 NM everywhere”.

The following concepts are examples of existing dynamic separation concepts based on using observations of wind to reduce existing separation standards.

1.3.4 Time Based Separation (TBS)

In headwind conditions, the wake vortex dissipates faster, therefore allowing aircraft to safely fly closer together on final approach. The TBS concept involves changing the separation rules on final approach from distance-based separation to time-based separation, which safely reduces approach separation to recover most of the capacity otherwise lost during strong headwind conditions. TBS software uses real-time information about the weather, airspeed, ground speed, heading and altitude to display time-based separation and arrival speed information to the approach controller. TBS has been in operation at Heathrow Airport since 2015 (NATS, 2015).

1.3.5 Wake Turbulence Mitigation for Departures (WTMD)

WTMD is a concept focusing on wind-dependent departure operations, which would be applied to airports with closely spaced parallel runways (CSPRs). WTMD takes advantage of a live forecast of strong crosswinds that would transport the wakes generated by heavy category aircraft on the downwind runway away from the upwind runway. This makes the departures on the upwind runway independent from downwind runway traffic in terms of wake effects; therefore, there is no need to maintain wake standards between upwind runway departure traffic and traffic on the downwind runway. Wake separation standards would still be applied between consecutive departures from the same runway and for departures from the downwind runway following departures

from the upwind runway. This procedure increases departures under favorable wind conditions.

1.3.6 Wake Turbulence Mitigation for Arrivals (WTMA)

WTMA is another wind-based solution, which allows for closer spacing of aircraft during periods of high crosswind conditions. WTMA uses wind forecast data to predict when wakes generated by an aircraft approaching a downwind runway cannot impact the aircraft landing on an upwind runway. When such crosswind conditions exist, the runway of interest is considered to be a wake independent runway. The concept also depends on favorable wind conditions and therefore excludes those airports that do not have heavy crosswind conditions.

1.4 Research Questions

When trying to demonstrate the safety of new concepts and procedures, common questions arise: Will a given procedure maintain the same level of safety that is observed today with respect to wake vortices? What is the minimum separation that can be achieved while still maintaining a given level of safety? Addressing such questions often involves Monte-Carlo simulation, and in the case of wake encounters, requires use of rare event simulation. Key questions that are addressed with this research are listed below:

- What are the capacity benefits of using a pairwise dynamic separation policy in NextGen flow corridors?
- Will a dynamic pairwise separation policy maintain the acceptable levels of safety with respect to wake vortex encounters?

- How do changes in different parameters like fleet mix, separation policy and meteorological conditions impact the capacity and safety of the flow corridor? What are the most important factors?

To answer these questions, a capacity simulation model and a safety simulation model are developed. The safety simulation incorporates a rare event probability estimation technique. This requires answers to the following questions:

- How can the rare event simulation technique be adapted for the problem of estimating wake vortex encounters? How well does the rare event simulation technique perform in estimating probabilities associated with the wake encounters?

The rest of this thesis is organized as follows: Chapter 2 provides a brief literature review, Chapter 3 documents the data collection and analysis efforts to identify trailing pairs in cruise and their separations distances. Chapter 4 deals with sensitivity analysis of a flow corridor's capacity to different simulation parameters with dynamic and static separation policies. Chapter 5 presents a rare event simulation methodology for estimating the probability of potential wake encounters for trailing pairs and hence flow corridors. Chapter 6 presents the conclusions and proposed future work.

CHAPTER 2: LITERATURE REVIEW

2.1 Flow Corridor Research

A field study of Air Traffic Control operations by Reynolds et al. (2002) found that controllers rely on underlying airspace structure to reduce the complexity of the planning and conformance monitoring tasks. Inspired by these findings, the flow corridor concept was suggested as an en-route airspace structure that would decrease the controllers' workload. Studies at George Mason University by Alipio et al. (2003) and Yousefi et al. (2004) were initial studies that provided the concept description, presenting the idea of flow corridors and how they operate.

Other research on flow corridors investigated the potential locations for the corridors. For example, Sridhar et al. (2006) grouped airports into regions and modeled a series of tubes connecting major regions. Xue and Kopardekar (2009) identified 60 corridor candidates using a Hough transform to identify groups or clusters of great circle trajectories that could form the tube network. Other research focused on benefit analysis that investigate the capacity gains of using corridors, delay reductions (Yousefi et al., 2010) and sector-load reductions below MAP values (Wing et al., 2008).

The other important factor that should be studied is the safety of such a concept of operation. Shortle et al. (2012) conduct a safety analysis on the Automated Airspace

Concept (AAC) as a part of safety-capacity tradeoffs in NextGen concepts using dynamic event trees. Ye et al. (2014) analyzed the collision risk-capacity tradeoff for a 2-lane flow corridor using a combined discrete–continuous simulation method. Zhang (2014) investigated the safety of flow corridors with respect to collision risk. However, there are no studies on safety of the corridors regarding wake vortex encounter risk. This research will focus on this gap in the literature.

2.2 Wake Vortex Risk

Wake vortices are generated as a byproduct of aerodynamic lift for every aircraft in flight. The pressure difference below and above the wings causes the air to go around the wingtip from the high-pressure region below the wing to the low-pressure region above the wing.

A vortex layer, produced in the near-field of the wing, gradually rolls up and generates a pair of counter-rotating trailing wake vortices. The initial strength of these vortices is a function of the aircraft's weight, airspeed, and wingspan and the air density. Vortex circulation intensity (Γ) represents the strength of the vortices, and the initial circulation is approximated by $\Gamma_0 = \frac{Mg}{\rho sBV}$, where M is the weight of the aircraft, ρ is air density, V is the airspeed, B is the wingspan, and $s = \pi / 4$ is a constant. The initial lateral spacing between the two vortices is sB which is usually about 78.5% of the wingspan, but can change with different wing loading and aircraft configuration. Generally, heavier aircraft generate stronger vortices. Although they tend to have larger wingspans (which appears in the denominator of the initial circulation strength), the increase in wingspan is not enough to counter the effect of higher weight.

Above the effects of the ground, due to mutual induction of the vortex pair, wake vortices descend downward while ambient wind can transport them laterally. The wake vortex descent rate is a function of the vortex circulation and aircraft span, and it decreases as the vortex circulation decays due to environmental influences.

The lifetime of these vortices, their transport and rate of decay is a function of meteorological conditions.

Wake vortices decay faster following the time the vortices link and form crude vortex rings, the "linking time" is dependent on the intensity of ambient turbulence, stronger ambient turbulence causes earlier linking and shorter vortex lifetimes, whereas calmer atmosphere results in more persistent wake vortices. Interaction with the ground makes the evolution of wake vortices more complex. Wake vortices that descend into ground effect (IGE) begin to separate laterally and decay more quickly than those that remain out of ground effect (OGE).

Lifetimes of wake vortices range from about 20 seconds to several minutes, depending upon the generating aircraft, proximity to the ground, and meteorological conditions.

2.3 Wake Vortex Encounters Frequencies in En-Route Airspace

The wake vortex hazard in terminal areas in take-off and approach phases of flight are well known and have been studied extensively. However, in the en-route phase and cruise altitudes, wake vortex encounters have been considered as rare, unlikely events. Nevertheless, the number of wake vortex encounters reports that are submitted voluntarily to the NASA Aviation Safety Reporting System (ASRS) show that these

encounters occur. For example, from 89 wake vortex encounter reports submitted during the second half of 2018 to ASRS, 15 reports indicated a wake vortex event in the cruise phase of flight (versus arrival or departure phases) (ASRS Database Online). Since these reports are voluntary, the database cannot be used to numerically quantify the prevalence of wake encounters within the National Airspace System (NAS). Also, it should be noted that a reported encounter is not the same as an actual encounter.

Studies and data that are collected at low altitudes near the airports are the basis of most current separation standards. Few studies have investigated wake vortex encounters at cruise altitudes, and most of the existing research is based on simulation, since data collection at high altitudes (above FL200) is a difficult task (Melgosa, 2017).

Nelson (2006) presents arguments that wake encounters at cruise altitude are a potential safety issue and that en-route wake vortex encounters will increase over time with increasing disparity in aircraft sizes, reduction of the minimum vertical separation distances, and increased air traffic. The argument is supported by analysis of simulation and flight test results obtained from earlier studies of wake encounters at low altitudes. Hoogstraten et al. (2015) also used a simulation framework and a wake vortex model to calculate the probability of severe wake vortex encounters in upper European airspace and predicted occurrence of a severe WVE once every 38 days in European airspace. They also had the same conclusion as Nelson (2006) and identified geometry of encounter as an important factor, where aircraft that are climbing or descending behind a heavy aircraft have a higher risk of encountering wake vortices.

Lau et al. (2018) also used simulation to predict the number of en-route wake vortex encounters, their main spatial encounter configurations, and their locations, over the European sky. They used an air traffic flow management model coupled with a wake vortex decay and transport model to predict the number of encounters defined as the residence of the intruder aircraft within the wake turbulence corridor of the generator aircraft. Their analysis of different encounter geometries implied that the number of wake encounters in the presence of strong winds is smaller than the number of encounters in low wind days because the vortices drift away from the intruders' trajectories, outweighing the drift of vortices into the intruders' trajectories. They predicted about 10 encounters for strong wind days and 19 encounters for low wind days over European airspace. However, since real wake vortices cover only a small fraction of the probabilistic volumes considered in their model, the number of real encounters would be substantially lower than the predicted potential encounters.

Schumann and Sharman (2015) used a simulation tool and analyzed the frequency wake encounters for historical aircraft movement data and meteorological data. The method was applied to data from radar-observed traffic over North America in 46 days in 2010 and 2011 and validated for upper airspace against pilot reports of wake encounters. Several suspected wake encounter cases were also inferred from turbulence reports. They found many events of close proximity between aircraft and active wakes, typically at 20–30 km horizontal separation, often for similar flight directions, at cruise levels of the upper airspace and even more often at lower altitudes in high traffic regions. Only about 0.4% of wake encounters were found to occur with both aircraft flying at constant

altitudes. 46% of computed encounters occurred when both aircraft were descending, 23% of encounters occurred when both aircraft were ascending, and the other encounter scenarios each occurred with a frequency of less than 8 percent. They also concluded that wake-vortex encounters occur frequently, though not all identified encounters are of safety concern.

En-route wake vortices generated by common airliners were also studied for the effects they might have on high/medium altitude long endurance RPAS (remotely piloted aircraft Systems) which are lighter and have larger wingspan and are susceptible to wake vortex turbulence (Marcos Benítez, 2016, Perez-Batlle et al., 2016). The project goal was modelling a vortex conflict detection system that warns the RPAS of vortex areas, so it can change its trajectory and escape a hazardous situation. They created a wake vortex generation and encounter model to define the airliner-RPAS vortex separation requirements. Results indicated that some current separation standards are not conservative enough when the RPAS faces an airliner wake vortex.

Most recently the problem of wake vortex encounters in cruise was studied by Melgosa et el. (2017) and Melgosa et al. (2018). They developed a simulation environment within the framework of the R-WAKE project to investigate the risks of potential wake vortex encounters in the en-route airspace, considering current and predicted operational scenarios, to support new separation standards for increasing airspace capacity. The R-WAKE simulation environment has different modules including simulators for weather, traffic, wake vortices, wake vortex interactions and different tools for safety and risk assessment. The framework was used to prove the safety relevance of

wake vortex encounters in cruise altitudes. Subsequently this high-fidelity simulation framework was used under realistic conditions to identify and characterize the suspected hazard areas (SHA) that flights should avoid under certain conditions if they are crossing a piece of airspace after another flight. They performed a large number of simulations to generate the SHAs, resulting from the combination of different separation distances, aircraft types (including realistic masses and cruise speeds), altitudes and atmospheric conditions and relative encounter geometries. They also demonstrated that the current en-route separation standards may be overly conservative in some cases, and may not protect enough in some specific situations.

There are also many studies concerning the occurrence and frequency of wake encounters for arriving/departing aircraft at airports, though that is not the focus of this research. For example, Kos et al. (2001) use a simulation-based risk assessment approach for landing aircraft and demonstrate its application to the case of multiple aircraft landing on a single runway. Shortle and Jeddi (2007) used a hybrid simulation methodology consisting of flight-track data and simulation of wake-evolution models to predict the frequency of potential wake alerts in landing. Wang and Shortle (2012) investigated the impact of stochastic variability of flight tracks on the probability of potential wake encounters for a single runway and for parallel runways. The results of this sensitivity analysis showed that the mean and standard deviation of separation, and the vertical standard deviation are the key parameters affecting potential wake encounters. In another study, Holzäpfel and Kladetzke (2011) used the WakeScene-D software package with modules for aircraft trajectories, meteorological conditions, wake vortex evolutions, and

potential hazard area to estimate the probability of encountering wake vortices for different traffic and crosswind scenarios during departure. Körner and Holzäpfel (2018) assessed possible wake vortex encounters in LIDAR field measurements accomplished by DLR and NASA at major international airports. They analyzed applied separations depending on the aircraft pairings and compared to the ICAO and RECAT standards. The results showed that in 0.02% of the landings, the encounters exceed a roll-control ratio limit, beneath which encounters are considered acceptable by pilots.

2.4 Dynamic Wake Separation

In future air traffic management, the static separation requirements between aircraft will be replaced by dynamic separation requirements that can vary based on meteorological conditions and aircraft state information. Dynamic separations are envisioned in both Europe (Single European Sky Air Traffic Management Research) and the U.S. (NextGen). Aside from the wind-based concepts mentioned in the introduction (e.g., WTMD; see Chapter 1), many dynamic separation concepts are in the exploratory stage. Feuerle et al. (2013) developed a new concept for wake-vortex hazard mitigation, with the basic idea that a criticality parameter is transmitted between aircraft to ensure a safe separation even within new self-separation concepts. The criticality parameter gives an indication about the severity of the vortices to surrounding aircraft which gives the following aircraft the possibility to assess the risk of preceding vortices. Rad et al. (2013) developed a concept for approach procedures that dynamically calculates the minimum safe distance, adjusts the follower aircraft speed and the corresponding approach types. Matayoshi and Yoshikawa (2014) argue that, based on a history of safe operations, the

risks at current separations are practically safe for all weather conditions even though that the actual wake risk varies with the weather. They suggest determining a target risk level within current separation risks and reducing separation until the expected risk at the reduced separation reaches the target risk level. Since the maximum risk at the reduced separation (target risk level) is within the level of risk admitted by current separations, the wake safety risk at the reduced separation would be acceptable.

2.5 Wake Vortex Turbulence Modeling

Fast-time models are developed to predict the behavior of wake vortices behind the generating aircraft. These parametric models are designed to reliably predict the position and strength of the wake vortices in real time, as a function of atmospheric and aircraft input parameters. Results of these fast time numerical models can be used for developing tighter separation standards, determining wake separation guidance for new aircraft, providing guidance for setting vertical separation standards, and testing of new concepts for safe increase in airport capacity (Proctor and Hamilton 2009).

These models are often developed using theoretical concepts and are calibrated using data obtained from field measurements or numerical simulations. Deterministic fast-time models predict the discrete vortex trajectories and circulation strengths as a function of time. Examples of models currently in use include AVOSS Prediction Algorithm (APA), the TASS Driven Algorithm for Wake Prediction (TDAWP), the Deterministic 2-Phase (D2P) model and Deterministic/ Probabilistic wake Vortex Model (DVM/PVM). In this research we use the first phase of APA algorithm (out of ground effect) to predict the transport and decay of wake vortices in cruise altitudes. We

implement the model using description available from published source (Robins and Delisi, 2002).

2.5.1 AVOSS Prediction Algorithm (APA)

The APA algorithm was first developed during the NASA Aircraft Vortex Spacing System (AVOSS) program and has undergone several iterations since. These algorithms are based on the work of Greene (1986) and Sarpkaya (2000). The original APA model V3.2, which was described in detail by Robins and Delisi (2002), is the framework for most recent versions of the algorithm. The APA model predicts wake vortex trajectories and circulation within a plane perpendicular to the path of the generating aircraft. Atmospheric inputs include vertical profiles of the ambient crosswind, temperature, and turbulence intensity (EDR).

In the APA algorithm, vortices are considered to migrate through four distinct phases. Phase I deals with the evolution of the vortices away from the ground (Out of Ground Effect). In OGE, the evolution of the vortices is computed by solving a system of 3 ordinary differential equations for 3 variables: v (speed of descent), z (altitude) and y (lateral position) using a constant time step (based on Sarpkaya, 2000). In version 3.2, the possibility of the vortex separation distance decreasing as a function of time is included to model the linking process after crow instability (Crow, 1970, Crow and Bates 1976),, but in later versions the separation distance is constant throughout the Out-of-Ground phase.

Phase II begins when vortices descend below 1.5 b_0 (the initial separation of the vortices). At this point in the vortices' evolution, as they approach the ground, the effect

of the ground causes the distance between the vortices to increase. This effect is modeled by introducing two image vortices that represent the presence of the ground. In this phase, the algorithm solves 8 ordinary differential equations (OEDs) that describe the motion of a system of four-point vortices. The circulation of the vortices decreases at the same rate as that occurring just before the transition to Phase II. Phase III and IV describe the behavior of the vortices under In Ground Effect when vortices descend below 0.6 b_0. For phase III, 16 OEDs are solved, and for phase IV, 24 OEDs are solved. The primary advantage of using four phases for modeling is that it allows the model to capture the ground effect on wake turbulence.

2.5.2 TASS Driven Algorithm for Wake Prediction (TDAWP)

Another model developed by NASA is TDAWP (Proctor et al., 2006). The Terminal Area Simulation System (TASS) is a fluid dynamics large eddy simulation model that numerically solves the Navier-Stokes equations for wake vortices. However, it is slow and computationally expensive. The TDAWP model is a simple set of algorithms created to generate similar results as the TASS model in a faster fashion (Shortle 2007). The model consists of two equations, one for the prediction of vortex transport and one for wake vortex decay. The model provides real-time predictions of wake vortex position and strength based on weather conditions. The TDAWP model does not include influence from the ground, but it includes the effects of crosswind shear on vortex descent rate and allows the prediction of change in lateral separation due to crosswind.

2.5.3 Deterministic/Probabilistic 2 phase Model (D2P/P2P)

D2P / P2P was developed by DLR, German Aerospace Laboratory (Holzapfel 2003). The model tries to capture the evolution of the wake vortices in two phases, a diffusion phase followed by a rapid decay phase. Similar to Sarpkaya's model, two parallel vortices are assumed to decay and descend at equal rates. However, in D2P, circulation decay is governed by an algebraic relationship representing the decay of a single potential vortex. D2P consists of a small set of differential equations which are obtained using results of large eddy simulations. The equations incorporate effects from wind, stable stratification, ambient turbulence, and ground proximity. The differential equations can be solved quickly, and they provide a good approximation to the large-scale model.

The P2P model models the initial wake vortex produced at the wingtip (diffusion phase). This phase uses inputs such as aircraft weight, airspeed and wingspan. The second phase (rapid decay) uses the first phase results and adds atmospheric inputs and ground proximity effects. P2P is probabilistic in the sense that it uses several components that take into account deviations from deterministic vortex behavior caused by the stochastic nature of turbulence, vortex instabilities, deformations, and uncertainties in environmental and aircraft parameters. The output of P2P consists of confidence intervals for vortex position and strength. Model design allows for the continuous adjustment of decay parameters and uncertainty allowances, based on a newly available of data. Before P2P, all the wake vortex prediction models were deterministic.

2.5.4 Deterministic/Probabilistic Wake Vortex Model (DVM/PVM)

Both models have been developed by Université catholique de Louvain (UCL) (de Visscher et al., 2010). The Deterministic wake Vortex Model (DVM) software constitutes the core of the WAKE4D which is a 3-D space plus time (4-D) wake vortex prediction platform software, also developed by UCL that simulates the transport and decay of the wake vortices generated by an aircraft evolving along a given fight path. DVM integrates various physical models to predict the transport and decay of the wake vortices in one “slice" of space along the fight path. It accounts for the effects of the profiles of wind (headwind and crosswind components), crosswind shear, turbulence and stable stratification, and ground proximity on both transport and decay of the wake vortices.

2.5.5 Comparison of Models

Several studies have compared the results of fast-time models to quantify the differences between the models and demonstrate the strengths and weaknesses of each model.

Shortle (2007) compared the predicted output for wake circulation, strength, and wake altitude over time for APA, D2P and TDAWP. The results demonstrate the fundamental differences of the models as shown in Figure 1. The two phases of the D2P model are obvious – there is the short diffusion period with minimal loss of strength before the second phase of rapid decay begins. In this example, the TDAWP model predicts the weakening to occur at a slower rate and does not predict the circulation to weaken to zero. APA predicts a nearly even amount of decay across time. All three

models predict similar initial descent for the vortices; however, they are different predictions for the final descent of the vortices.

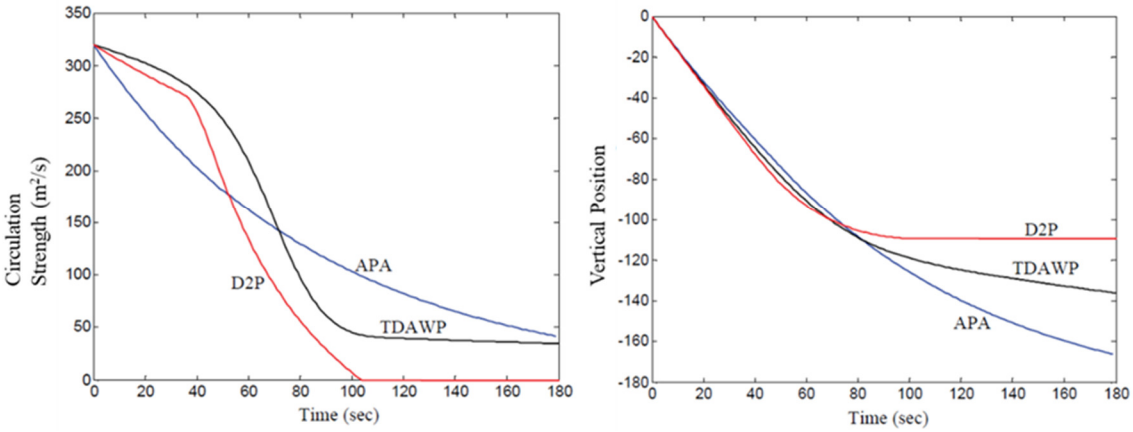

Figure 1 Predictions of different models for circulation and altitude vs time (Shortle 2007)

Proctor and Hamilton (2009) reported similarity in OGE wake predictions between TDAWP and D2P, even though the two models have very different formulations and their development was driven by parametric results from two different LES models. Both D2P and TDAWP predict two-phased circulation decay; however, the TDAWP predicts slightly longer lifetimes for wakes. The Sarpkaya model predicts very different circulations from TDAWP or D2P. It also predicts longer lifetimes for vortices than either TDAWP or D2P in near neutral stratification, but shorter lifetimes in stratified environments. Also, in predictions of the Sarpkaya model, vortex descent speed slows down faster resulting in a smaller descent of the vortices.

Prius and Delisi (2011) evaluated seven fast-time models, including 4 different versions of APA, TDWAP, DVM and a new fast time model VIPER. They compared

model outputs with LIDAR observations in different airports and concluded that these models perform in a similar way over a large range of ambient conditions and their predictions are in agreement with LIDAR observations. However, when the ambient turbulence is weak or there is stable stratification, these models perform differently.

All of these models are validated against field data, and predicted acceptable results, but observing these differences indicate that wake turbulence models are not precise models.

2.6 Rare Event Simulation

With all wake mitigation procedures and separation laws in place, wake encounters are inherently rare, and their probability is very small. As new procedures, concepts, and technologies, such as dynamic self-separation, are proposed to improve airspace capacity, such changes must be demonstrated to be safe prior to implementation. Thus, common questions arise: Will a given procedure maintain the same level of safety that is observed today with respect to wake vortices? What is the minimum separation that can be achieved while still maintaining a given level of safety? Addressing such questions often involves Monte-Carlo simulation of rare events. However, estimating rare event probabilities with crude Monte Carlo simulation can be very inefficient.

The main challenge to estimate rare event probabilities is computation time. The following example illustrates the problem: Assume γ is the true probability of a rare event. The typical approach to estimate this probability is to simulate *n* i.i.d. replications and let $X_i = 1$ if the event occurs, and 0 otherwise. Then $\hat{\gamma} = \sum_{i=1}^{n} X_i/n$ is an unbiased estimator of the rare event probability γ, with $\text{var}[\hat{\gamma}] = \gamma(1 - \gamma) / n$. For a rare event,

the relative error, which is the standard deviation of the estimator divided by its mean, is approximately $1/\sqrt{\gamma n}$. For example, if $\gamma = 10^{-9}$, then achieving a relative error of 10% requires at least 10^{11} replications, which may be intractable, particularly if the simulation time for each replication is non-trivial. In the above example, if the time needed for each simulation replication is one second, then the required time for achieving a 10% relative error is more than 3,000 years. Thus, other methods are needed. In the literature there are two common approaches for improving the efficiency and variance reduction in rare event simulation – *importance sampling* and *splitting*.

2.6.1 Importance Sampling

Importance sampling (IS) works by changing the probability laws of the system itself. The underlying sampling distribution is changed in a way that makes the occurrence of the rare event more likely, so the events of interest are sampled more frequently. Using a new distribution introduces a biased estimator, so corrections must be applied. This is achieved by multiplication of the estimator with a likelihood ratio. IS is particularly useful in systems where the stochastic process reaches the rare event with a small number of "catastrophic jumps." The main challenge in the IS method is finding the optimal change of measure – i.e., the choice of the sampling distribution that minimizes the variance of the estimator. Importance sampling has been applied in many domains. A few examples are digital communication systems (Smith et al, 1997), radar systems (Mitchell, 1981), medical image analysis (Naiman and Priebe, 2001), finance (Fuh et al., 2013), and so forth.

2.6.2 Splitting

The main idea of the splitting technique (e.g., L'Ecuyer et al. 2009) is to split the simulation into separate independent runs when trajectories get "near" the rare event. This tends to focus computation effort on runs that are more likely to hit the rare event. Unlike IS, one advantage is that the probability laws of the system remain unchanged. Therefore, the stochastic model capturing the system evolution can be developed independently of the splitting method. Splitting is more useful when a system takes many small steps towards the rare event. The splitting method has been applied to other real-world problems such as collision risk in aviation (Blom et al. 2006, Blom, Bakker, and Krystal 2009, de Oliveira et al. 2010), cascading blackouts (Shortle 2013), queueing networks (Garvels 2011) and network reliability (Murray, Cancela, and Rubino 2013).

In this study we use splitting method to estimate the rare probability of potential wake encounters for a pair of trailing aircraft which are supposed to maintain their separation distance and altitude. For a rare event -in which the follow aircraft enters the potential wake region of the generating aircraft- to happen, the follow aircraft should gradually deviate from its predefined trajectory, which suggest the use of splitting method.

2.6.3 Basic Splitting Method

The basic setting of the problems in the literature is as follows: Assume a Markov process $X \equiv \{X_t, t \geq 0\}$ with state space χ, let S and $\mathcal{R}$ be two disjoint subsets of χ , where S is the initial state set, and $\mathcal{R}$ is the rare event set. The process starts at $X_0 \in S$, leaves the set *S*, and then eventually reaches $\mathcal{R}$ or goes back to set *S*. If we define $\tau_S =$

$inf\{ j > 0 : X_{j-1} \notin S \; and \; X_j \in S\}$, the first time when the Markov chain returns to S after leaving it , and $\tau_{\mathcal{R}} = inf\{ j > 0 : X_j \in \mathcal{R}\}$, the first time when the chain reaches the rare event set, then the small probability that we want to estimate is $Pr[\tau_{\mathcal{R}} < \tau_S]$, the probability that the Markov chain reaches the rare event set before going back to S.

To estimate this probability, the splitting algorithm uses an importance function $h : \chi \to \mathbb{R}^+$ which is a map of the state space to an *importance value* indicating how close the process is to the set of rare events. Based on this, we assume $S = \{x \in \chi : h(x) \leq 0\}$ and $\mathcal{R} = \{x \in \chi : h(x) \geq l\}$ where $l > 0$ is a constant. In the multilevel splitting method, we split the interval $[0, l)$ into m disjoint subintervals in form of $[0, l_1)$, $[l_1, l_2)$,…, $[l_{m-1}, l_m = l)$, $l_1 < l_2 < \cdots < l_m$ each representing a stage. For $k = 1, \ldots, m$, let $\tau_k = inf\{ j > 0 : h(X_j) \geq l_k\}$, then $D_k = [\tau_k < \tau_S]$ denotes the event that the process reaches level k before reaching level 0. With these definitions, an unbiased estimator for the desired probability is $\gamma = P[D_m] = \prod_{k=1}^{m} p_k$, where $p_1 = P[D_1]$ and for $k > 2$, p_k is the conditional probability $p_k = P[D_k \mid D_{k-1}]$.

In implementing the splitting algorithm, the number of stages, m, and the thresholds l_i should be selected in a way that a sample path reaching a threshold has a noticeable probability of reaching the next threshold. In other words, going from one stage to the next is not a rare event, otherwise there is no benefit in using the splitting technique.

Estimating the rare event probability is done by estimating p_1 and then estimating the subsequent conditional probabilities separately. In the first stage, we start N_0 independent runs from the initial states, where the initial state $X_0 \in S$ of each chain is

randomly generated from the probability distribution of *S*. These chains are simulated until the time $T = min(\tau_1, \tau_S)$. Upon hitting the first level, the state of the process is saved. If the number of chains reaching level 1 is R_1 then we estimate $p_1 = \frac{R_1}{N_0}$. Using the saved states of chains that reach level 1, we get an empirical distribution for initial states of stage 2. Then the algorithm samples from this empirical distribution and simulates N_1 independent chains until they reach level 2 or go back to level zero. If the chains reach the next level, then $p_2 = \frac{R_2}{N_1}$. The estimation is done in successive stages in the same manner for $p_3, \dots, p_m$.

2.6.4 Fixed-Splitting, Fixed-Effort Splitting, and Fixed Number of Successes

Many variations of the splitting method are discussed in the literature (Garvels 2000). In *fixed splitting*, we clone each of the R_k chains that reach level *k* in c_k copies, for a fixed positive integer c_k. In this method, the number of independent chains simulated at each level is random. The advantage of fixed splitting is that it can be implemented recursively in a depth-first manner. Therefore, the computer needs to store, at most, a single system state per level, just keeping the simulation history of the current run. However, the efficiency of fixed splitting is extremely sensitive to the choice of splitting factors (c_k). If the splitting factors are too high, the number of chains explodes, whereas if they are too low, the variance is very large because very few chains reach the rare event.

In the *fixed effort* approach, a predetermined total number of runs at each level (N_k) is set. Random assignment and fixed assignment are two ways of achieving this

goal. In random assignment, we draw the N_k starting states at random, with replacement, from the R_k available states. In fixed assignment, we split each of the R_k states approximately the same number $c_k = \left\lfloor \frac{N_k}{R_k} \right\rfloor$ or $\left\lfloor \frac{N_k}{R_k} \right\rfloor + 1$. The fixed assignment gives a smaller variance than the random assignment because it corresponds to stratification over the empirical distribution of entrance state at level *k*.

The fixed effort approach has the disadvantage of requiring more memory than fixed splitting, because it must use a breadth-first implementation. Garvels and Kroese (1998) conclude from their analysis and empirical experiments that fixed effort performs better than fixed splitting, mainly because it reduces the variance of the number of chains that are simulated at each stage. It turns out that with optimal splitting factors, this is not always true and fixed splitting is asymptotically better under ideal conditions. But due to the sensitivity to the splitting factors, and since the optimal splitting factors are unknown in real-life applications, the more robust fixed-effort approach is usually preferable.

Another variation of the splitting method introduced by Amrein and Kunsch (2011) is called *fixed number of successes* (FNS). This method controls the imprecision of the estimator rather than the computational effort. At each level, the total number of trajectories that must reach the next level is fixed (R_k is fixed); independent replications at the current level continue until the fixed number of successes is achieved. According to the authors, this approach is often superior to fixed splitting and fixed effort, because the levels are learned adaptively, so the probability of reaching the next level is approximately the same at all levels and it never estimates the probability to be zero.

Also, it is less sensitive to tuning issues like the choice of level sets and the number of replicates per level.

CHAPTER 3: ANALYSIS OF CURRENT AIRCRAFT SEPARATION IN CRUISE

3.1 Motivation for Collecting and Analyzing Historical Data

It is desirable to use simulation as a tool to estimate the safety and capacity of current operations as well as proposed changes for future operations. To determine the current safety levels, parameters in a simulation model need to be quantified using data from real flights. Statistics such as average and variance of separation distance, average and variance of airspeed, average and variance of altitude, and so forth should be estimated from historical flight data to calibrate parameters of the simulation model in order to generate trajectories with similar characteristics. The objective of this section is to collect and analyze historical track data for *trailing pairs* of aircraft *in cruise altitudes*.

3.2 Methodology for Data Collection and Processing to Identify Trailing Pairs

This research uses historical data from https://ADSBExchange.com, which is a co-op of Automatic Dependent Surveillance-Broadcast (ADS-B), Mode S, and Multilateration (MLAT) feeders from around the world. The data exchange is claimed to be the world's largest source of unfiltered flight data. Their historical data (by date and time) was previously available free of charge, which is not the case anymore.

Flight track data is provided in 60-second intervals, typically on the 30-second mark of any minute. A query is issued on live position data and results are returned in a JSON (JavaScript Object Notation) format. Essentially, the query returns 65 seconds of

historical data on all aircraft, including known position data, altitude, and timestamps. Therefore, given the fact that a query is issued every 60 seconds, no data is lost. The result of this process is daily generation of 1,440 JSON files which get zipped into a single file for that day. The historical data is available for each day beginning June 9th, 2016.

The historical data provided by the ADS-B Exchange include many data fields. The important ones are ICAO number (which is broadcast by aircraft and is used to identify the aircraft), receiver identification number (used to identify the receiver that logged the data), timestamp (which is reported in epoch milliseconds and is converted to human readable time), latitude, longitude, altitude (which is in feet at standard pressure), speed, speed type (ground speed, true air speed, etc.), vertical speed, track angle across the ground (which is clockwise from 0° north), aircraft model, and wake turbulence category of the aircraft. Figure 2 shows snapshots of recorded aircraft positions over the U.S. at different times of a single day.

The purpose of this data collection and analysis effort is to identify the trailing pairs in cruising altitudes over 30,000 feet and to calibrate simulation parameters using statistics from the historical track data.

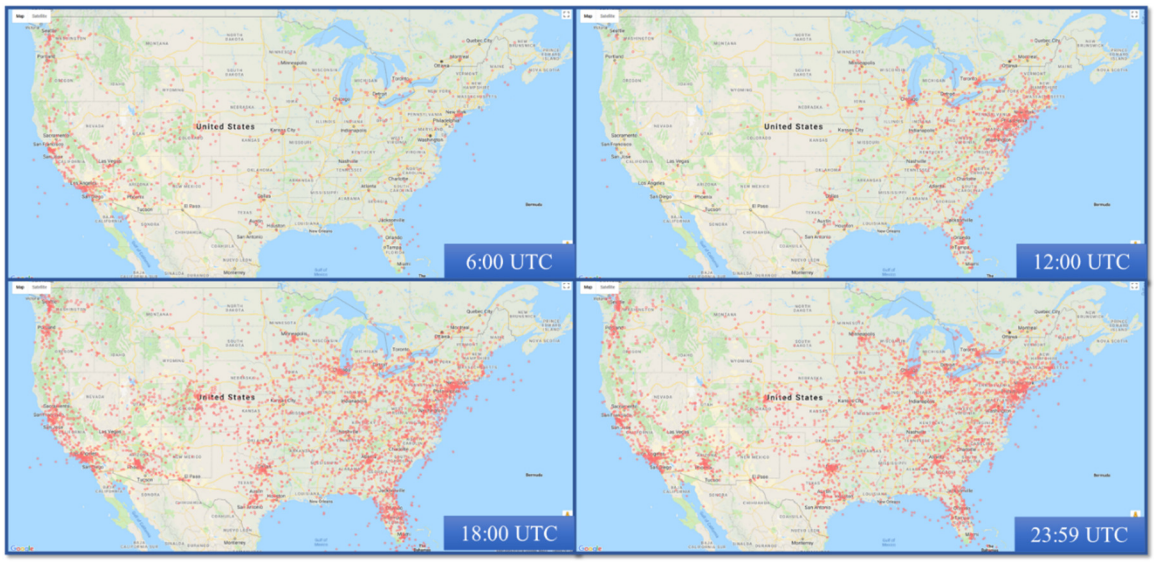

Figure 2 Snapshot of aircraft position over United States

The historical ADS-B Exchange data is from all around the world, but we are only interested in flights above the United States and Europe where there is a good coverage of feeders. Figure 3 shows a snapshot of the locations of active feeders on a typical day. The positions are moved slightly for security and anonymity reasons.

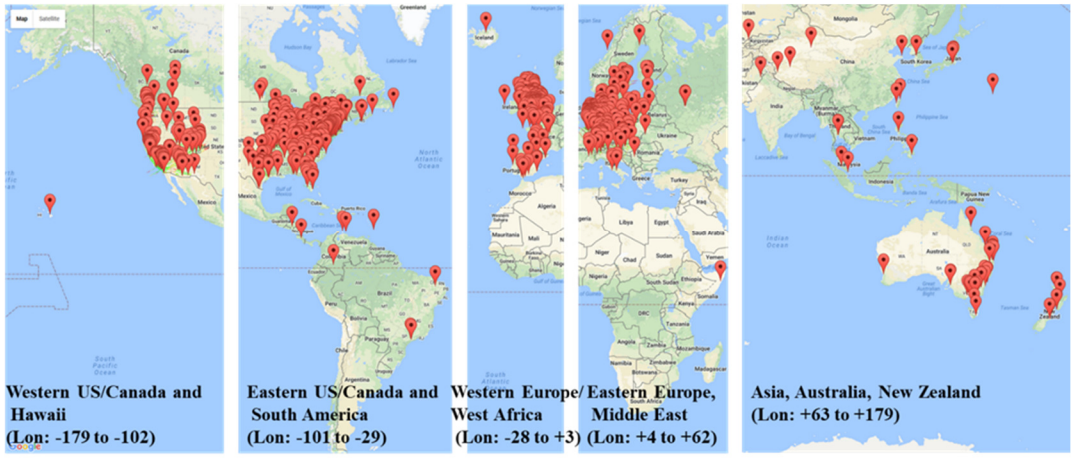

Figure 3 Snapshot of active feeders in a typical day

To clean the data, we remove all rows with missing latitude, longitude, or altitude and filter the data based on coordinates to include only aircraft over the U.S. and Europe. In each minute's JSON file, there might be multiple known positions for a specific aircraft. To reduce the workload, we remove all duplicate rows except the one which has the timestamp closest to the 30 second mark of that minute. This process is repeated for 1,440 JSON files for each day. Then, for each aircraft, we use a simple linear interpolation to get the latitude, longitude, altitude, and airspeed of that aircraft on the exact 30 second mark of each minute. This procedure results in matching timestamps for all aircraft in each minute allowing correct calculations of aircraft separations. At each timestamp we calculate the distances between all pairs of aircraft which fly on the same high altitude (with a tolerance of ±200 ft) over 30,000 ft. If the distances are less than a certain threshold (80 nautical miles), we store them in another database. The ground speed data available in ADS-B Exchange is not very reliable as there are a lot of missing data or bad data (very low or high speeds). To get better data for aircraft speed, we calculate the ground speed using the position of aircraft at different timestamps.

In summary, after processing the data for a given day, we have information on each aircraft throughout the day, which includes latitude, longitude, altitude, and ground speed at the 30-second mark of each minute. Additionally, we create another database that stores the distance between pairs of aircraft at the 30-second mark of each minute if they are flying at the same altitude and if their distance is less than a certain threshold.

The main goal of this data collection effort is to identify current separation standards for trailing pairs of aircraft, so first we must come up with a definition for pairs

of aircraft that we consider trailing. As a preliminary filter, we consider two aircraft as a trailing pair if they are within d nautical miles of each other for more than t minutes. These criteria give trailing pairs, but also select pairs on crossing tracks and pairs that fly on parallel paths very close to each other. Figure 4 shows sample pairs extracted considering only these two criteria, 4-a shows aircraft with crossing paths, 4-b shows aircraft with parallel paths close to each other.

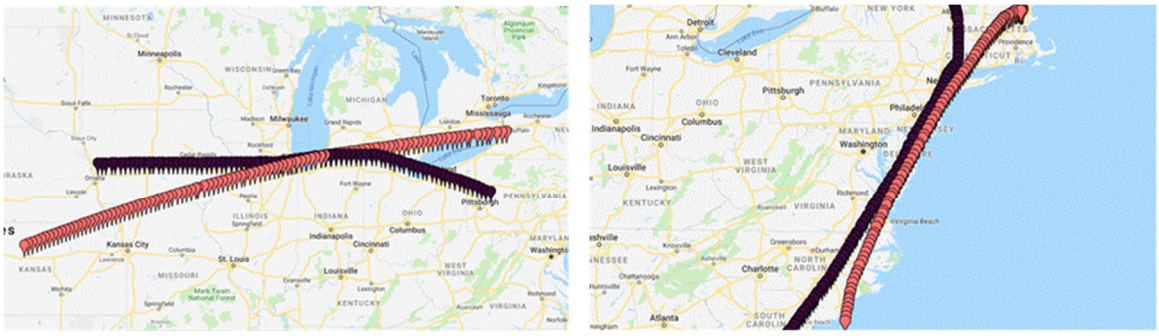

4-a 4-b

Figure 4 Examples of pairs of aircraft that fly close to each other for few minutes but are not trailing each other

To identify the actual trailing pairs, we apply another filter that uses the coordinates for each aircraft over time to determine if they are flying on the same path. The heuristic calculates the closest point of each track to the other track, and if most of these closest distances are within 2 nautical miles, the heuristic decides that the aircraft are on the same path. Figure 5 depicts an example of a trailing pair of aircraft obtained from this filter.

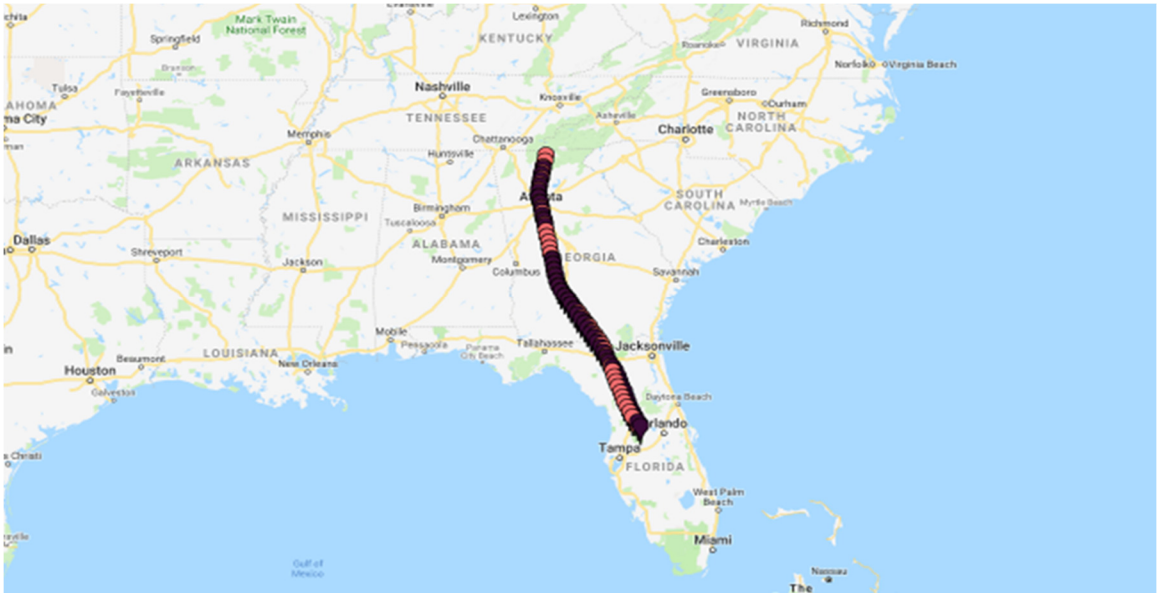

Figure 5 An example of trailing pairs

3.3 Analysis and Results

To identify trailing pairs which are flying close to each other and are of concern in wake vortex scenarios, the proximity parameters are set as $d = 20$ nautical miles and $t = 10$ minutes. After processing and analyzing 5 weeks of data for flights over the U.S. (three consecutive weeks in summer 2017 and two consecutive weeks in winter 2018), we identify about 3,000 trailing pairs. For flights over Europe we process the data for two consecutive weeks in summer 2017, and we identify about 2,000 trailing pairs.

Charts in Figure 6 show the distribution of minimum distance for trailing pairs found in the U.S. and Europe. Minimum distance is the minimum in-trail distance for a given lead-trail pair observed over the in-trail time horizon of that pair. Current separation rules do not allow aircraft to get closer than 5 nautical miles to each other, and the historical data verifies that actual aircraft separations follow this rule. The mode of

the distribution for both U.S. and Europe is about 14 nautical miles which is significantly higher than the 5 nautical mile minimum separation and implies that very large spacing buffers are added to the minimum separation.

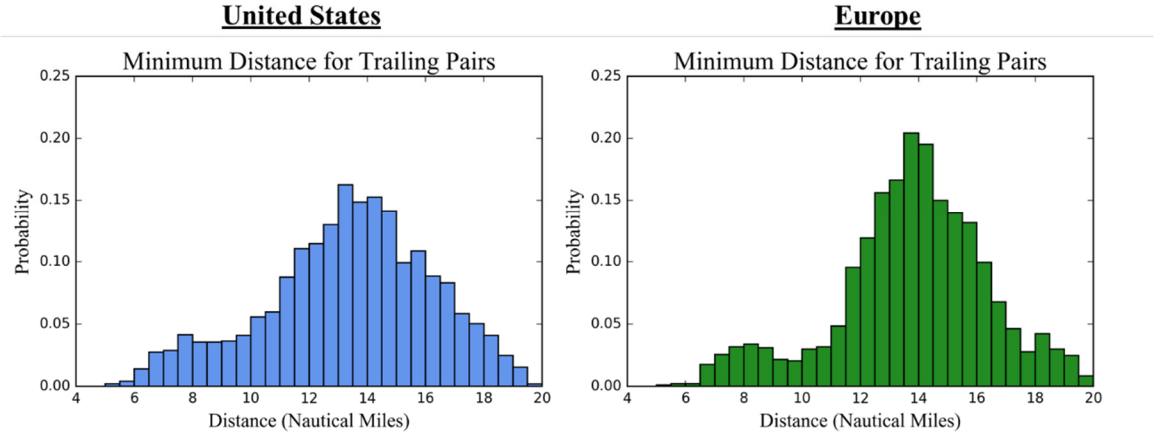

Figure 6 Distribution of distance at closest point of approach for trailing pairs

Figure 7 shows the distribution of average distance between trailing pairs, where average distance is the average in-trail distance for a given lead-trail pair observed over the in-trail time horizon of the pair. The mode of the distribution is about 16 nautical miles for both U.S. and Europe. However, for trailing pairs in Europe, the histogram has a more defined peak and the average distance has less variance. Figure 8 shows the distribution of standard deviation of in trail distance for pairs of aircraft in the U.S. and Europe.

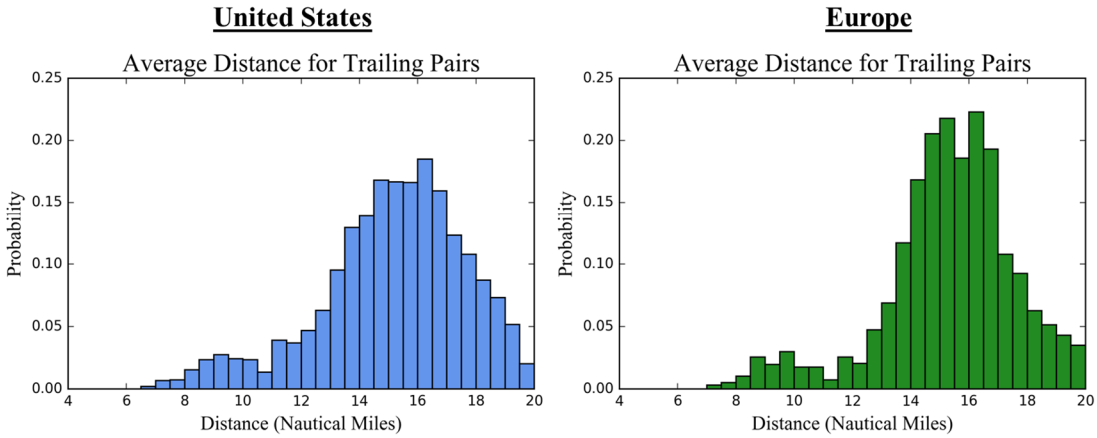

Figure 7 Distribution of average distance for trailing pairs while trailing

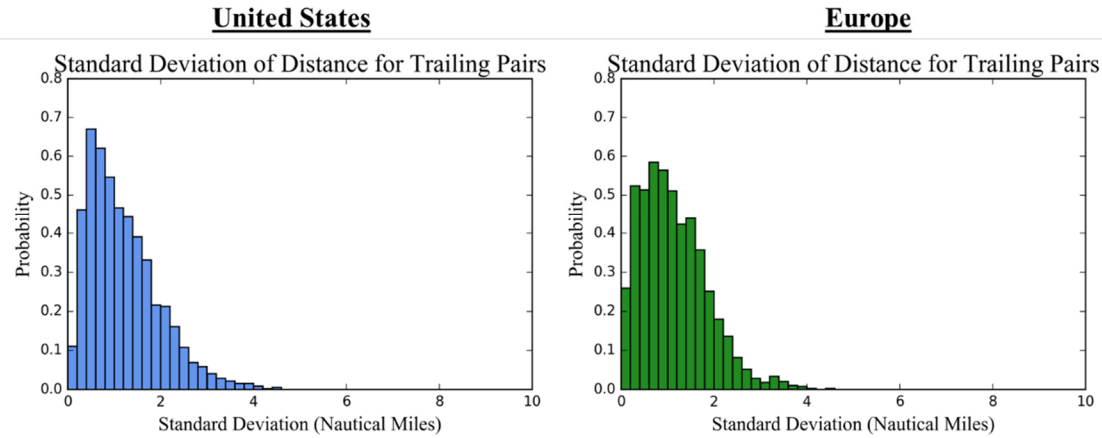

Figure 8 Distribution of standard variation of distance for trailing pairs

To see if different aircraft types have different separation distributions, we group the results by the wake vortex categories of the leading and following aircraft. Table 2 shows the wake categories of 123 aircraft types in 6 categories (Lower Small, Upper Small, Large, Lower Heavy, Upper Heavy, and Super) for RECAT II in Southern California TRACON (SCT) (Johnson, 2017).

Table 2 RECAT II 123 aircraft types categorized for SCT

A (Super)	B (Upper Heavy)	C (Lower Heavy)	D (Large)		E (Small Plus)	F (Small)	G
A388	A332	A306	A318	DH8A	ASTR	BE10	A124
	A333	A30B	A319	DH8B	B190	BE20	A342
	A343	A310	A320	DH8C	BE40	BE58	B703
	A345	B762	A321	DH8D	B350	BE99	B74S
	A346	B763	AT43	E135	C560	C208	C135
	B742	B764	AT72	E145	C56X	C210	DC87
	B744	C17	B712	E170	C680	C25A	E3TF
	B748	DC10	B721	E75L	C750	C25B	E6
	B772	K35R	B722	E75S	CL30	C402	L101
	B773	MD11	B732	E190	E120	C441	VC10
	B77L		B733	E45X	F2TH	C525	
	B77W		B734	F16	FA50	C550	
	B788		B735	F18H	GALX	P180	
	B789		B736	F18S	H25B	PAY2	
	C5		B737	F900	LJ31	PA31	
			B738	FA7X	LJ35	PC12	
			B739	GLF2	LJ45	SR22	
			B752	GLF3	LJ55	SW3	
			B753	GLF4	LJ60		
			C130	GLF5	SH36		
			C30J	GL5T	SW4		
			CL60	GLF6			
			CRJ1	GLEX			
			CRJ2	MD82			
			CRJ7	MD83			
			CRJ9	MD87			
			CRJX	MD88			
			CVLT	MD90			
			DC91	SB20			
			DC93	SF34			
			DC95				

The original data also has a field for the wake turbulence category of the aircraft and has 3 categories Light, Medium and Heavy, but this data is missing for most flights. Hence, we determine the wake turbulence category using the previous table. Considering only the types of aircraft listed in this table we can identify the wake turbulence categories of both the leading and following aircraft for about 95% of the pairs.

After grouping pairs by wake category, it is observed that more than 80 percent of the identified trailing pairs fall into the Large-Large category. Most other pair combinations suffer from small sample sizes (Table 3). With insufficient observations,

we cannot compare the categories in terms of average separation distance. In general, we do not observe any obvious differences between separation distributions for different categories of leading and trailing aircraft.

Table 3 Number of pairs of aircraft in each Lead-Follow wake category

United States

Number of Pairs		Trailing aircraft					
Leading aircraft		F	E	D	C	B	A
	F			2			
	E		8	18	1	1	
	D	2	22	2446	88	36	1
	C		1	50	55	8	
	B		1	30	13	49	2
	A					5	1

Europe

Number of Pairs		Trailing aircraft					
Leading aircraft		F	E	D	C	B	A
	F						
	E			2			
	D	1	1	1646	21	25	4
	C			13	11	5	
	B			39	6	89	13
	A			3		13	15

F: Lower small E: Upper small D: Large
C: Lower heavy B: Upper heavy A: Super

Even though we do not observe any obvious differences between distributions of separation distance for pairs in different lead-follow wake categories, to estimate the parameters of our wake encounter model, we try to eliminate any volatility that might be caused by such differences. Therefore, we select a list of comparable aircraft models in terms of wake category and estimate the parameters based on data for trailing pairs in which both the leading and following aircraft belong to this list. The selected list of aircraft consists of large aircraft including: Airbus A318, Airbus A319, Airbus A320, Airbus A321, Boeing B737-600, Boeing B737-700, Boeing B737-800, and Boeing B737-900. Using these new criteria to identify the desired trailing pairs gives about 1,400 pairs

in the U.S. and 1,500 pairs in Europe. Figure 9 shows the distribution of average distance for trailing pairs which belong to the selected types of aircraft. Fitting a normal distribution to these data gives $\mathcal{N}(15.1, 2.5^2)$ for average separation distance in the U.S. and $\mathcal{N}(15.2, 2.3^2)$ for average separation distance in Europe.

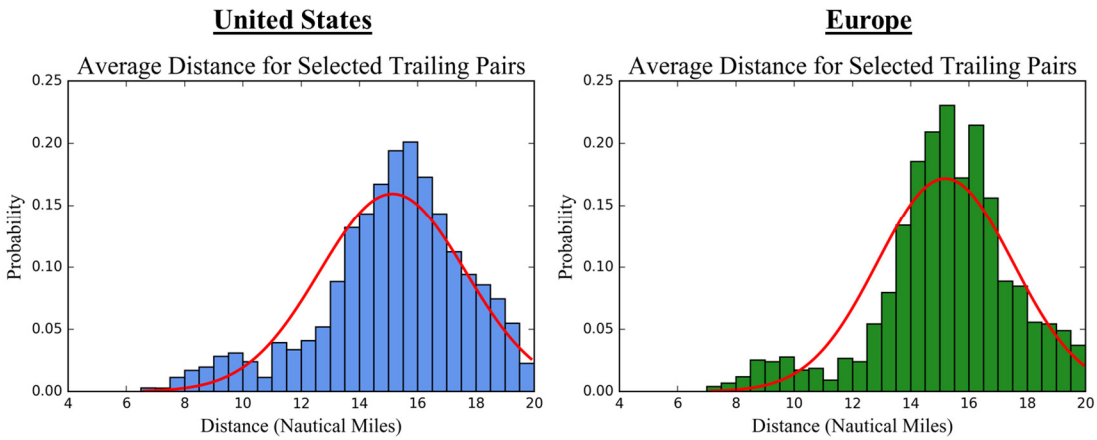

Figure 9 Distribution of average separation distance for trailing pairs (upper medium aircraft)

Gamma distributions are fitted to the observed distributions of standard deviation of separation distance. For trailing pairs in both the United States and Europe, the average standard deviation of separation distance is estimated to be around 1.1 nautical miles. Figure 10 shows the histograms and fitted distributions for selected trailing pairs.

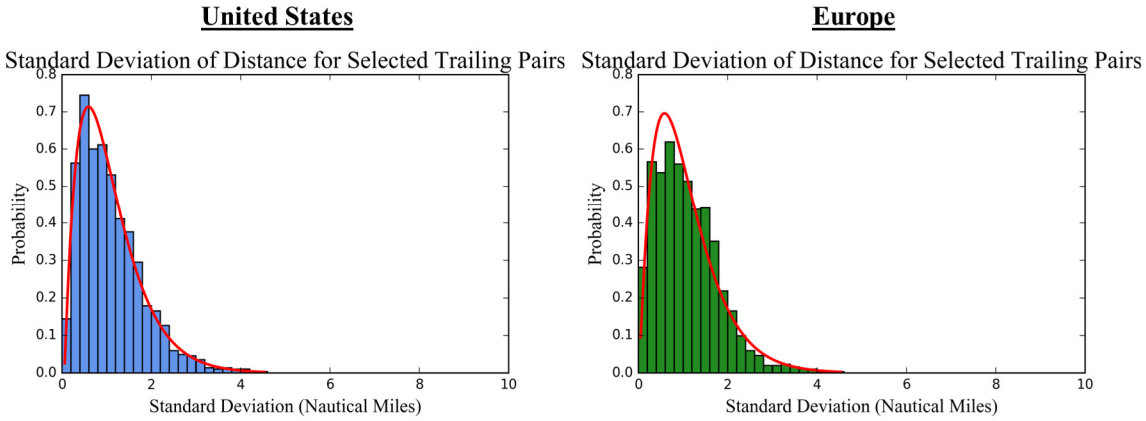

Figure 10 Distribution of standard deviation of separation distance for trailing pairs (upper medium aircraft)

Other important parameters which can be verified using historical track data are average airspeed and the standard deviation of airspeed for the leading and following aircraft. Wake models generally require *airspeed* as an input parameter, historical track data provides *ground speed* of the aircraft. Since we do not have access to supporting weather data on wind speed, we use the calculated ground speeds to get an estimate for average and standard deviation of airspeed for both aircraft. These estimates are not ideal since the ground speed might be more volatile than air speed because of the wind.

Since there are a lot of missing data, we calculate the average ground speed of the aircraft at each timestamp using the position aircraft at two consecutive timestamps. Figure 11 shows examples of the groundspeed versus time for pairs of aircraft.

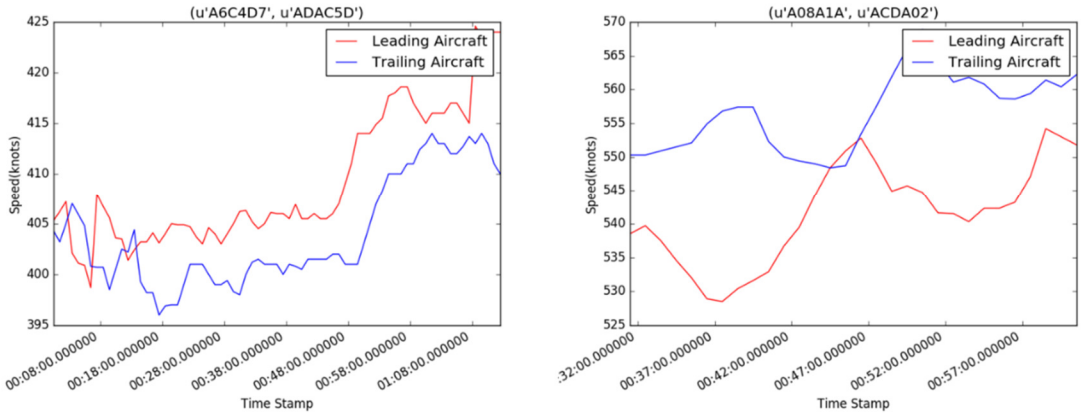

Figure 11 Examples of groundspeed versus time for pairs of trailing aircraft

Figure 12 shows the histograms and the fitted normal distributions for average ground speeds of pairs of aircraft in the U.S. and Europe. For the U.S., the fitted normal distributions of average ground speed for both the leading and trailing aircraft have parameters $\mu \cong 436$ knots and $\sigma \cong 50$ knots. These parameters for normal distributions fitted on data from Europe are $\mu \cong 446$ knots and $\sigma \cong 35$ knots. Data indicates that average speed of leading and trailing aircraft follow the same normal distribution. The ground speed average is greater in Europe and has less volatility in comparison with the U.S.

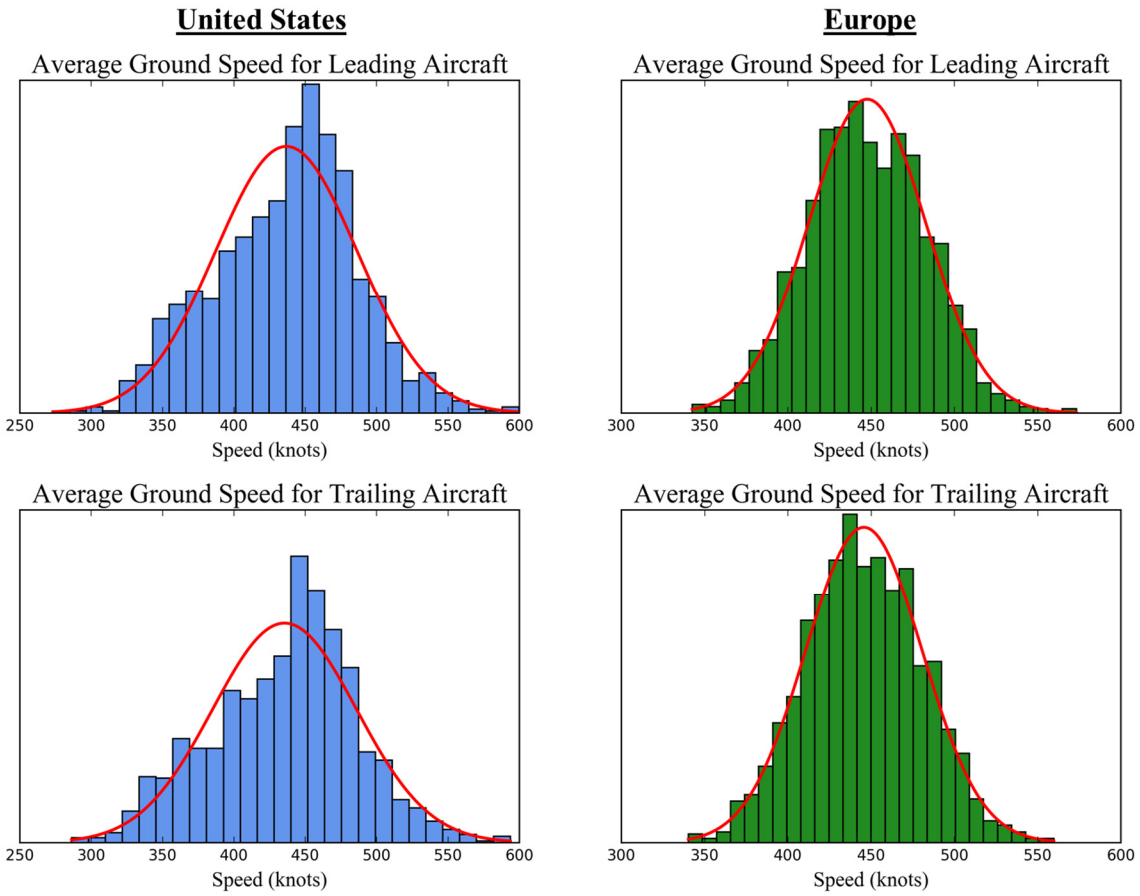

Figure 12 Distribution of average ground speed for trailing pairs

Figure 13 depicts the histograms and fitted gamma distributions of the standard deviation of ground speed for the leading and trailing aircraft in the U.S. The average standard deviation of ground speed for both leading and trailing aircraft is about 16 knots.

United States

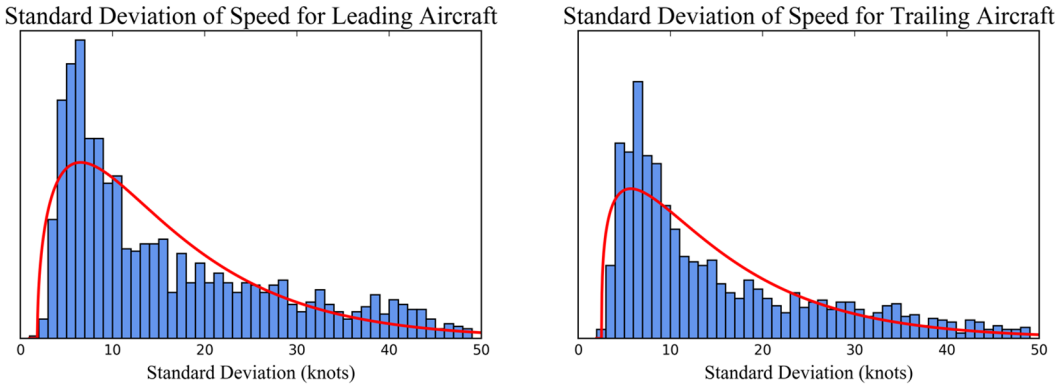

Figure 13 Distribution of Standard deviation of ground speed for leading and trailing aircraft

Another important parameter in simulating movements of aircraft is the variance of altitude. Altitude from the ADS-B track data is measured in feet at standard pressure. To estimate the variance of altitude, we extract intervals of level flight from the historical aircraft tracks. We consider an aircraft in level flight if it keeps the same altitude ($\pm$200 ft) for more than 10 minutes. Then for each of these intervals we calculate the standard deviation of altitude over that interval. Analyzing data for aircraft flying over the U.S. for three days, we find more than 30,000 intervals of level flight over 30,000 feet. Figure 14 shows the resulting distribution of standard deviation of altitude. The histogram suggests a very good performance in maintaining the altitude – the average standard deviation estimated from historical data is about 10 ft.

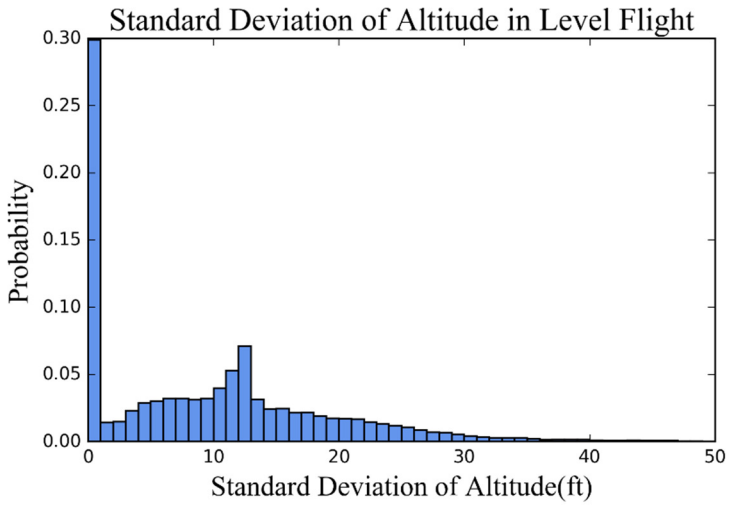

Figure 14 Standard deviation of altitude for aircraft in level flight over 30,000 ft

The statistics calculated in this section will play a significant role in quantifying the parameters of the simulation models in the next chapters.

CHAPTER 4: CORRIDOR CAPACITY WITH DYNAMIC WAKE SEPARATION

This chapter explores the capacity benefits of employing a dynamic wake separation policy in comparison with a static separation policy in a single lane en-route flow corridor. Wake durations on flight paths vary greatly depending upon meteorological conditions such as wind, ambient turbulence intensity, and atmospheric stability. They also depend on the weight and airspeed of the generating aircraft. Current separation rules prescribe static minimum wake vortex separations based on weight categories of the aircraft. Traditional ICAO separation minima or new categories of RECAT I, or even extensive tables of pairwise separation in RECAT II, all specify static separation minima based on a *worst-case* analysis of aircraft within a weight category (e.g., based on the heaviest aircraft within a given category in front of the lightest aircraft, assuming meteorological conditions that lead to the longest lasting wakes). These static minima are all independent of the weather and atmospheric conditions as well as variations in the actual weight and airspeed of the generating aircraft.

4.1 Dynamic Separation Concept for En-route Flow Corridor

Dynamic separation is a general concept in which separation minima can change dynamically depending on a number of factors including atmospheric conditions and aircraft state information. Dynamic concepts exist both in the terminal and en-route environment. There are some well-established terminal dynamic concepts, such as

WTMD and WTMA for example (see Chapter 1), which depend on crosswind only, and TBS which depends on headwinds. Dynamic separation is also part of the envisioned RECAT Phase III concepts, where the Phase II pairwise separations will function as the base, and real time meteorological data, provided by ground or airborne sensors, will be used to dynamically adjust them.

Dynamic separation concepts in en-route operations are not well-defined, but are still in the concept exploration and development phases. There is a plan to apply the dynamic pairwise separations in RECAT III to the en-route operations in the future. In this research, we define a possible dynamic concept for en-route flow corridors for the purpose of exploring potential capacity benefits.

The new concept is proposed within the environment of a single lane flow corridor. Flow corridors help accommodate high levels of traffic by reducing airspace complexity and allowing for self-separation-capable aircrafts. In our case study, we use a single lane corridor which is assumed to be 400 NM (nautical mile) long at FL350. Passing is not allowed in the corridor, and we assume that all aircrafts are flying at the centerline of the corridor. Aircraft in the corridor are responsible for self-separation. An aircraft can adjust its airspeed to maintain the target separation from its leading aircraft. **Error! Reference source not found.** shows a simple single-lane corridor.

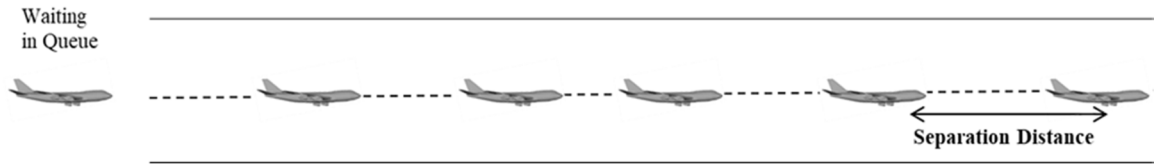

Figure 15 A single-lane corridor

In the dynamic separation concept, a dynamic separation function computes minimum separation based on a variety of parameters like atmospheric conditions and aircraft state parameters. This separation distance is updated periodically, reducing or increasing the separation distances in varying conditions. Figure 16 shows the dynamic separation concept.

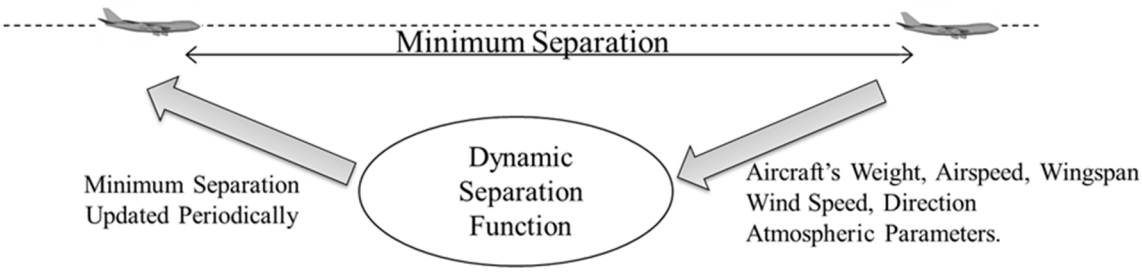

Figure 16 Concept of dynamic wake vortex separation

In our study, the proposed dynamic separation concept is more specific. The dynamic separation function is based purely on the generator aircraft's weight and airspeed. It is assumed that the trailing aircraft has access to the actual weight of the leading aircraft, meaning the maximum weight for the leading aircraft does not need to be assumed. However, the decrease in weight due to fuel burn over the length of the corridor is not considered. Furthermore, we assume that the trailing aircraft has access to the

airspeed of the leading aircraft, broadcast via ADS-B Out. The minimum required separation distance is assumed to be updated every T=5 minutes using a real time wake prediction model to adjust for changes in airspeed. Meteorological conditions such as ambient turbulence and stratification are taken into account, but they do not change during the flight in corridor. **Error! Reference source not found.** shows the dynamic separation concept proposed in this study.

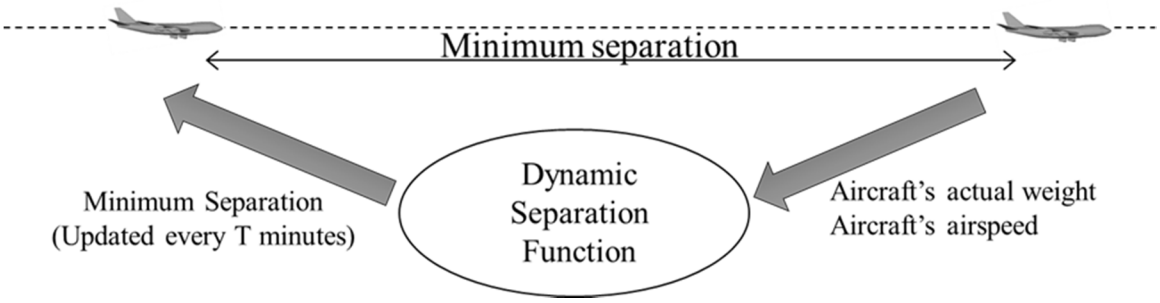

Figure 17 Proposed dynamic separation concept

We use throughput as a metric for capacity of the corridor, it is estimated using simulation for different scenarios and different policies.

$$\text{Throughput} = \frac{number\ of\ aircrafts\ which\ exit\ the\ corridor - 1}{exit\ time\ of\ the\ last\ aircraft - exit\ time\ of\ the\ first\ aircraft}$$

4.2 Methodology for Developing Simulation Model

4.2.1 Aircraft Types in Corridor

In 2017, the U.S. commercial aircraft inventory was 7,309 aircraft. The most popular aircraft were the Boeing 737-800 with 794 units (10.9% of total), the Boeing

737-700 with 585 units (8.0%), the Airbus A320 with 505 units (6.9%), the Boeing 757-200 with 456 units (6.2%) and the Bombardier CRJ200 with 393 units (5.4%) (source: Forecast International). We use these top 5 popular models to choose different fleet mixes for our simulation purposes. All of these aircraft types are narrow body jets except for the CRJ200, which is a regional jet. Table 4 summarizes the properties of these aircraft.

Table 4 Properties of aircraft in the fleet mix

Aircraft Type	MTOW (Kg)	Wingspan (m)	Wake Category	Cruise Speed (Knots)	Maximum speed (Knots)	Stall speed
B737-800	79016	34.32	D	455	470	149
B737-700	70080	34.32	D	450	470	143
A320-200	78017	35.8	D	450	470	145
B757-200	115660	38.1	C	460	495	164
CRJ200	24041	21.21	E	425	465	116.6

4.2.2 Arrival Process and Separation Laws

Aircraft arrive at the corridor according to a Poisson process. Therefore, inter-arrival times follow an exponential distribution. We allow for an immediate entrance to the corridor if an aircraft arrives at the corridor when its leading aircraft has already passed the required separation distance; otherwise, the aircraft must wait in the queue (Figure 18).

Figure 18 Different states of the corridor when an aircraft arrives

When aircraft are in corridor, they follow a set of self-separation laws. These laws are as follows:

- If an aircraft does not see any other aircraft in front of itself in the corridor, it tries to maintain its own predetermined target airspeed.
- If the aircraft's target airspeed is less than the airspeed of its leading aircraft, it tries to maintain its own predetermined target airspeed.
- If the distance between an aircraft and its leading aircraft is more than the cautionary distance (separation distance plus a buffer distance), the aircraft tries to maintain its own predetermined target speed.
- If the target speed of the trailing aircraft is greater than the airspeed of its leading aircraft and the aircraft is within the cautionary distance, the trailing aircraft tries to maintain the separation distance and to fly at the same speed as the leader.

The first three scenarios correspond to situations where an aircraft is flying independent of other aircraft in corridor, maintaining its own target speed. The last scenario is to make sure that two aircraft never get very close to each other in order to avoid wake vortex encounters. Figure 19 shows these different control laws for different separation scenarios.

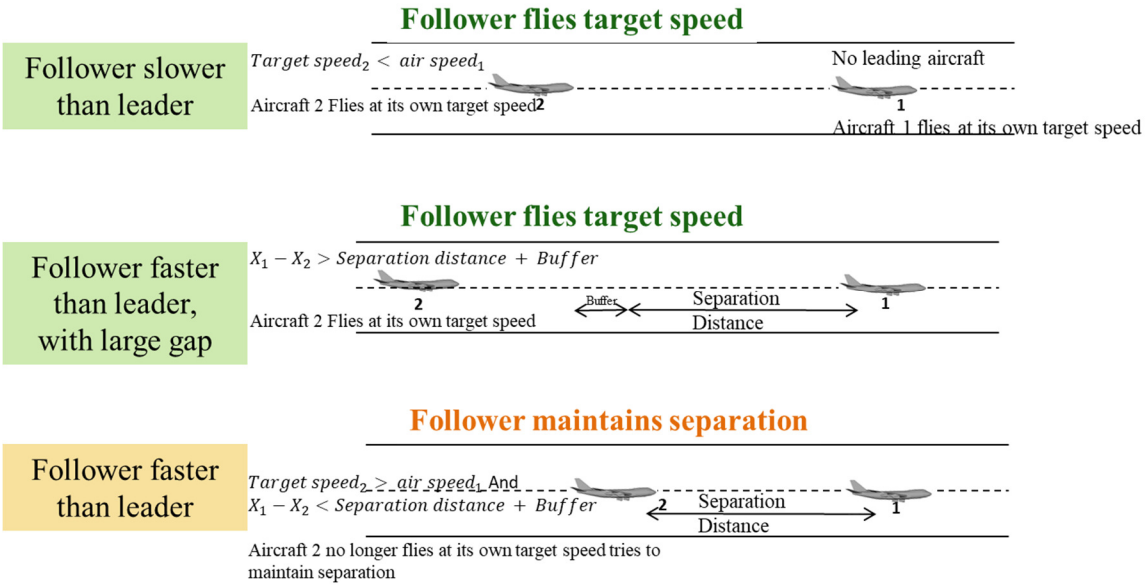

Figure 19 Different control laws for different scenarios

To simulate the trajectory of an aircraft when it is flying its own target speed, we use a mean reverting Ornstein-Uhlenbeck process to control the velocity, which is given by the following stochastic differential equation:

Equation 1 Mean reverting OU process

$$dv = -\rho(v - \mu)dt + \sigma dW_t$$

Here, v is the velocity (airspeed) of the aircraft, μ is the target velocity, ρ is the reversion rate, σ is the volatility parameter and W_t is the Wiener process (standard Brownian motion). Under this process, random perturbations occur, but the process is mean reverting, so the velocity tends to return to the preferred target average.

To simulate the self-separation operations, a proportional derivative (PD) controller is used. The controller adjusts the acceleration of the aircraft as the control

parameter to maintain the separation distance which is decided using a fast-time wake prediction model (APA) in a static or dynamic way. The following stochastic differential equation represents the PD controller:

Equation 2 PD controller

$$dv_f = k_p(x_l - D - x_f)dt + k_d(v_l - v_f)dt + \sigma_f dW_t$$

Here, x_f and v_f (x_l and v_l) are the along-track position and velocity of the following (leading) aircraft, σ_f is the volatility parameter and D is the along-track target separation.

The output acceleration from the PD controller is bounded within a certain range to match the physical constraints of the aircraft and the maximum comfortable acceleration for passengers. Lower and upper bounds for airspeed are also defined to avoid a stall and going over the maximum design speed, respectively.

If we consider only one pair of trailing aircraft, where the leader maintains its target speed and the follower maintains the separation distance via a PD controller (the output is not bounded), it can be shown that the mean and variance of the along track separation between the leading and trailing aircraft are

$$E[x_l - x_f] = D \text{ and } var[x_l - x_f] = \frac{\sigma_f^2}{2k_p k_d}$$

and the variance of the velocity of the following aircraft is:

$$var[v_f] = \frac{{\sigma_f}^2}{2k_d}$$

It should be noted that for a PD controller, the response is characterized by damping ratio (ζ) and the natural frequency (ω_n). A damping ratio greater than one means that the system gradually approaches the target, and a damping ratio less than one

means the system overshoots before returning to the target. The natural frequency specifies how quickly the system approaches the target. The control equations are given below:

Equation 2 Control equations

$$k_p = \omega_n^2$$
$$k_d = 2\zeta\omega_n$$

We can also write the variance equations as follows:

Equation 4 Variance equations

$$var[\,x_l - x_f\,] = \frac{\sigma_f^2}{4\zeta\omega_n^3}$$

$$var[\,v_f\,] = \frac{{\sigma_f}^2}{4\zeta\omega_n}$$

Using these results, the parameters k_d, k_p, (or ζ, ω_n) and σ can be chosen so that the aircraft separation and velocity have some prescribed variability.

4.2.3 Determining the Control Parameters

Error! Reference source not found. summarizes the list of parameters in the simulation which are used to model along track movements of the leading and following aircraft and their estimated values using historical data on trailing pairs of aircraft over the United States, which were obtained in the previous chapter by analyzing historical track data.

Table 5 Parameters of model estimated from historical flight data over the U.S.

Observable Parameter	Associated Model Parameters	Estimated Value
Average (target) separation distance	D	15.1 nm
Standard deviation of separation distance	$\frac{\sigma_f}{\sqrt{2k_d k_p}}$	1.1 nm
Target speed for leading aircraft	μ	436 kts
Standard deviation of speed for leading aircraft	$\sigma_l/\sqrt{2\rho}$	16 kts
Standard deviation of speed for following aircraft	$\sigma_f/\sqrt{2k_d}$	16 kts

We want to set the parameters of the controllers to get the same averages and standard deviations of trailing aircraft pairs as estimated using historical track data. For the PD controller, we have three variables and two equations, so if we set a value for the damping ratio, we can solve for the other parameters. However, this works only for one pair of trailing aircrafts. In the flow corridor model, there is additional variance in separation distance and airspeed since an aircraft can follow different control laws at different times. For example, a faster trailing aircraft that reaches the corridor late, flies for a time at its own airspeed until it reaches the cautionary distance with its leading aircraft, then it slows down and tries to maintain the separation distance, and when its leader exits the corridor, the aircraft again speeds up to its own target airspeed. This change in airspeed to close a gap adds additional variance. Updating the separation distance every few minutes is another source of variance. This is all different than the situation when there is just one pair of aircraft in the corridor and there is no change in

control laws for each aircraft, so all variance can be modeled using the noise parameters with the equations previously given.

For these reasons we cannot just solve for the gains and noise parameters in the OU process and the PD controller using the estimated values from historical track data, since, with additional sources of variance, the variance in separation distance and airspeed would be much higher than what was estimated. Experiments in which we use a modified approach to determine the gains and noise parameters are described later in this chapter.

4.2.4 APA Implementation

The APA algorithm was discussed in Chapter 2. In the corridor simulation model, we use a GMU implementation of the wake model described in the original APA paper by Robins and Delisi (2002). For an en route corridor, the wake vortices are evolving away from the ground, so we only use the equations in phase I of the APA model, where the algorithm solves a system of three ordinary differential equations using a constant time step (based on Sarpkaya, 2000). Wake vortex decay in out-of-ground effect (OEG) is mainly driven by atmospheric turbulence and stratification. So, in addition to properties of the generating aircraft, the important input parameters for APA are the Eddy Dissipation Rate (EDR) and Brunt–Väisälä Frequency (BVF) (or vertical temperature profile). Away from the ground, the vortices are transported laterally at the speed of the local crosswind, so the other model input is the vertical profile of the lateral wind. Output of the APA model is predicted position and strength of the wake vortices within a plane

perpendicular to the path of the generating aircraft at every time step. Since we do not consider the crosswind in our experiments, there is no lateral transport and we only have vertical descent of the vortices due to mutual induction.

To verify our implementation of the APA, we compared the results of our implementation with the results given by a newer version of the algorithm implemented by NASA. For a variety of meteorological conditions, the results are very close. Figure 20 shows both the output of the NASA model and GMU implementation in neutral stratification for different ambient turbulence conditions. In the case of very high ambient turbulence, the prediction for circulation decay is very close to the expected results even though the descent prediction is completely different. Figure 21 compares the outputs of two models in moderate turbulence intensity for different stratification levels. Outputs of both models are almost congruous, so we are confident in verifying our implementation.

In the flow corridor, the target separation must be greater than the minimum accepted separation distance, which is 5 nautical miles. Thus, the separation minimum is set equal to either 5 NM or the required separation determined by results of the APA model, whichever is greater.

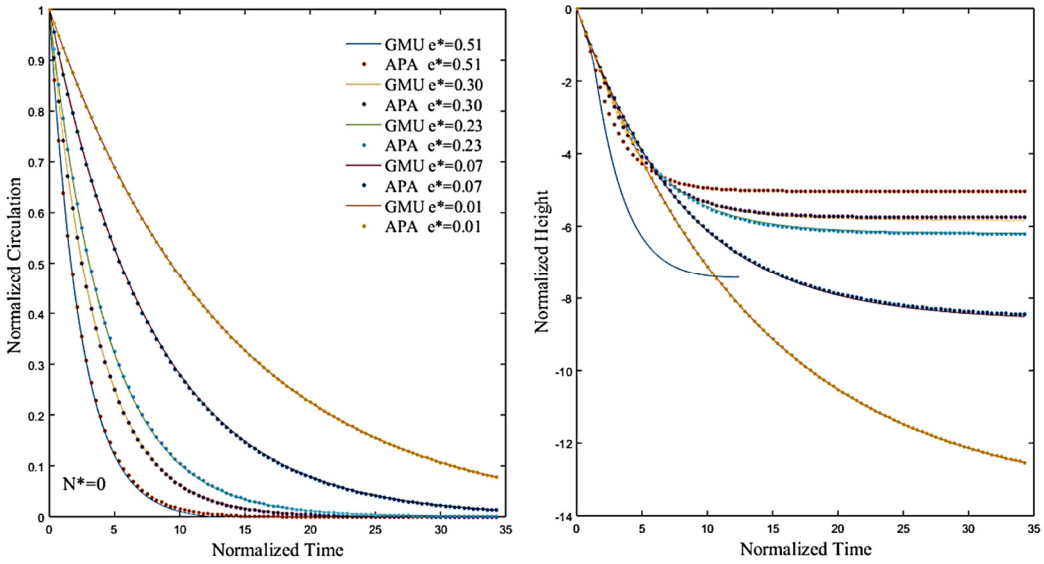

Figure 20 Comparing the outputs in neutral stratification for different turbulence intensity levels

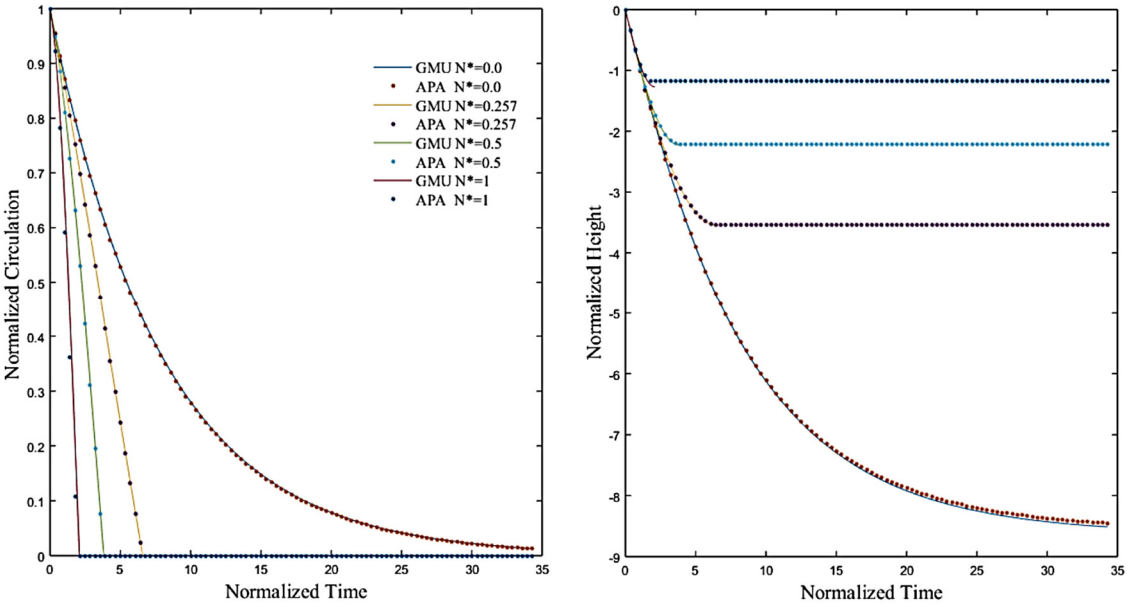

Figure 21 Comparing the outputs in moderate turbulence intensity for different stratification levels

4.2.5 Static and Dynamic Separation Scenarios

To investigate the potential capacity benefits of dynamic separation, we define the methods for setting the static separation and dynamic separation requirements.

Static separation is determined based on a "worst-case" analysis. Specifically, the static minimum separation distance is pre-determined for each pair of aircraft with atmospheric parameters set at their values in the worst-case scenario – i.e., neutral stratification (N=0) and very weak turbulence intensity level (EDR=10^{-7}). Other variable input parameters are the leading aircraft's weight and speed. The weight of the lead aircraft is selected as 90% of its MTOW to be on the conservative side, and the airspeed is set as the nominal cruise speed for each type of aircraft. The actual target speed and initial speed of all aircraft are generated from normal distributions with mean equal to the cruise speed. Also, to decide the separation distance, we need to know the maximum circulation threshold that is safe for trailing aircraft.

It is obvious that for different airspeeds and different weights of the generating aircraft we get different separation distances. However, while increasing the weight of the generating aircraft always results in a bigger required separation distance, this is not the case with increasing airspeed. Increasing the airspeed of the generating aircraft decreases the minimum required separation time (since airspeed is in the denominator of the initial circulation strength). However, this decrease does not necessarily translate to a decrease in separation distance, since with higher airspeed the aircraft might travel a greater distance in a shorter time. Also, the worst-case airspeed that gives the largest separation distance changes with weight.

This behavior is shown in Figure 22. The plots show the time and distance travelled by the generating aircraft until the vortex circulation strength decays to less than 180 m^2/s. The minimum separation time is monotonically decreasing as a function of the airspeed of the generating aircraft, but the minimum separation distance is not. Therefore, the airspeed used in the static scenario is not necessarily the airspeed that gives the largest separation. As a result, we assume that we do not have any information about the speed, so in the APA model we set the airspeed of the generating aircraft as its cruise speed.

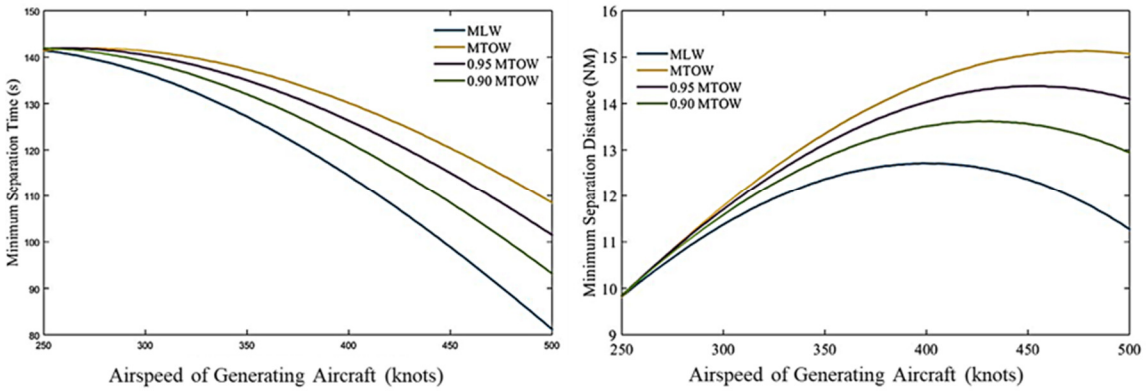

Figure 22 Separation distance and separation time for different weights and airspeeds of generating aircraft

For dynamic separation, a critical assumption is that we have information about the actual weight of the aircraft, but this information may be sensitive due to economic and political aspects. Therefore, the willingness of airlines to share this piece of information is presently very limited (Feuerle et al., 2013). So, this obstacle must be dealt with before implementing the dynamic policy in the real world. For simulation purposes,

we generate random weights from a uniform distribution for each aircraft and they are considered as actual weights of the aircraft. Lower bounds and upper bounds of these uniform distributions for each aircraft type are selected as 75% of the MTOW and 95% of MTOW. Similar to the static case, the target and initial airspeed for each aircraft are generated randomly from normal distributions with mean equal to the nominal cruise speed of the aircraft. The difference is that in the separation function for the dynamic case, the input speed is the actual speed of the aircraft at each time step, versus a fixed value in the static case.

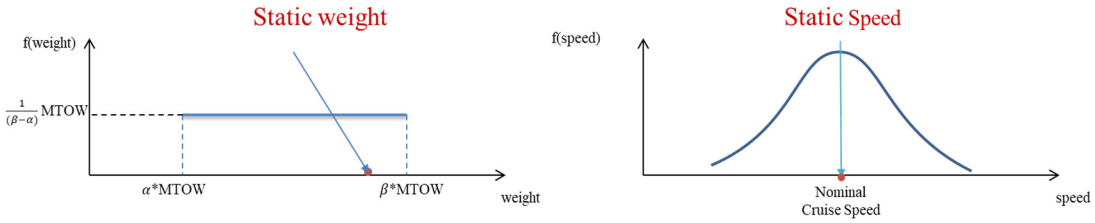

Figure 23 Probability distribution function for weight and speed of aircraft in dynamic separation

The outputs of APA model are used to decide the separation distance. For each following aircraft, a maximum tolerable circulation threshold is defined based on its weight category. The time that it takes for the wake vortices of the generating aircraft to get weaker than this threshold is extracted from APA output. Then the separation distance is calculated by multiplying this time by the airspeed of the generating aircraft.

4.2.6 Summary of Parameters in Simulation Model

The parameters in the simulation model can be put in 6 categories:

- Separation policy: static or dynamic policy, minimum accepted separation distance.
- Atmospheric parameters: air density, EDR, BVF.
- Fleet mix: types and percentage of aircraft in fleet.
- Control parameters: proportional gain, derivative gain, and noise.
- Distributions: selected distributions for weight and speed and their respective parameters (range, mean, variance).
- Arrival process: selected process and its parameters for aircraft arrivals.

4.3 Experiments and Results

4.3.1 Selecting the Parameters of the Control Model

Experiments are designed to investigate how changes in input parameters impact the throughput of the corridor. The first step is adjusting the gains and volatility parameters in the PD controller in a way that the distributions for the average separation distance, standard deviation of separation, and standard deviation of aircraft speed in the flow corridor match the results from analyzing historical track data.

The first method is setting the volatility parameter for aircraft dynamic systems model equal to zero (i.e., set $\sigma_f = 0$ in equation 2). In this method, the proportional and derivative gains and volatility parameters are determined by selecting a value for the damping ratio ($\zeta = 1.5$) and solving for σ_f and ω_n using parameters estimated from historical data (Equation 4). Then we set the volatility parameter to zero. In this scenario,

when an aircraft reaches the desired separation and airspeed, it maintains the speed and distance with zero variance.

We run the simulation with a fleet mix that consists of 3 types of aircraft in the large category (B737-800, B737-700, A320) and with the dynamic separation scenario based on airspeed. Figure 24 shows the distributions for average separation distance, standard deviation of distance and standard deviation of airspeed. The distributions are similar to the results from analyzing historical data. However, the average standard deviation of separation distance is smaller, and the average standard deviation of speed is higher than the estimated values from historical data. Therefore, we try other methods to see if we can get distributions that are closer to what we got from analyzing track data.

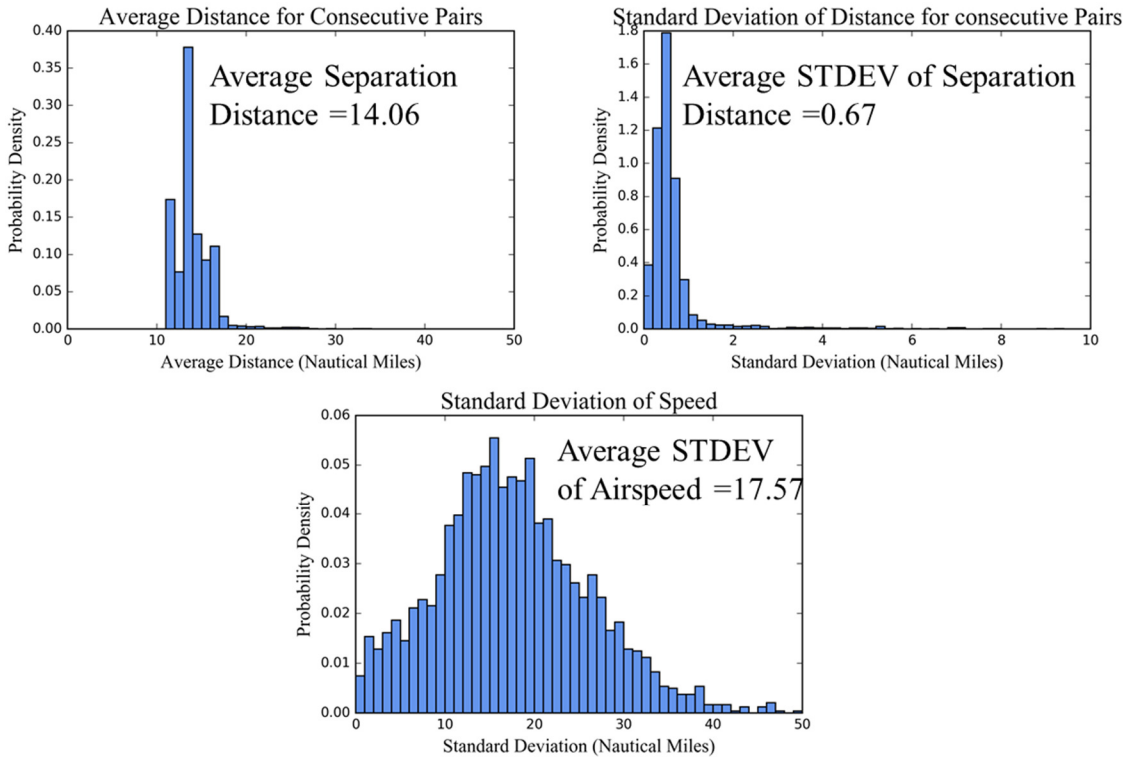

Figure 24 Distributions for trailing pairs, obtained from flight track simulation in the flow corridor model (parameters tuned via first method)

In the second attempt to tune our parameters, we look at the left-hand tail of the fitted distributions of standard deviation of distance and standard deviation of airspeed. Specifically, we look at their 5-percentile value. These numbers are associated with pairs of aircraft with minimum variance in their separation distance and airspeed – i.e., pairs in which the trailing aircraft tries to maintain the target separation that is already achieved, so there is not much variance in airspeed of the lead-follow pair. The 5-percentile values for standard deviation of distance and standard deviation of airspeed are 0.07 NM and 2.52 knots respectively. To solve for the volatility parameter, natural frequency, and damping ratio, we set the damping ratio as before to be consistent with previous

experiments. Lesser variances for separation distance and velocity (0.07 NM and 2.52 kts instead of 1.1 NM and 16 kts) mean that the PD controller has a quicker response and a higher natural frequency. Figure 25 shows the related histograms for pairs of trailing aircraft in the corridor.

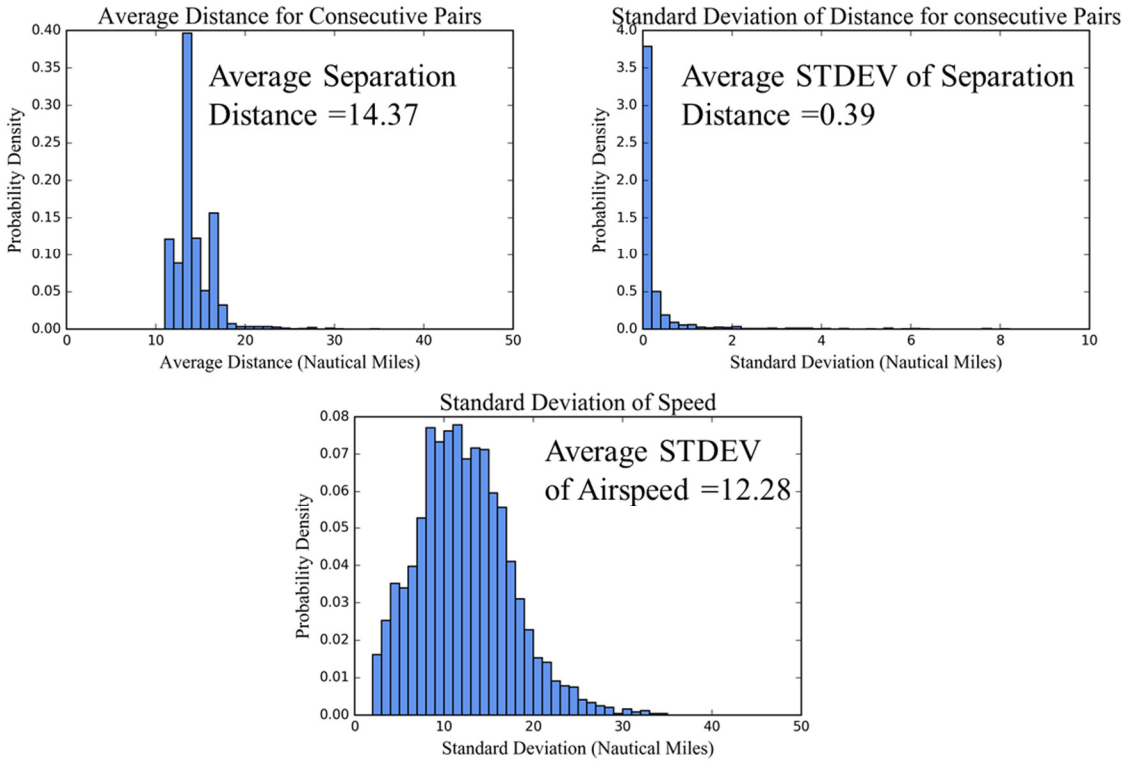

Figure 25 Distributions for trailing pairs, obtained from flight track simulation in the flow corridor model (parameters tuned via second method)

There is also another choice to remove the PD controller all together. In this approach, an aircraft changes its airspeed immediately when needed. For example, if the aircraft has a higher target airspeed than its leader, it flies its own target speed until it reaches the separation distance and then instantaneously changes its airspeed to that of

the leader so that the prescribed separation can be maintained. Figure 26 shows the related histograms for pairs of trailing aircraft in the corridor using this method. This is a baseline that shows what would happen if the aircraft could adjust speeds on the spot without any limits on maximum acceleration or deceleration.

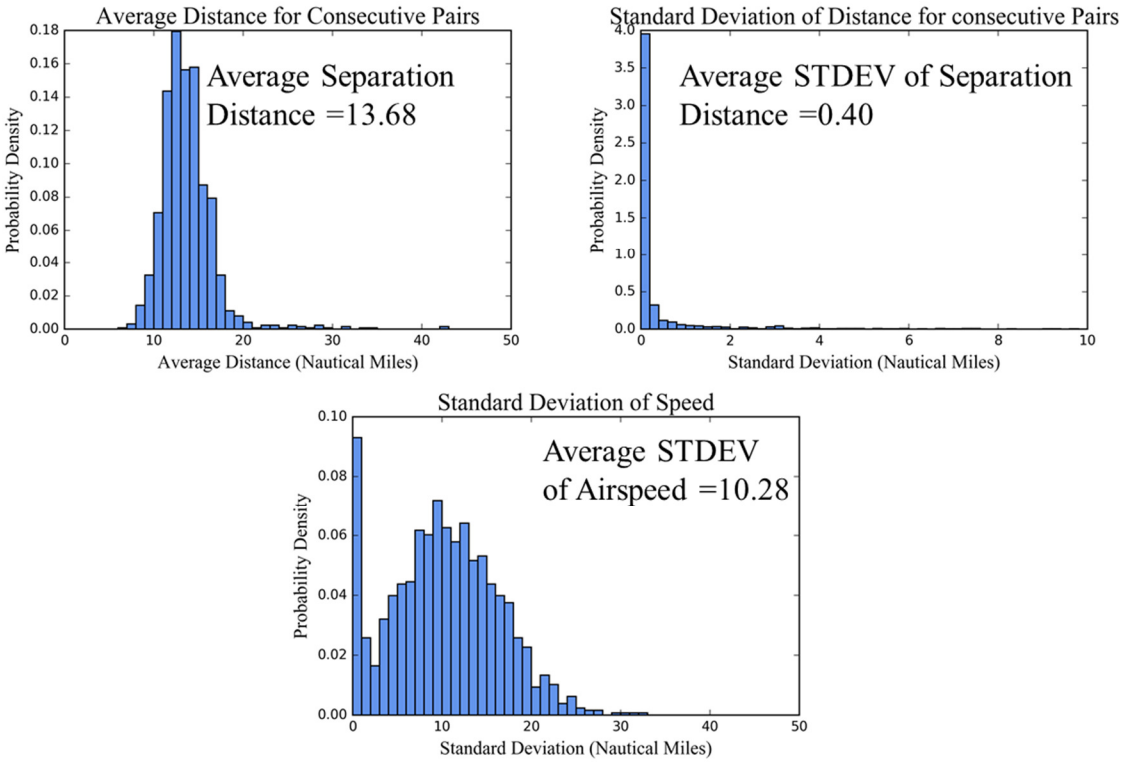

Figure 26 Distributions for trailing pairs, obtained from flight track simulation in the flow corridor model (instant adjustment of speed method)

None of the methods gave us completely similar distributions to the distributions obtained from historical data, but after comparing the histograms in figures 24, 25 and 26 with historical distributions in Figures 9, 10 and 13, we select the first method to tune parameters of our PD controller and the rest of the experiments are performed with this

set of parameters, unless mentioned otherwise. This translates to having perfect controllers, so sources of variance in separation distance and velocity are intrinsic features of the flow corridor like changes in target airspeed or target separation distance.

4.3.2 Sensitivity Analysis: Arrival Rate

The first set of experiments examines the effects of the arrival rate. Figure 27 shows results for two different fleet mixes and two different separation policies. In the uniform fleet mix, all aircraft are B737-800, and in the mixed fleet, all five types of aircraft in Table 4 appear with equal probability. All simulations are conducted under the assumption of neutral stratification and very weak turbulence intensity.

As expected, throughput increases as the arrival rate increases for both policies and fleet mixes. At some point, the corridor becomes saturated and it is not possible to increase throughput anymore by increasing the arrival rate. This maximum throughput approximates the corridor capacity. With both fleet mixes, the dynamic separation gives a higher throughput than the static separation. The increase in throughput for the mixed fleet is about 18% while the increase for a uniform fleet is about 6%. With a mixed fleet, faster aircraft tend to fly slower than their nominal cruise speed when they are flying behind a small aircraft. Because of the higher variability in airspeeds, the separation reduction achieved by employing a dynamic separation policy results in relatively higher capacity benefits for a mixed fleet.

Comparing fleet mixes, a uniform fleet has a higher maximum throughput than the mixed fleet because all the aircraft are traveling at similar speeds. In the mixed fleet,

the CRJ200 has a smaller nominal cruise speed which tends to slow down the aircraft behind it (since no passing is allowed in the single corridor).

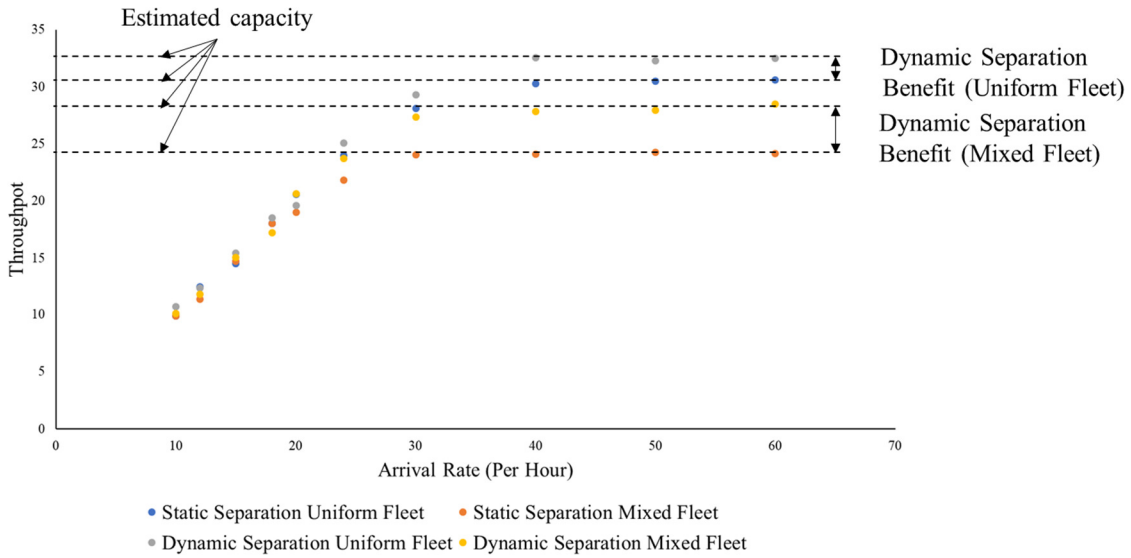

Figure 27 Throughput vs arrival rate for different policies and fleet mixes

4.3.3 Sensitivity Analysis: Separation Policy

As observed from the previous experiment, employment of a dynamic separation policy increases the capacity of the corridor. Two factors differentiate the dynamic policy from the static policy – variable weight of each aircraft and variable airspeed of each leading aircraft. To see which of these factors contributes most to increasing the capacity, we test three versions of the dynamic policy:

- One in which the weights are known, while the airspeed of the leading aircraft is unknown and is assumed as a typical cruise speed for the associated type of aircraft.

- One in which the airspeeds are known in real time. Aircraft weights are constant and assumed to be 0.9 * MTOW for the associated type of aircraft. The minimum separation distance is updated every 5 minutes to account for changes in speed.
- One in which both weights and airspeeds are known.

First, we test the four policies with a fleet mix with all 5 types of aircraft. The results are shown in Figure 28.

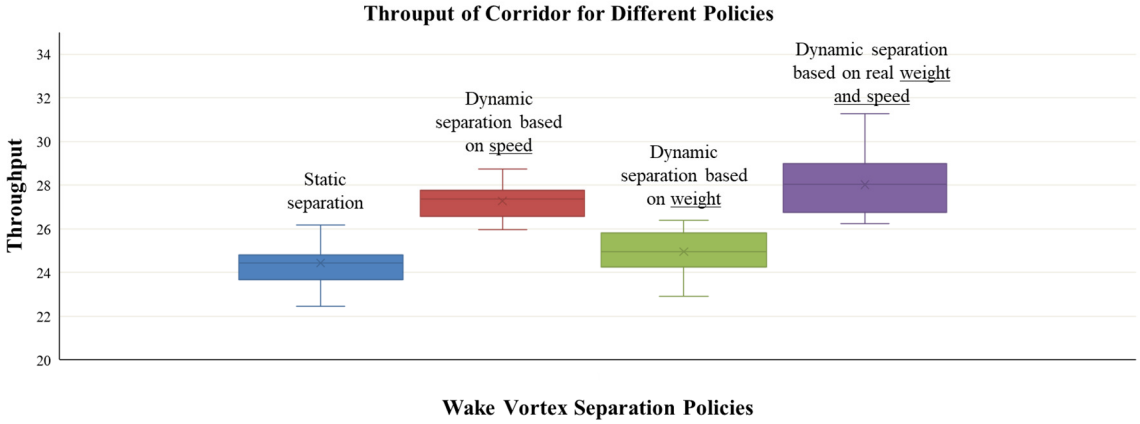

Figure 28 Flow corridor capacity with different separation policies for a mixed fleet with 5 type of aircraft

The dynamic separation policy increases the throughput of the corridor in comparison with a static separation policy. Using a two sample t-test we get a p-value less than 10^{-10} which confirms a statistically significant difference between the two policies. For this fleet mix, the speed-based policy works better. This can be explained by the fact that with the introduction of the slower aircraft, many aircraft fly with airspeeds

slower than their nominal cruise speed, so the weight-based policy that uses the nominal cruise speeds to determine the required separation gives more conservative separations.

We also run this experiment with a more homogenous fleet consisting of the first four aircraft in Table 4. Results are shown in Figure 29. This time, the weight-based separation policy works better than the speed-based policy. These experiments show that, based on the fleet mix, different factors might be important in increasing the flow corridor capacity.

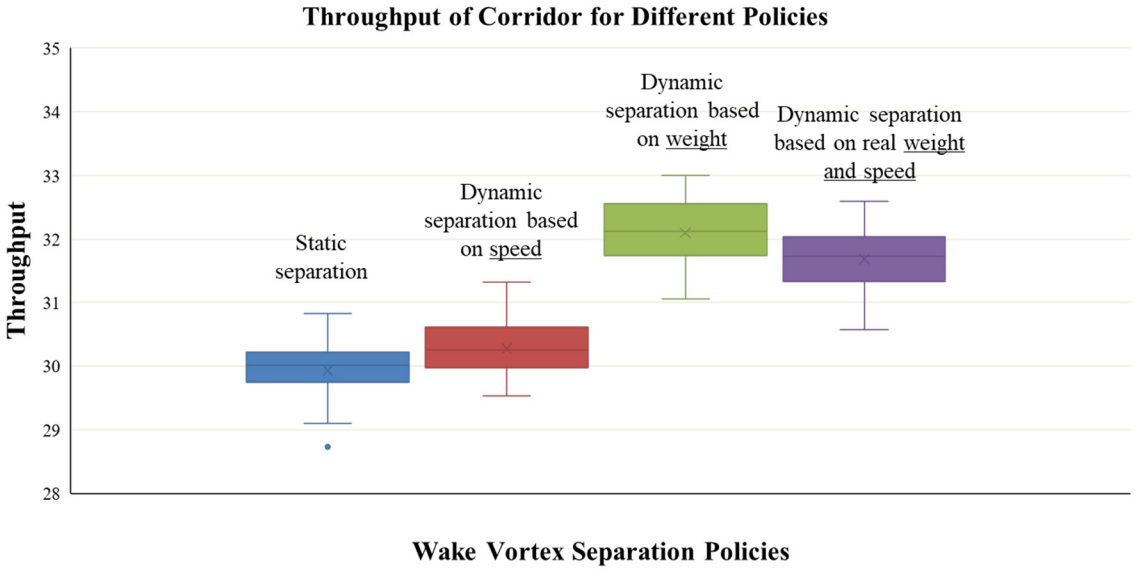

Figure 29 Flow corridor capacity with different separation policies for a mixed fleet with 4 type of aircraft

Another simulation parameter regarding the separation policy is the minimum acceptable separation distance. In all previous experiments, this minimum was set at 5 nautical miles. A set of experiments with a reduced minimum separation was done in which the new minimum was set at 3 nautical miles. Experiments show that at low

turbulence intensity levels, increases in throughput are negligible, since the separation distance calculated for aircraft via the APA model is almost always greater than the minimum separation. However, at higher ambient turbulence, this reduction results in a significant increase in throughput, because vortices decay faster so the determining factor in separation distance is the minimum separation distance.

4.3.4 Sensitivity Analysis: Meteorological Conditions

The following experiments explore the impact of ambient turbulence on throughput for different fleet mixes using a dynamic separation policy. Results are shown in Figure 30. An increase in the ambient turbulence results in faster decay of vortices and smaller separation distances, hence an increase in the throughput of the system. The maximum possible throughput happens when all separation distances are equal to the minimum separation distance, which is selected as 5 nautical miles. In general, a uniform fleet leads to higher throughput for the corridor independent of ambient turbulence or the type of control law that we use. With increasing ambient turbulence, we see an increase in throughput; for the uniform fleet we get to the maximum throughput with lower ambient turbulence in comparison with mixed fleets for which higher levels of ambient turbulence are needed to reduce the separation distances, since smaller aircraft in the mix are more susceptible to wake vortices.

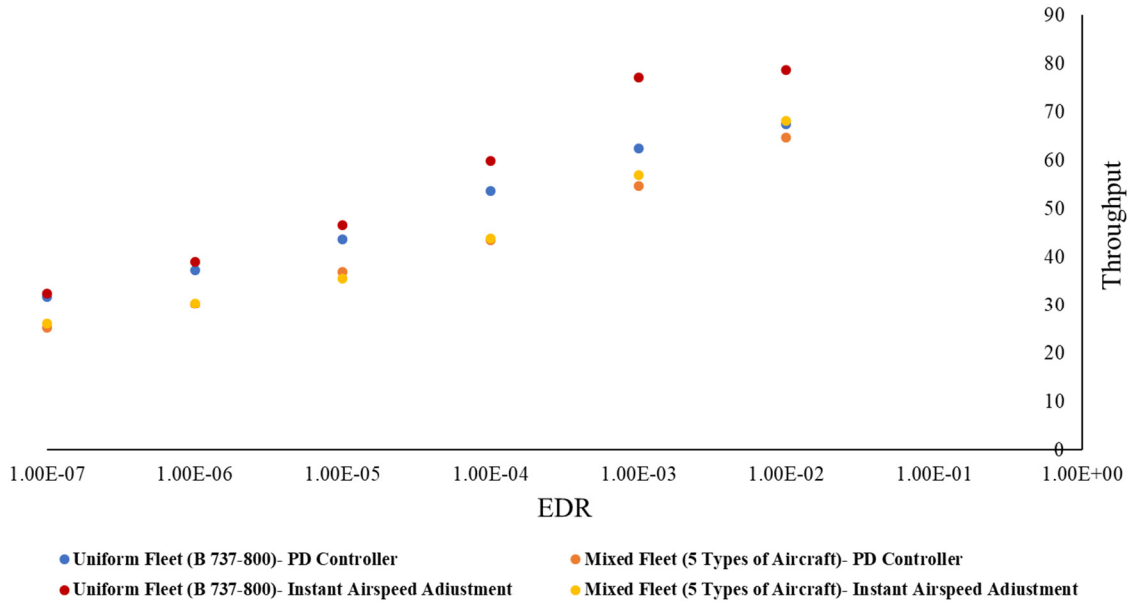

Figure 30 Throughput vs ambient turbulence for different fleet mixes

The effect of the control law is negligible for lower ambient turbulences, when aircraft are spaced out in the corridor. However, in higher levels of ambient turbulence, when separation distances decrease and aircraft are flying closer to each other, we see higher path delays for the PD controller and consequently lower throughput. This happens because a small reduction in the speed of the leading aircraft leads to a bigger reaction in the following aircraft and more reduction in its airspeed. When there is a chain of leaders and followers, this can add up and bring aircraft at the back of the chain to their minimum allowable speeds in the simulation. This is similar to traffic jam phenomena for vehicles in a highway. When aircraft are further apart, they recover faster from this chain reaction. Figure 31 shows the airspeed plot of 10 consecutive aircraft in the corridor for low and high ambient turbulence. When the average separation distance is about 13 NM the aircraft recover from this slow down effect in shorter time in

comparison with the case when the aircraft are closer to each other. Also, the decrease in airspeed is smaller when aircraft are spaced out.

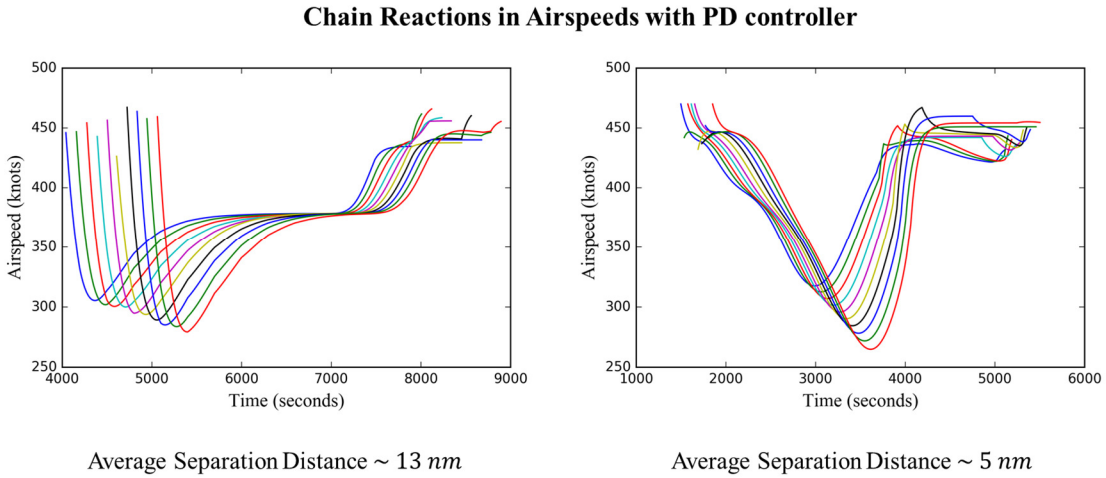

Figure 31 Chain reactions in airspeed of aircraft in corridor

Figure 32 shows the effect of different stratification conditions on throughput for different fleet mixes. More stable stratification results in faster decay and smaller separation distances, resulting in an increase in the throughput of the system. For both conditions of high stratification and very strong turbulence, the throughput of the system is almost the same. Both conditions lead to the fast decay of wake vortices, which in turn leads to separation minima from the APA model that are smaller than the required 5 NM separation distance, so all separation minima are set to this 5 NM requirement.

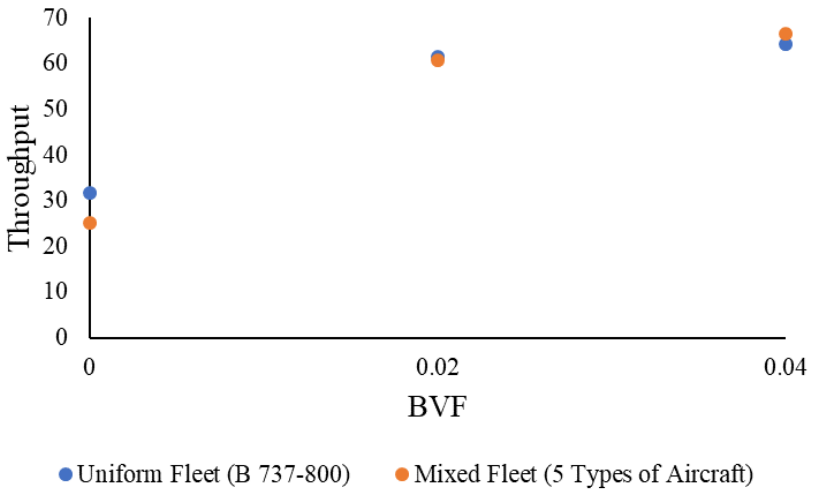

Figure 32 Throughput vs stratification for different fleet mixes

Here, we again see the problem of slow down using a PD controller in the simulation when aircraft fly closer to each other. If we use the control model with instant adjustment of speed, the throughput of the system increases to about 75 aircraft per hour in comparison to about 66 with the PD controller. The gains of this PD controller model were selected to reflect the distributions from the historical data analysis, however, using a controller with smaller time constant leads to higher throughputs.

These sensitivity analyses show that assuming worst-case meteorological conditions to determine static separation requirements seriously impacts the capacity of the flow corridor. With more aircraft equipped to sensors and data about surrounding meteorological conditions, using a dynamic separation policy can significantly increase the capacity of the flow corridor.

4.3.5 Sensitivity Analysis: Noise in Flight Track Data

Previously, we adjusted the gains and volatility parameters in the PD controller in a way that the distributions for the average separation distance, standard deviation of separation, and standard deviation of aircraft speed in the flow corridor match the results from analyzing historical track data. However, the historical track data that we used is noisy and should be smoothed using a smoothing method such as moving average. Figure 33 shows a sample unfiltered plot of separation distance as a function of time for a pair of trailing aircraft and the corresponding ground speed vs time for both aircraft.

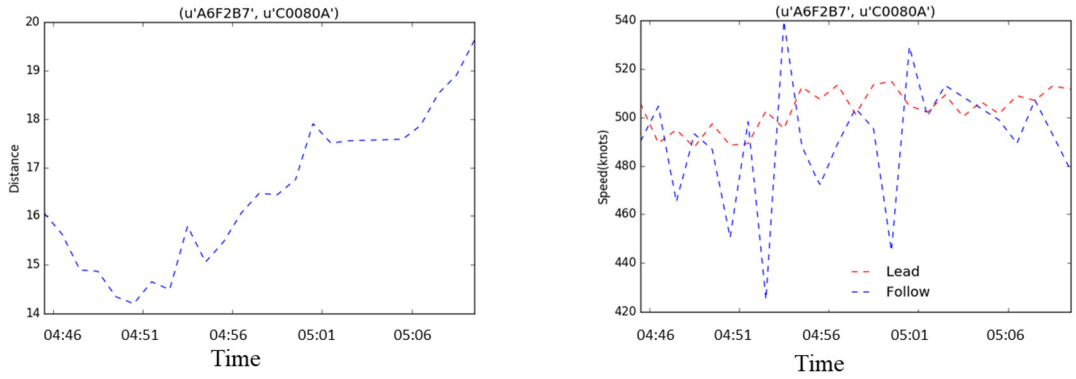

Figure 33 An example of plots from unfiltered distance and speed data

Figure 34 shows the same plots when we use a 10-minute exponential moving average. It is clear that using a moving average decreases the volatility of separation distance and speed. For this specific pair, the average separation distance using exponential moving average

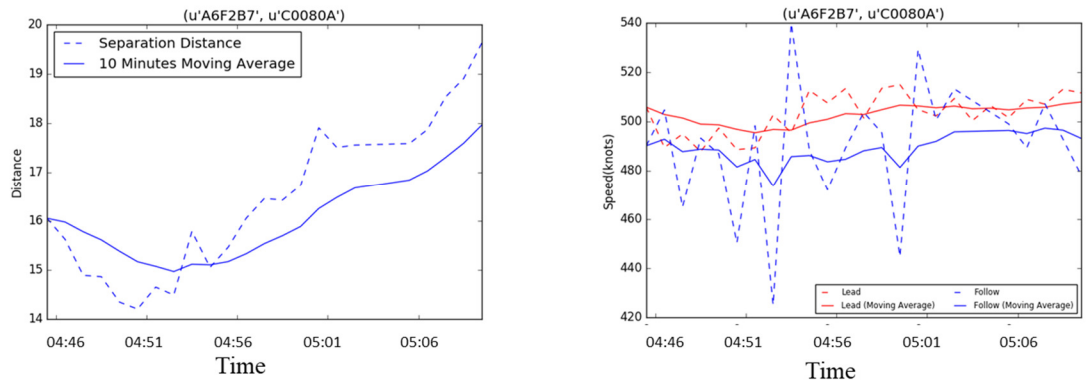

Figure 34 An example of plots from filtered distance and speed data using moving average

To investigate how filtering the noise of historical track data would change our results, we calculate the gains and volatility parameters of PD controller using the new histograms we get from filtered data for the average separation distance, standard deviation of separation, and standard deviation of aircraft speed. Figure 35 shows the throughput of the corridor for different separation policies in a corridor with 5 types of aircraft using these new parameters.

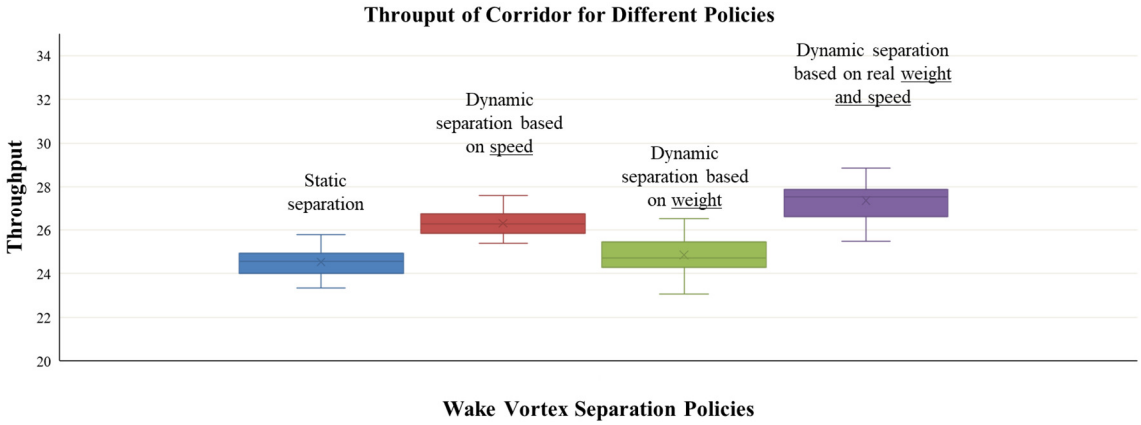

Figure 35 Flow corridor capacity with different separation policies for a mixed fleet with 5 type of aircraft (flow corridor parameters are estimated using filtered data)

This is very similar to results from the actual data. Using the moving average filter does not change the average separation. It reduces the average standard deviation of distance and also reduces the average standard deviation of speed. However, in the end the results are not significantly different from results using unfiltered data for different policies.

4.4 Conclusions

These experiments confirm that in many meteorological conditions, using dynamic separation instead of static separation can increase the throughput noticeably. Knowing the real weight of aircraft and calculating the separation distance based on actual weight of the aircraft can also lead to increased capacity of the flow corridor. The fleet mix is also a key factor in determining the capacity of the flow corridor. A uniform fleet, where all aircraft are the same wake turbulence category, increases the capacity of the corridor. In future work, an expanded corridor model should be studied that would allow for multiple lanes, lane changing maneuvers and passing of aircraft with higher velocities.

The next step is studying the safety of the dynamic separation procedures in corridors (using rare event simulation method) via analysis of the likelihood of potential wake encounters in the corridor.

CHAPTER 5: RARE EVENT SIMULATION FOR POTENTIAL WAKE ENCOUNTERS

The previous chapter investigated potential capacity benefits that can be achieved in the flow corridor using a dynamic wake separation policy. This chapter investigates the safety of the corridor with respect to wake encounter risk.

The risk of wake vortex encounters has been studied extensively in the terminal area during take-off and landing. Fewer studies have focused on wakes at cruise altitudes. One approach is to combine track data, which can either be historical surveillance data or synthesized tracks generated from a computer simulation, and a model of wake vortex behavior, such as the model from Robins and Delisi (2002). Hoogstraten et al. (2015) developed a simulation framework using recorded track data and a wake simulation model to analyze the risk of wake turbulence in upper airspace. Results include estimating the probability of encounter, determining the main factors contributing to risk and recommending mitigating measures. It was found that encounter geometry is an important contributing factor after weight, and most encounters happen when one or both aircraft are climbing or descending. Nelson (2006) reviewed several studies related to en-route wakes and argued that en-route encounters are likely to increase over time with increasing disparity in aircraft sizes (e.g., super heavy aircraft which generate powerful wakes sharing airspace with very light jets which are more susceptible to wakes).

This chapter explores the performance of a rare event simulation technique in the context of estimating probabilities of potential wake encounters for pairs of trailing aircraft. The ultimate purpose is to evaluate the safety of flow corridors regarding wake encounters. To achieve this goal, we look at the wake encounter probability for a single pair of trailing aircraft. This is done using a rare-event splitting method, for which we identify good strategies for applying the method to the problem of estimating wake encounter probabilities. Suggestions for the choice of the level function and the locations of levels are given. The model is run using distributions obtained using the historical track data. A sensitivity analysis shows the relative importance of various input parameters in the model. Finally, we use the results to provide arguments for safety of the whole corridor.

5.1 Methodology for Corridor Wake Safety Analysis

In this work, aircrafts are modeled as point masses, where aircraft states include the along-track position, along-track airspeed, across-track position, and altitude. We consider the acceleration of each aircraft as the control parameter in the along-track dimension. Movements of the aircraft in all three dimensions are assumed to be independent from each other. An example of a more complex model with six coupled state variables, derived from basic aerodynamic principles, is given in Glover and Lygeros (2004).

5.1.1 Along-Track Movements

The model simulates two aircraft – a leading aircraft and a trailing aircraft. Different control laws govern the along-track movements of the two aircraft. The leading aircraft tries to maintain a preferred target speed without considering the position or the speed of the trailing aircraft. Conversely, the trailing aircraft adjusts its velocity to maintain a target separation from the leading aircraft using a proportional-derivative (PD) controller. To model the along-track movement of the leading aircraft, we adopt the Ornstein-Uhlenbeck (OU) process to control the velocity, which is the same as equation 1 in the previous chapter:

$$dv_l = -\rho(v_l - \mu)dt + \sigma dW_t$$

Here, v_l is the velocity (airspeed) of the leading aircraft, μ is the target velocity, ρ is the reversion rate, σ is the volatility parameter and W_t is the Wiener process (standard Brownian motion). It can be shown that, in steady state, the velocity has a normal distribution with mean μ and variance $\sigma^2/2\rho$. The reversion rate and volatility parameter can be chosen so that the velocity stays in a desired interval around the target velocity with some specified probability.

For the following aircraft, a PD controller, similar to the one employed in the flow corridor, is used to make the trailing aircraft track the leading aircraft as the reference point. The trailing aircraft tries to maintain a desired along-track separation D and to fly at the same speed as the leader. We use a similar stochastic differential equation to model the PD controller:

$$dv_f = k_p(x_l - D - x_f)dt + k_d(v_l - v_f)dt + \sigma dW_t$$

Here, x_f and v_f (x_l and v_l) are the along-track position and velocity of the following (leading) aircraft, and D is the desired along track separation.

5.1.2 Vertical Movements

For the vertical dimension, each aircraft tries to maintain a target altitude. A similar mean reverting OU process, with parameters μ_z, ρ_z and σ_z, is used to model vertical position. The parameters are chosen so that aircraft altitudes have some chosen standard deviation. The previous model for capacity of the corridor did not consider altitude changes, but it is important to model the vertical movements for safety analysis. Figure 36 shows a sample path of vertical movements of an aircraft. The axes are not to scale, and the actual motion would be represented as a smoother curve.

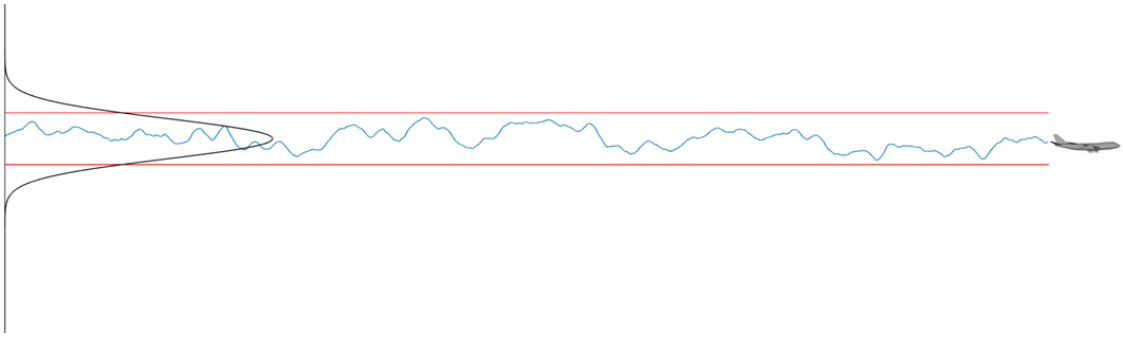

Figure 36 Sample path for vertical trajectory of an aircraft (axes not to scale).

For two aircraft in trail, both z_l and z_f (the altitudes of the leading and trailing aircraft) have normal distributions with mean μ_z and variance $\sigma_z^2/2\rho_z$ so the relative vertical position of the trailing aircraft to the leading aircraft $z_l - z_f$ has a normal distribution with mean zero and variance σ_z^2/ρ_z, since the vertical movements of the

aircraft are assumed to be independent. Figure 37 shows a snapshot of the steady-state relative position of two aircraft in the along-track and vertical dimensions. The figure is obtained by simulating trajectories of 50,000 pairs of aircraft, according to the previously described control laws for 30 simulated minutes, and recording their relative position at the end of the simulation.

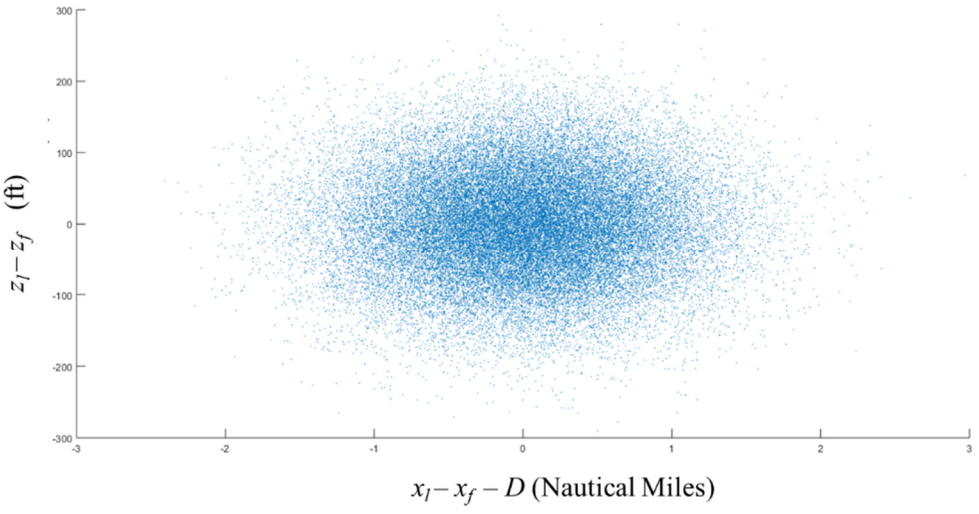

Figure 37 Snapshot of relative location of aircrafts in steady state

Figure 38 shows normalized histograms for the along track and vertical distances of the aircraft in steady state. The fitted probability density function matches the theoretical probability density function.

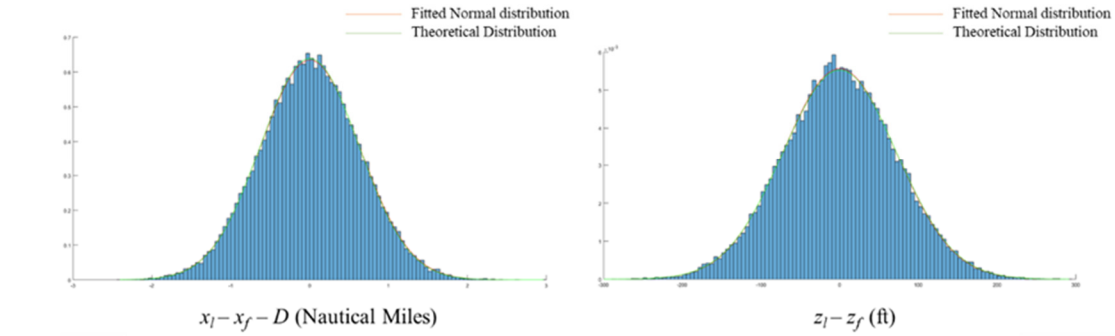

Figure 38 Histograms for relative positions (along track and vertical) in steady state

5.1.3 Lateral Movements

Similar to the vertical dimension, we use a mean reverting OU process for modeling the lateral motion of aircraft. This dimension is treated independently of the other two dimensions. The parameters of the process are chosen in a way such that specified navigation performance targets are met (e.g., the aircraft remains within a certain distance of the centerline 95% of the time).

5.2 Modelling the Wake Vortex Region

Wake vortex behavior can be quite complex. Factors affecting the wake behavior include the weight, air speed, wing shape and wingspan of the generating aircraft as well as meteorological conditions such as air density, wind speed, wind direction, turbulence, and temperature stratification. A variety of models have been developed in the literature to capture this behavior (e.g., Robins and Delisi 2002). Many of these models involve numerically solving a set of differential equations. One challenge is that embedding these models into a simulation requires resolving the system of differential equations at every time step for every active aircraft in the simulation. This is because each new time step

results in a new set of initial conditions and a new "starting point" for the wake of each aircraft. An aircraft may change altitude, heading, or airspeed at each time step resulting in new initial conditions for the wake.

This chapter demonstrates a proof-of-concept for the rare event splitting method in estimating the probability of potential wake vortex encounters for a single pair of trailing aircraft. The results are used to argue the safety of the flow corridors regarding wake vortex risk. Since the focus of this chapter is on implementation of the rare event simulation methodology, the wake model is simplified as much as possible. This characterization allows us to focus tests on basic properties of the splitting methodology. Future work can embed the more complicated models into this framework.

We first consider a two-dimensional model in which only along-track and vertical movements are considered (lateral movement is ignored). Wang and Shortle (2012) have shown via sensitivity analysis that the variability parameters in these two dimensions are key parameters in terms of reducing encounters. Figure 39 shows a high-level geometric model of the wake region, characterized by a triangle in two dimensions. The dimensions of the region – namely the length of the wake region, the minimum predicted descent, and the maximum predicted descent – may be different for different aircraft with different velocities at varying meteorological conditions. The region does not predict the exact position of the wake, but rather defines an area that is likely to contain the wake. So, if another aircraft enters the triangle, it may or may not hit the wake. We refer to these events as potential wake encounters.

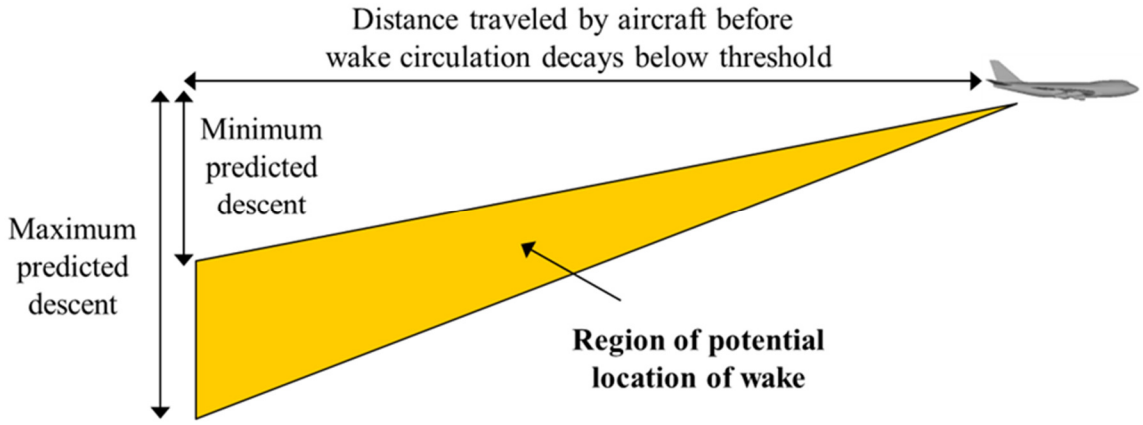

Figure 39 Wake region behind the leading aircraft in two-dimensional model

In the three-dimensional model we allow for lateral movement. In higher altitudes, the vortices remain spaced slightly less than a wingspan apart, drifting with the crosswind. To take into account the possible lateral drift of the wake vortices, the 3D model is a polyhedron in shape of a wedge which is shown from different views in Figure 40. The maximum lateral drift is an input for the model. The symmetry of the model assumes that the crosswind is unknown with a maximum value and equal uncertainty in either direction.

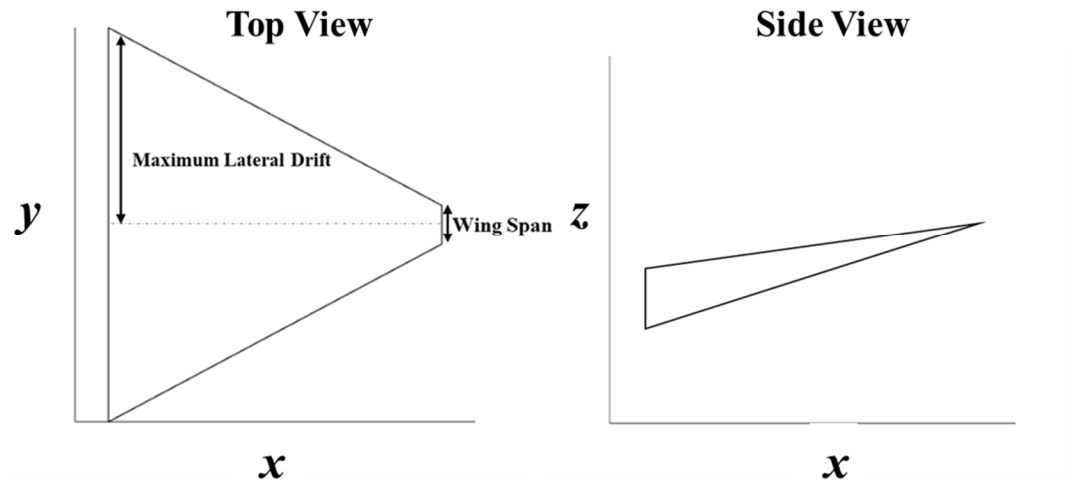

Figure 40 Wake region behind the leading aircraft in 3D model

5.3 Splitting Methodology

For a pair of trailing aircraft that are trying to maintain their separation distance and altitude, the rare event of a potential wake encounter happens when the following aircraft gradually deviates from its trajectory (safe state) and enters the potential wake region of the generating aircraft (rare event). We define our problem similar to the basic setting of splitting problems in the literature. We have a stochastic process $X \equiv \{X_t, t \geq 0\}$ with state space χ, where X_t is a strong Markov process. In our case, X_t consists of the positions and airspeeds of each aircraft (see state variables defined in the previous section). We define two disjoint subsets of χ, S and W, where W is the rare event set and S is a set of "safe" states considered as initial conditions to the simulation. In our case, the rare event set W is the wake region. The set S is defined as a region that is behind and above the leading aircraft (Figure 41), where the lower right corner of the region is the target location of the trailing aircraft.

The process starts at some state on the boundary of the safe set. It then leaves S and either eventually returns to S or reaches W. The goal is to estimate the probability γ that a trailing aircraft enters W prior to returning to S, starting from a point on the boundary of S. Since the process tends to revert to the lower right-hand corner of S, the termination time of the simulation is not an issue. The rare event probability is:

$$\gamma = \Pr\{X(t) \text{ reaches wake region before returning to safe region} \mid \text{trailing aircraft has just left safe region}\}.$$

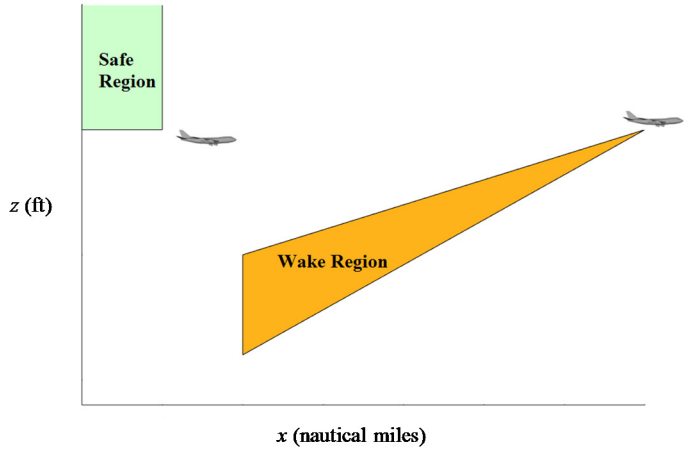

Figure 41 Side view of the wake region behind the leading aircraft

To implement splitting, a set of intermediate level sets must be defined (as an example, see Figure 21). The simulation splits whenever it gets to a new level. We define a sequence of m levels $\{l_0, l_1, l_2, \ldots, l_m\}$ such that l_0 is the boundary of S and l_m is the boundary of W. Let D_k be the event that the trailing aircraft crosses level l_k before returning to the safe state. Let $p_1 = \Pr\{D_1\}$ and $p_k = \Pr\{D_k \mid D_{k\text{-}1}\}$ for $k = 2, \ldots, m$. That is, p_k is the probability of crossing level k given that level k-1 has been crossed. Since $D_M \subset D_{M-1} \subset \cdots \subset D_1$, the probability of reaching the rare event before returning to the safe state is $\gamma = \Pr\{D_m\} = \Pr\{D_1\}\Pr\{D_2|D_1\} \ldots \Pr\{D_m|D_{m\text{-}1}\} = p_1 p_2 \ldots p_m$.

We use a fixed effort splitting method, where the number n of simulation runs from each stage are fixed and pre-selected. In the first stage, we start n independent runs from the initial states (i.e., the boundary of the safe set), where the initial states are randomly generated based on the steady state probability distribution for the relative

position of the trailing aircraft. At time zero, the leading aircraft is assumed to be at a fixed point. At each time step we update the position and velocity of both aircraft and continue until the relative position reaches level 1 or returns to the safe set. If the run reaches level 1, the simulation is stopped, and the end state is saved in a set called L_1. Let R_1 be the number of runs reaching the first level. The probability of reaching level 1 is estimated as $\widehat{p_1} = R_1/n$. In stage $k \geq 2$, the initial states are generated by randomly sampling n states with replacement from the set L_{k-1}. Each run is simulated independently until it reaches level k or goes back to level k-2, in which case the run is truncated. This is done to reduce time simulating trajectories back to the safe set.

In doing this truncation, we have to correct the bias. This is done as follows. For each stage k, we randomly sample r_k chains from all the killed chains in the stage, where r_k is a pre-selected integer. For these selected chains, we continue simulating them until they return to the safe set or reach level k. Every chain that reaches level k gets a weight $W_k = M_k / r_k$, where M_k is the number of killed chains in that stage. For example, if we have $M_k = 100$ killed chains and we select $r_k = 5$ of these to simulate to completion, then each of these is representative of 100/5 = 20 killed chains. Therefore, if a sampled chain reaches level k, it is cloned to $\lfloor W_k \rfloor + 1$ or $\lfloor W_k \rfloor$ copies (since the number of copies must be an integer), with probabilities $\delta = W_k - \lfloor W_k \rfloor$ and $1 - \delta$ respectively. For $k > 2$, the probability of reaching level k form level k-1 is estimated as $(R_k + W_k S_k) / n$, where R_k is the number of chains that reach level k without down crossing level k-2 and S_k is the number of chains that reach level k after down-crossing level k-2.

5.4 Test Cases and Results

5.4.1 Preliminary Test Case

To test our methodology, we consider a pair of aircraft in cruise phase. Using the APA wake vortex prediction algorithm (Robins and Delisi 2002), we calculate approximate boundaries of our wake region. We choose a B737-800 aircraft as the leading aircraft, with a wingspan of 34.32 m and a mass of 66.36 tons (maximum landing weight). The altitude is set at 35,000 feet with air density equal to 0.38 kg/m^3. The atmospheric parameters EDR and BVF are set to 10^{-7} m^2/s^3 and 0 per second, respectively. Figure 42**Error! Reference source not found.** shows the predicted altitude and circulation of wake vortices using the APA model with the selected parameters. The results are used as a rough reference point for setting the dimensions of the wake zone in Figure 39.

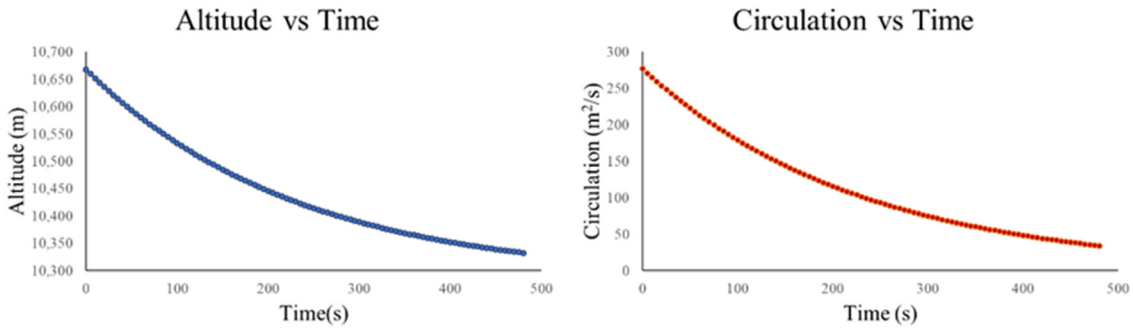

Figure 42 Decay and transport of wake vortices in time

The leading aircraft flies at a target speed of 450 knots. The following aircraft flies on the same path maintaining a two-minute separation (which equates to 15 NM)

with a standard deviation of 5 seconds (which equates to .625 NM). In the vertical dimension, the aircraft remain within 100 feet of the desired altitude at least 95% of the time.

Assuming a critical circulation threshold of 180 m^2/s for the back end of the wake zone equates to about 100 seconds in Figure 20. We set the length of the wake zone as 12.5 NM, which is the distance equivalent of 100 seconds, assuming a speed of 450 knots. Since the trailing aircraft is trying to maintain two-minute separation, this corresponds to a 20-second buffer beyond the back end of the wake region. The altitude chart in Figure 20 indicates that the vortices descend about 133 m (or about 435 feet) in the first 100 seconds and about 338 m in the first 500 seconds (which equates to a rate of about 222 feet in 100 seconds). Since the shape of the wake region is assumed to be triangular (Figure 17), we use the initial descent rate (435 feet per 100 seconds) multiplied by 100 seconds to set the maximum predicted descent and the average descent rate (222 feet per 100 seconds) to set the minimum predicted descent.

In simulating the motion of the two aircraft, we assume that the wake region is rigidly attached to the lead aircraft. That is, if the lead aircraft moves up, the entire wake region instantly shifts with it. In reality, only the portion of the zone very near the aircraft where the wake is generated would shift. Defining the wake region in this way is a simplification, but it eliminates the need for keeping a time history of the wake at each point. In future work, this assumption could be relaxed using more complex wake models, though we do not expect the main results to change much.

5.4.2 Splitting Schemes and Results

The first splitting scheme is inspired by the triangular shape of the wake region and uses nested triangles around the wake region as intermediate levels (Figure 43). Two variations are implemented. In the first variation, the intermediate levels are evenly spaced in distance from each other. In the second variation, the intermediate levels are spaced *in probability* – meaning that the probability of reaching level *j* from level *j*-1 is approximately the same for all j. It should be noted that the probability of reaching level *j* depends on the starting point in level *j*-1 and not all points on the contour of a given level have the same probability of reaching the next level.

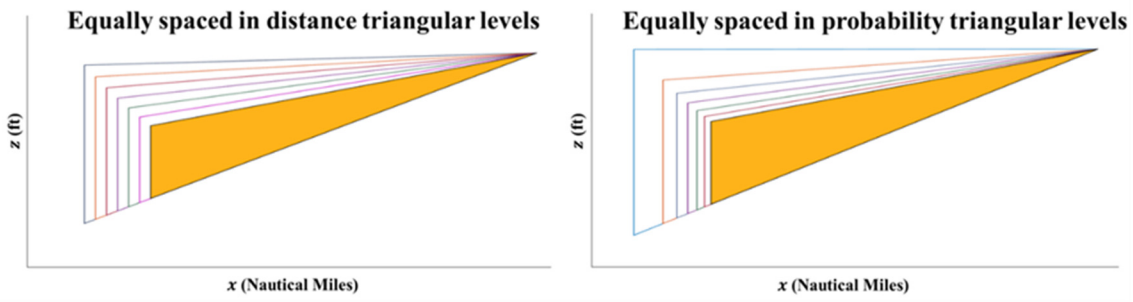

Figure 43 Geometry of intermediate levels in first splitting scheme

Figure 44 shows the variance of the simulation estimator for different simulation experiments. The variance is proportional to the computation time required to achieve a given relative error, so an n-fold reduction in variance corresponds to an n-fold increase in simulation efficiency. Three different numbers of levels and two different level sets are used: 5, 7 and 10 levels and equal-distance and equal-probability levels. In each experiment, 100 replications are simulated with n = 2,000 runs simulated in each level for

each replication. (For example, with 10 levels, each replication consists of 2,000 runs at each level for a total of 20,000 runs. With 5 levels, there are half as many runs. However, the levels are further apart, so it takes longer to simulate between one level and the next. So, the total run time is similar in each case.) The levels that are evenly spaced in probability result in a smaller variance in comparison with levels that are evenly spaced in distance.

Figure 45 shows the level probabilities from the previous experiments – that is, the probability of reaching level j starting from level j-1 prior to returning to the safe set. The probability of reaching the first level is significantly smaller than the other level probabilities, even when we try to use levels that are evenly spaced in probability. This is a result of the difference in geometry between the boundary of the safe region where the simulation starts, and the boundaries of the levels as shown in Figure 41.

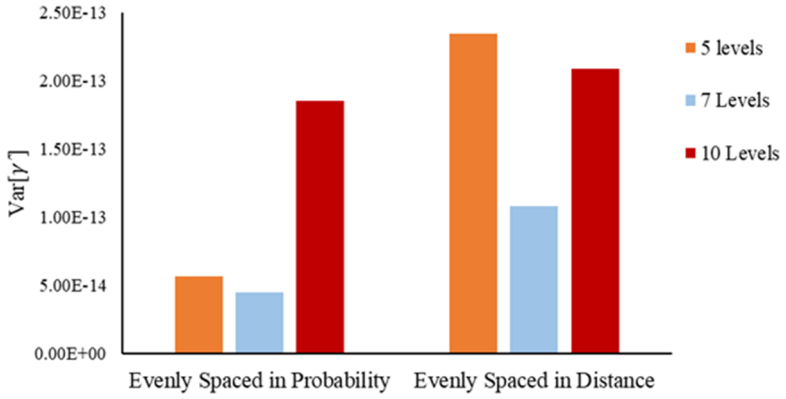

Figure 44 Sample variance using splitting with triangular intermediate levels

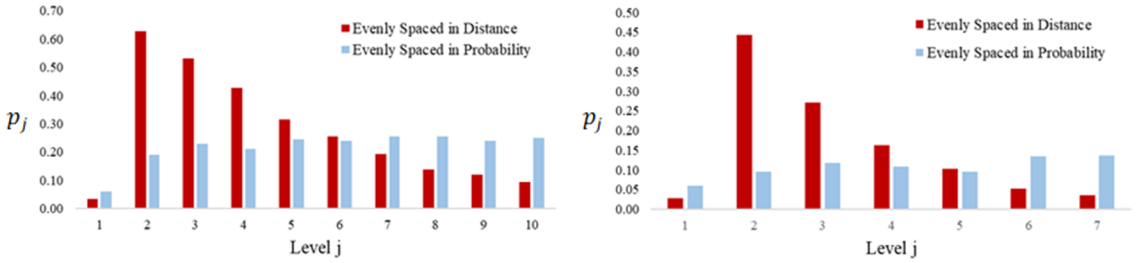

Figure 45 Level probabilities in 10-level and 7-level sets

To solve this problem, we introduce a different scheme for intermediate levels as shown in Figure 46. The idea is to have levels with similar geometry near the safe region boundary and then transition to levels with similar geometry to the wake region closer to the rare event. Figure 47 compares the variances achieved by this new level set with the variances achieved by the previous level set (nested triangles). This new scheme offers smaller variance, and in this experiment, is also about 2 times faster than the previous schemes due to simpler calculations that are needed to check if the trailing aircraft reached the first three intermediate levels.

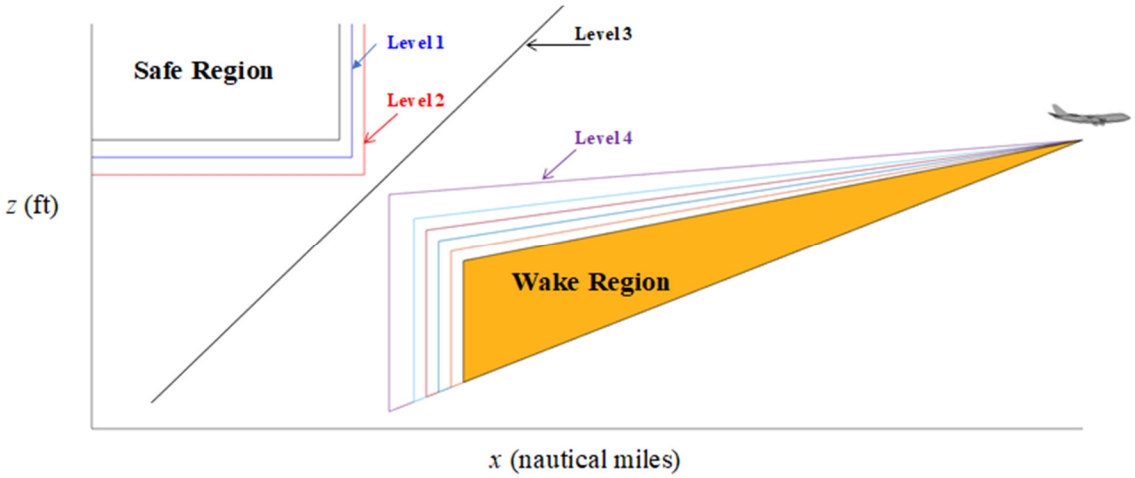

Figure 46 New level sets for splitting method

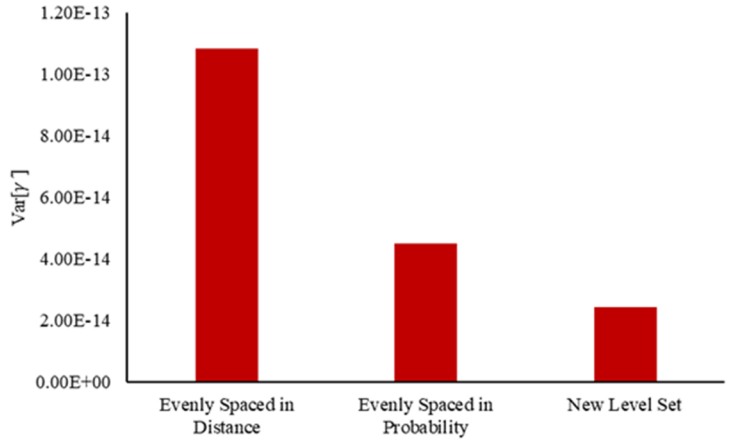

Figure 47 Comparison of variances for 7 intermediate levels with different locations and geometries

In addition, a number of standard Monte Carlo simulation experiments are performed with a similar computing budget. The standard simulation approach is significantly less efficient than splitting, since no potential wake encounters are observed in any of these experiments (so the estimated encounter probability is zero).

Experiments with a three-dimensional model are done in a similar manner to the first splitting scheme adding a lateral dimension to the trajectories of the aircrafts and the

boundaries of the wake region. Since aircraft are trying to remain at the centerline of the path and perturbations are not extreme, the lateral (across-track) deviation of the aircraft is not large enough to help the trailing aircraft avoid the wake region (which is conservative in size). The lateral dimension is unique in that the aircraft is trying to fly through the middle of the zone in this dimension. In the along-track and vertical dimensions, the aircraft is trying to fly behind and above the zone. The probability of a potential encounter is similar to the two-dimensional model.

5.5 Estimating Current Encounter Probabilities Trailing Aircraft in Cruise

In this section, we use the parameters from Table 5 as baseline values for our rare-event wake encounter model, and we perform sensitivity analysis to understand the most important parameters that impact the probability of an encounter. In addition to the parameters of the along-track movement, we have the standard deviation of altitude from track data as $\sigma_z/\sqrt{2\rho_z} = 10$ ft, which is used for determining the parameters of the vertical movement.

The objective in setting the parameters of the two-dimensional model (D, σ_f, k_d, k_p, μ, σ_l, ρ, σ_z, ρ_z) is to get the same averages and standard deviations estimated from historical data. As before, for the PD controller, we have 3 variables and two equations, so we set the damping ratio to 1.5 to have an overdamped control system, and we solve for σ_f and the natural frequency (ω_n). This model does not try to model the actual dynamics of the aircraft, but to give a realistic distribution for the relative positions of aircraft in trail.

We use the same simplified two-dimensional wake region model as before, in which only along-track and vertical movement of the aircraft are considered. The shape of the wake region is a triangle which is rigidly attached to the generating aircraft as shown in Figure 39. The dimensions of this triangle are approximated using the APA model for a Boeing 737-800 with a mass of 66.36 tons (maximum landing weight), a wingspan of 34.32 m, and an airspeed of 436 knots, which is the average ground speed from historical data. Weather condition parameters are set as EDR equal to 10^{-7} m^2/s^3 and BVF equal to 0 per second. These weather conditions – i.e., low atmospheric turbulence and neutral stratification – result in slower decay and transport of wake vortices and are considered the worst-case scenario for wake vortex encounters.

We consider a critical circulation threshold of 180 m^2/s for the following aircraft. The amount of time needed for the vortex circulation strength of the generating aircraft to fall below this threshold is estimated as 104 seconds using the APA model. This gives a length of 12.6 NM for the wake region, which is the distance that an aircraft travels in 104 seconds with an airspeed of 436 knots. Using a target separation distance of 15.1 NM estimated from track data adds about a 20-second buffer to the 12.6 NM minimum separation distance. Minimum and maximum predicted descent after 104 seconds are also estimated using the APA model as described before and are equal to 230 ft and 460 ft respectively.

We use the fixed-effort splitting method with nested triangular intermediate levels, which are evenly spaced in distance, to estimate the probability of the rare event in which the following aircraft leaves the safe region – where it is flying above the lead

aircraft in a distance greater than the target separation – and enters the wake region before returning to the safe state.

The probability of entering the wake region is not equal to the probability of the wake encounter, as this wake region does not predict the exact position of the wake vortices and is defined as a region that is likely to contain the wake. Furthermore, the analysis does not consider *where* the aircraft enters the wake zone, which may impact wake severity.

Using the parameters estimated from historical data, the estimated probability of potential wake encounter is less than 1E-40 with a very high relative error. Thus we require much more computational effort to obtain a good relative error for such a small probability.

5.5.1 Sensitivity Analysis

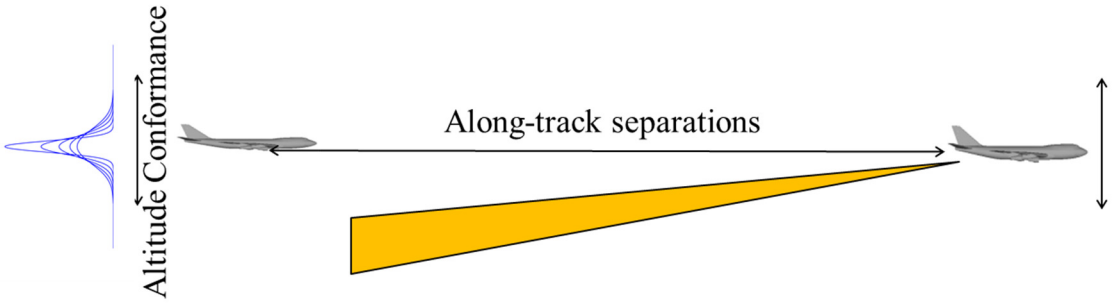

Figure 48 Parameters impacting the encounter probability

The next step is performing a sensitivity analysis to see which parameters have the largest effect on the probability of a potential wake encounter (Figure 48). The first

parameter is altitude conformance. Since wake vortices begin to descend below the altitude of the generating aircraft after their formation, if the following aircraft flies at the same altitude as the leading aircraft, it should avoid the wake vortices. Thus, the variability in altitude is a source of risk in wake encounters. Figure 49 shows the sensitivity of potential encounter probability to the altitude conformance. The potential wake encounter probability is sensitive to the variability in altitude conformance and an increase in the variability of altitude can result in significant changes in the potential encounter probability.

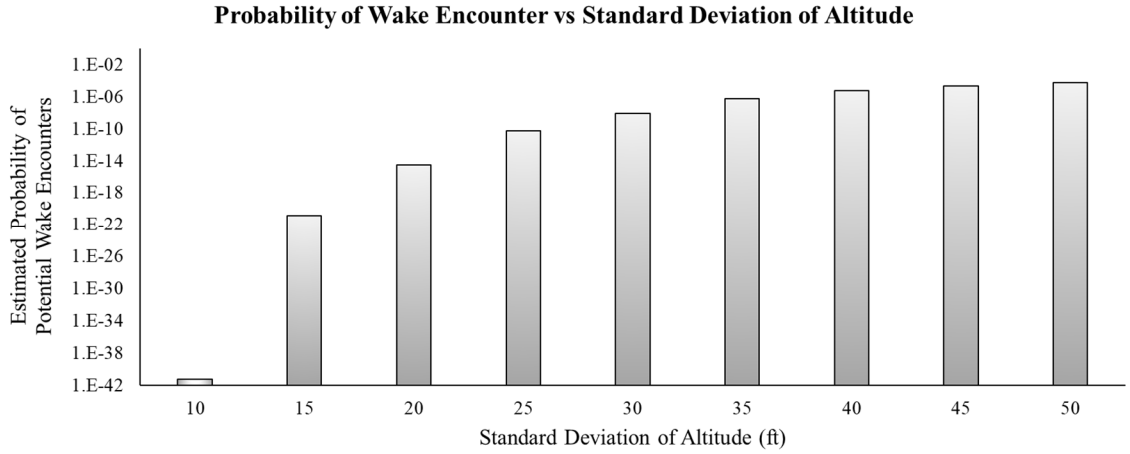

Figure 49 Sensitivity Analysis: Altitude Conformance

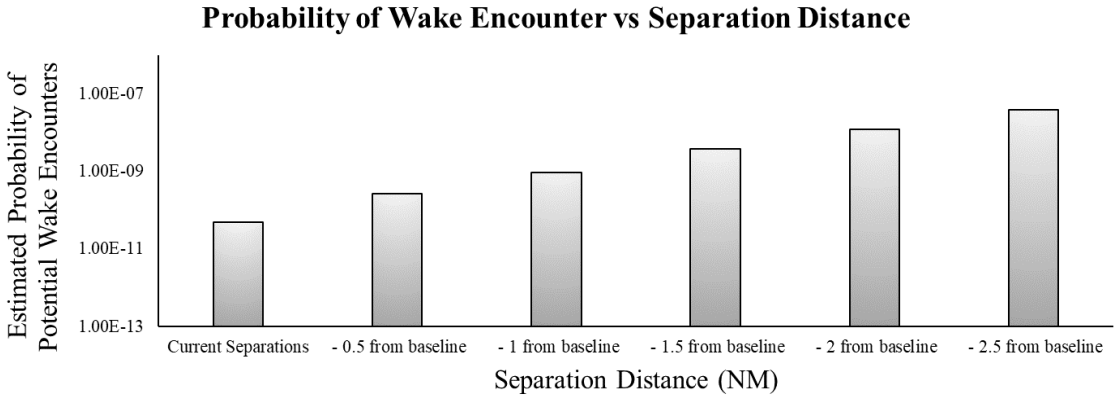

Figure 50 Sensitivity analysis: Along-Track Separation

The second parameter is longitudinal separation. Decreasing the longitudinal separations result in an increase in the corridor capacity. Figure 50 shows the probabilities of potential wake encounters for hypothetical decreases in longitudinal separation distance. For this chart, we set the standard deviation of altitude to 25 ft, since probabilities estimated with the baseline value of 10 ft were all very small (less than 10E-30), and we got very high relative errors for them with simulation times of about 1 hour. Decreasing the longitudinal separation also causes an increase in potential encounter probability, but the encounter probability is less sensitive to longitudinal separation in comparison with altitude conformance.

5.6 Safety Analysis: Scenarios involving Change of Altitude

Studies show that for aircraft flying in high altitude in trail of each other, the higher risk of encountering wake vortices happens when an aircraft is trying to descend behind a heavy aircraft or when a heavy aircraft is ascending in front of other traffic. To

model scenarios involving changes of altitude, we use the historical data to get more information about how aircraft change their altitudes in cruise.

First, we extract intervals of level flight from the altitude plot of the aircraft. We only consider the cases of transition in altitude when an aircraft flies at least 10 minutes in each altitude, both altitudes are above 30,000 ft, the number of missing data points is limited, and the transition happens within a fixed time bound. Figure 51 shows an example of multiple altitude changes with such conditions.

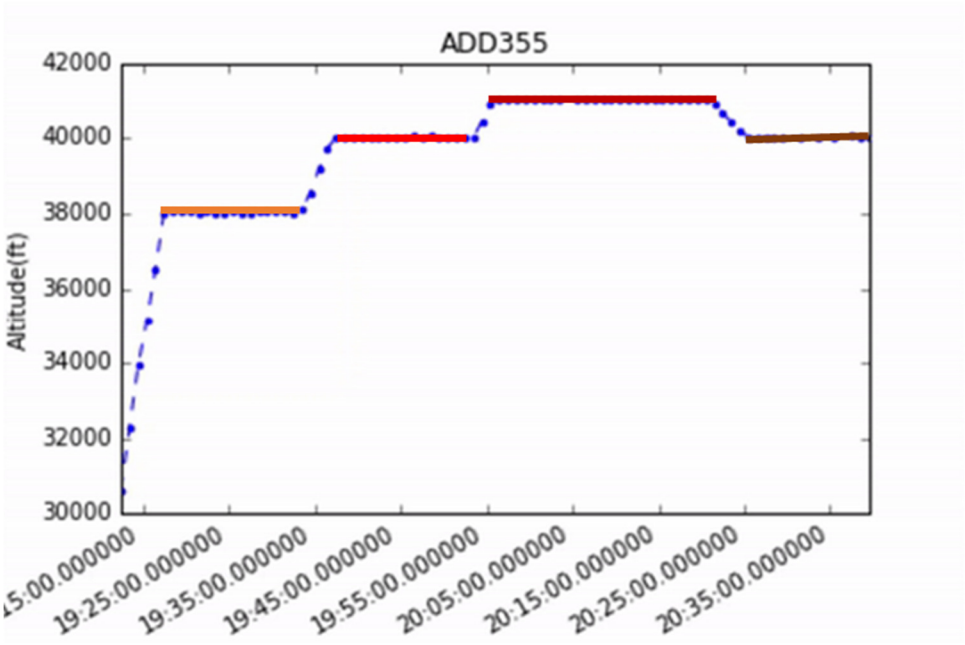

Figure 51 Altitude change and intervals of level flight for an aircraft in cruise

Processing three days of data on U.S. airspace, we find about 12,300 cases of level transitions in cruise, with about 7,500 cases of transitions to a higher flight level and about 4,800 cases of transitions to a lower flight level. Charts in Figure 52 show the

probability of specific level changes in both cases. The most probable changes in altitude are ascending or descending to a level 2,000 ft above or below. Other frequent transitions are to 1,000 ft and 4,000 ft above and below. To assess the safety of scenarios involving changes in altitude, we only consider these six frequent transitions with their respective probabilities.

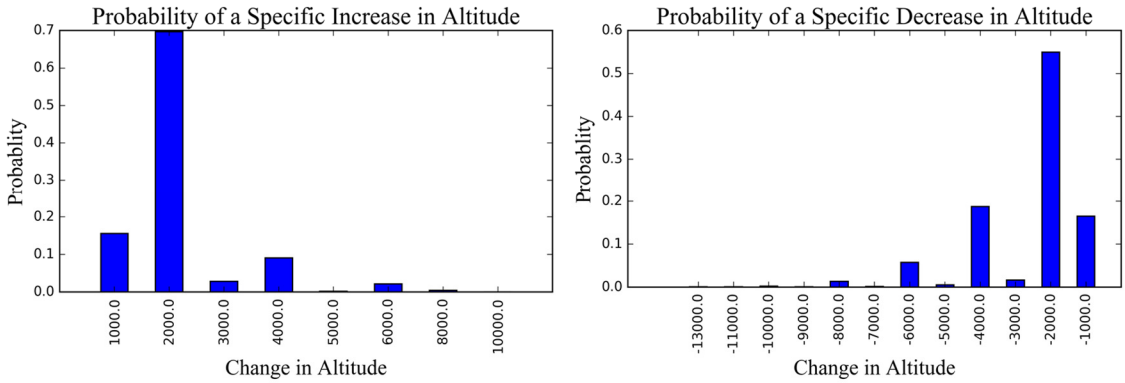

Figure 52 Level transition probabilities

The average rate of climb is about 890 fpm and the average rate of descent is about 960 fpm for altitude changes in cruise. These numbers are lower bounds for the actual rates of climb and descent. This is because of the resolution of historical data. For example, if an aircraft climbs 1,000 ft in less than one minute, it has a rate of climb more than 1,000 fpm, but the historical data has a resolution of one minute, so the calculated rate of climb for this aircraft is 1,000 fpm.

Two sets of experiments are designed to determine the wake encounter risks for pairs of aircraft trailing each other when one aircraft starts to change its altitude. In the

first set of experiments, the leading aircraft starts to ascend in front of the trailing aircraft, and in the second set of experiments the trailing aircraft starts to descend behind the generating aircraft. We assume that the wake region is rigidly attached to the generating aircraft and if the lead aircraft moves up or down, the entire wake region instantly shifts with it. In reality, only that part of the wake region very near the aircraft would shift.

A Monte Carlo simulation method is used for these experiments. We use parameters estimated from historical data to model pairs of aircraft trailing each other (these parameters are listed in Table 5). When one aircraft starts to climb or descend, the other aircraft tries to maintain its own target speed and altitude. The aircraft that changes its altitude does so with a fixed random rate of climb or descent that is generated from distributions from historical data. The wake region is the two-dimensional triangle shaped region as before. We do not consider the crosswind and lateral movements of the vortices or aircraft in these experiments.

A lateral offset mitigation procedure is investigated in which the aircraft that wants to change its altitude first starts a lateral offset procedure and goes to a parallel track which is x nautical miles offset from the previous track, and then starts to climb or descend, and then returns to the original track at the new level. To estimate the probability of potential wake encounters in this scenario, we use the 3D wake model which considers the uncertainty of crosswind in determining boundaries of the wake region based on the maximum predicted crosswind without knowing its direction. This results in a wedge shaped region in which the edges are the predicted position of the wake vortices under the condition of the maximum crosswind in that direction. For a

maximum crosswind of 10 knots, a 1 nautical mile lateral offset before changing altitude results in 0 encounter observations in the simulation model for 100,000 simulated pairs.

5.7 Safety Analysis for Flow Corridor

To analyze the safety of the flow corridors, we analyze the worst case scenario in terms of determining the wake vortex separation; this can happen for example, if we have wrong information about actual weight and airspeed of the aircraft, or if the airspeed of the lead aircraft changes somewhere between two consecutive updates of the of the wake vortex separation distance. For each lead-follow combination we find the minimum target separation for that pair combination in corridor. We can also get this minimum and maximum separations by running APA for a range of weights and airspeeds that are feasible in the corridor.

This minimum separation is used in the rare event simulation model as the target separation, while the dimensions of the wake region are determined based on the worst case scenario for that pair (very conservative wake region). Figure 53 shows such a situation. Results of the rare event simulation shows that even for these situations the estimated probability of the potential wake encounter is less than 10^{-15}.

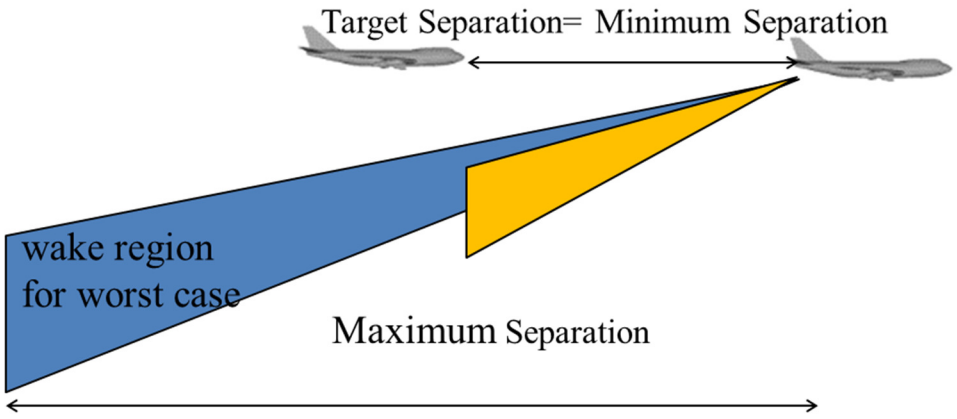

Figure 53 Aircraft follows the wrong separation distance

5.8 Conclusions

This chapter demonstrated a proof-of-concept for using a rare event splitting technique in simulating potential wake encounters. This work can be used in evaluating risk in high density environments where encounters are more likely to occur. While standard Monte-Carlo simulation did not generate any hits of the rare event set (for the problems and computational budgets considered in these experiments), the splitting method was able to generate results in reasonable time. Key decisions in implementing splitting are the choice of the level function and the locations of the levels. It was found that levels that are equally spaced in probability provide lower variance than levels that are equally spaced in distance. This is consistent with the standard theory of splitting (e.g., L'Ecuyer et al. 2009). A level function that attempted to mirror the shape of both the rare event set and the safe set was also found to reduce the variance. The wake model used in this approach was very simple – a geometric triangle. The rationale for this choice

was to focus testing on the splitting method using a "first-order" approximation of the wake.

Sensitivity analysis on results of the rare event model indicated that even though decreasing longitudinal separation between aircraft would increase the probability of potential wake encounters, longitudinal separation is not the most important parameter in avoiding potential wake encounters. The foremost factor is altitude conformance. If both aircraft precisely maintain the same altitude, the predicted number of wake encounters in trail is zero, because the wake vortices sink. With levels of altitude conformance less than 25 ft, the probability of potential wake encounters is less than 10^{-10}.

For flying in the Reduced Vertical Separation Minimum (RSVM) airspace, aircraft must be equipped with an automatic altitude control system that controls the aircraft altitude within ±65 feet about a specific altitude when the aircraft is operated in level flight. This is a 95% tolerance which means the standard deviation of altitude should be about 30 feet. The predicted wake vortex encounter for this level of altitude conformance is about 10^{-8} from Figure 49. This result is less than the estimates of Hoogstraten et al. (2015) which predicted a severe wake vortex encounter frequency of 1.6×10^{-6} per en-route flight over European airspace, which equated to approximately one every 38 days. This result considered all en-route flights, taking into account ascending and descending traffic. However, this dissertation only considered level flights. Since the ascending and descending cases have greater wake risk, we expect the estimates in our work to be less than the estimates in Hoogstraten et al. (2015).

CHAPTER 6: CONCLUSIONS

6.1 Summary and Results

In this dissertation, we provided a simulation framework to explore the benefits of a dynamic separation policy that takes advantage of knowing the actual weight and airspeed of the generating aircraft and real-time weather/wind data, versus a static separation policy in a single lane flow corridor. In order to have a simulation model that generates aircraft trajectories that are as close as possible to the real trajectories of aircraft in cruise, we first initiated an effort to collect and analyze historical flight track data. Processing five weeks of ADS-B data, we identified trailing pairs in cruise altitudes over the United States and Europe. Distributions for average separation distance, standard deviation of separation distance, standard deviation of ground speed, and standard deviation of altitude in level flight were obtained from analyzing the track data on trailing pairs.

Using these distributions, a simulation framework was developed to generate the trajectories of aircraft in a flow corridor. Capacity analysis was performed for different separation policies and different meteorological conditions. Results indicate that using a dynamic separation policy can significantly increase the capacity of the flow corridor.

The historical track data statistics were also used to calibrate a simulation model that generates trajectories for a pair of trailing aircraft in cruise. Safety analysis was

performed with a rare event splitting technique to estimate the probability of potential wake vortex encounters. Results of this safety analysis showed that with current levels of altitude conformance, it is very unlikely for aircraft trailing each other at the same altitude to have potential wake encounters. Sensitivity analysis that was performed on the parameters of the wake encounter model showed that altitude conformance plays a key role in determining the probability of the potential wake encounters. This is because wake vortices tend to sink and if the following aircraft flies at the same altitude as the leader aircraft, wake vortex encounters would be very rare. Furthermore, sensitivity analysis results indicate that with current levels of altitude conformity, the longitudinal separation can be safely reduced. Current operations are based on 5 NM minimum separation, but what we observed from data is that typical separations may be around 15 NM. We analyzed a 2 NM reduction in longitudinal separation from the baseline, which also showed acceptable safety levels regarding the wake encounters.

Safety of operations in the flow corridor with dynamic separation was analyzed using the same rare event simulation model considering the worst-case scenarios that could happen in determining the separation. Even with worst-case scenarios the flow corridor is considered safe in terms of wake vortex hazard.

6.2 Future Work

The current research would be improved with better modeling of the flow corridor, allowing for passing or adding additional lanes to the flow corridor. This would include lanes stacked vertically to investigate wake separation for ascending and descending traffic. For the dynamic separation policy, effects of using a different fast-

time wake model to determine the separation between aircraft should be studied. Also, the effects of sudden changes in meteorological parameters can be studied on both capacity and safety of the corridor. The PD controller can be modified or replaced with a more sophisticated controller to avoid creating chain slowdowns when simulating trajectories of the aircraft in the corridor. The next step in improving the safety analysis could be using a more complex model for the wake region.

REFERENCES

Alipio, J., Castro, P., Kaing, H., Shahid, N., Sherzai, O., Donohue, G. & Grundmann, K. (2003). *Dynamic Airspace Super Sectors (DASS) as High-Density Highways in the Sky for a New US Air Traffic Management System*. Proceedings of 2003 Systems and Information Engineering Design Symposium, 57 – 66.

Amrein, M., & Künsch, H. R. (2011). *A Variant of Importance Splitting for Rare Event Estimation: Fixed Number of Successes*. ACM Transactions on Modeling and Computer Simulation (TOMACS)21 (2):13.

Blom, H. A. P., Krystul, J., Bakker, G. J., Klompstra, M. B., & Klein Obbink, B. (2006). *Free Flight Collision Risk Estimation by Sequential Monte Carlo Simulation*. In Stochastic Hybrid Systems; Recent Developments and Research Trends, edited by C. G. Cassandras and J. Lygeros, 247–279. New York: Taylor & Francis.

Blom, H. A. P., Bakker, G. J., & Krystul, J. (2009). *Rare Event Estimation for a Large-Scale Stochastic Hybrid System with Air Traffic Application*. In Rare Event Simulation Using Monte Carlo Methods, edited by G. Rubino and B. Tuffin, 193–214. West Sussex, United Kingdom: Wiley.

Cheng, J., Tittsworth, J., Gallo, W., & Awwad, A. (2016). *The Development of Wake Turbulence Recategorization in the United States*. The American Institute of Aeronautics and Astronautics. AIAA Aviation.

Crow, S. C. (1970). *Stability Theory for a Pair of Trailing Vortices*. AIAA Journal, Vol. 8, No. 12, December 1970, pp. 2172-2179.

Crow, S.C. & Bate, E.R. (1976). *Lifespan of Trailing Vortices in a Turbulent Atmosphere*. J. Aircraft, Vol. 13, No. 7, July 1976, pp. 476-482.

De Oliveira, I. R., Vismari, L. F., Cugnasca, P. S., Camargo, J. B., Bakker, G. J., & Blom, H. A. P. (2010). *A Case Study of Advanced Airborne Technology Impacting Air Traffic Management*. In Computational Models, Software Engineering and Advanced Technologies in Air Transportation, Next Generation Applications, edited by L. Weigang et al., 177–214.

Feuerle, T., Steen, M., & Hecker, P. (2013). *New Concept for Wake-Vortex Hazard Mitigation Using Onboard Measurement Equipment*. Journal of Aircraft. 52. 10.2514/6.2013-4426.

FAA. (2018). *Aerospace Forecast Fiscal Years 2018-2038*.

Flight Safety Foundation. (2017). *Business Jet Pilots Describe A380 Wake Turbulence Encounter*. https://flightsafety.org/a380-wake-turbulence-encounter/.

Fuh, C.D., Teng, H.W. & Wang, R.H. (2013). *Efficient Importance Sampling for Rare Event Simulation with Applications*. Taiwan: National Central University. arXiv:1302.0583v1 [stat.ME]

Garvels, M. J. J., & Kroese, D. (1998). *A Comparison of RESTART Implementations*. Enschede: Department of Applied Mathematics, University of Twente.

Garvels, M. J. J. (2000). *The Splitting Method in Rare Event Simulation* Enschede: Universiteit Twente

Garvels, M. J. J. (2011). *A Combined Splitting-Cross Entropy Method for Rare Event Probability Estimation of Queueing Networks*. Annals of Operations Research 189 (1):167–85.

Glover, W., & Lygeros, J. (2004). *A Stochastic Hybrid Model for Air Traffic Control Simulation*. In Hybrid Systems: Computation and Control, edited by R. Alur and G. J. Pappas, 372–386. Berlin: Springer-Verlag.

Greene, G. C. (1986). *An Approximate Model of Vortex Decay in the Atmosphere.* Journal of Aircraft, Vol. 23, No. 7, 1986, pp. 566–573.

Hallock, J. N. (2005). *How the Present Separation Standards Were Created?* U.S. department of transportation, research and innovative technology administration, Volpe Center.

Holzäpfel, F. (2003). *Probabilistic Two-Phase Wake Vortex Decay and Transport Model*. Journal of Aircraft, Vol. 40, No. 2, pp. 323–331.

Holzäpfel F. and Kladetzke J. (2011). *Assessment of Wake Vortex Encounter Probabilities for Crosswind Departure Scenarios*. Journal of Aircraft, Vol. 48, No. 3, pp. 812–822.

Hoogstraten, M., Visser, H. G., Hart, D., Treve, V., & Rooseleer, F. (2015). *Improved Understanding of En Route Wake-Vortex Encounters*. Journal of Aircraft 52:981–989.

Johnson. E. (2017). *Wake Turbulence Administration Re-Categorization (RECAT) Basics.* 63rd Air Safety Forum.

Joint Planning and Development Office. (2011). *Targeted NextGen Capabilities for 2025.*

Joint Planning and Development Office. (2012). *Concept of operations for the next generation air transportation system*.

Körner, S. & Holzäpfel, F. (2018). *Assessment of the Wake-Vortex Encounter Probability on Final Approach based on LIDAR Measurements*. American Institute of Aeronautics and Astronautics.

Kos, J., Blom, H. A. P., Speijker, L. J. P., Klompstra, M. B., & Bakker, G. J. (2001). *Probabilistic Wake Vortex Induced Accident Risk Assessment*. Air Transportation Systems Engineering, edited by G. L. Donohue and A. G. Zellweger, 513–531. Reston, VA: American Institute of Aeronautics and Astronautics.

L'Ecuyer, P., Le Gland, F., Lezaud, P., & Tuffin, B. (2009). *Splitting Techniques*. In Rare Event Simulation Using Monte Carlo Methods, edited by G. Rubino and B. Tuffin, 39–61. West Sussex, United Kingdom: Wiley.

Lau, A., Berling, J., Koloschin, A., Holzäpfel, F., Linke, F. & Wicke, K. (2018). *Ground-based Wake Vortex Prediction in the En-route European Airspace*. Aviation Technology, Integration, and Operations Conference10.2514/6.2018-2879.

Marcos Benitez, M. (2016*). En Route Vortex Conflict Detection System for RPAS operations.* Universitat Politècnica de Catalunya, Barcelona, Spain.

Marr, B., & Lindsay, K., (2015). *Controller workload-based calculation of monitor alert parameters for en-route sectors.* 15th AIAA Aviation Technology, Integration, and Operations Conference, AIAA 2015-3178.

Matayoshi, N. & Yoshikawa, E. (2014). *Dynamic Wake Vortex Separation Combining with Traffic Optimization.* Proceeding of the 29th Congress of the International Council of the Aeronautical Sciences (ICAS), St. Petersburg, Russia, Sept. 2014.

Melgosa, M., Prats, X., Ruiz, S., Tarragó, J., Busto, J. & Steen, M. (2017). *A novel framework to assess the wake vortex hazards risk supported by aircraft in en-route operations*. A: SESAR Innovation Days. "Proceedings of the 7th SESAR Innovation Days". Belgrade: 2017, p. 1-6.

Melgosa, M., Ruiz, S., Busto, J., Steen, M., Rojas, J.I., & Prats, X. (2018). *Wake Vortex Hazards in En-Route Airspace and Suspected Hazard Area Identification Using High*

Fidelity Simulation Models. 37th AIAA/IEEE Digital Avionics Systems Conference (DASC).

Mitchell, R.L. (1981). *Importance sampling applied to simulation of false alarm statistics*. IEEE Transactions on Aerospace and Electronic Systems., vol. AES-17, pp. 15-24.

Murray, L., Cancela, H., & Rubino, G. (2013). *A Splitting Algorithm for Network Reliability Estimation*. IIE Transactions 45(2):177–89.

Naiman, D. and C. Priebe (2001). *Computing Scan Statistic p-values Using Importance Sampling, with to Genetics and Medical Image Analysis*. Journal of Computational and Graphical Statistics, 10, 296–328.

NATS. (2015) *Time Based Separation (TBS) continues to improve resilience at Heathrow*. https://www.nats.aero/news/newsbrief/december-2015/time-based-separation-tbs-continues-improve-resilience-heathrow/.

Nelson, R. (2006). *Trailing Vortex Wake Encounters at Altitude - A Potential Flight Safety Issue?*. AIAA Atmospheric Flight Mechanics Conference and Exhibit.

Pan-European ANS Performance Data Portal. *Executive Summary - draft Performance Review Report 2018.* https://ansperformance.eu/prcq/.

Perez-Batlle, M., Marcos, M., Pastor, E. (2016). *Effects of En-route Wake Vortex on RPAS Operations*. A: SESAR Innovation Days. "6th SESAR Innovation Days - Book of Abstracts". Delft: 2016.

Proctor, F., Hamilton, D., & Switzer, G. (2006). *TASS Driven Algorithms for Wake Prediction*. 44th AIAA Aerospace Sciences Meeting and Exhibit, AIAA 2006-1073, Reno, NV.

Proctor, F., & Hamilton, D. (2009). *Evaluation of Fast-Time Wake Vortex Prediction Models*.47th AIAA Aerospace Sciences Meeting, Orlando, FL, AIAA Paper 2009-344.

Pruis, M.J., Delisi, D.P. (2011). *Assessment of Fast□Time Wake Vortex Prediction Models using Pulsed and Continuous Wave LIDAR Observations at Several Different Airports*, AIAA Paper 2011□3035.

Rad, T., Schönhals, S., & Hecker, P. (2013). *Dynamic separation minima coupled with wake vortex predictions in dependent runway configurations*. Proceedings of the Institution of Mechanical Engineers, Part G: Journal of Aerospace Engineering, 228(8), 1450–1457.

Reynolds, T. G., Histon, J. M., Davison, H. J. & Hansman, R. J. (2002). *Structure, Intent & Conformance Monitoring in ATC.* Proceedings of the Advanced Workshop ATM 2002, vol. 2002, pp. 235-244.

Robins, R., & Delisi, D. (2002). *NWRA AVOSS Wake Vortex Prediction Algorithm Version 3.1.1*. National Aeronautics and Space Administration, Langley Research Center.

Rossow, V. J., & James, R. D. (2000). *Overview of Wake-Vortex Hazards During Cruise*. Journal of Aircraft, Vol. 37, No. 6, pp 960-975.

Roychoudhury, I., Spirkovska, L., Oconnor, M., & Kulkarni, C. (2018). *Survey of Methods to Predict Controller Workload for Real-Time Monitoring of Airspace Safety.* Report NO. ARC-E-DAA-TN60548, NASA/TM-2018-219985

Sarpkaya, T. (2000). *New Model for Vortex Decay in the Atmosphere*. Journal of Aircraft - J AIRCRAFT. 37. 53-61. 10.2514/2.2561.

Schumann U. & Sharman R. (2015). *Aircraft Wake-Vortex Encounter Analysis for Upper Levels*. Journal of Aircraft, Vol. 52, No. 4, pp. 1277–1285.

Shortle, J. (2007). *A Comparison of Wake-Vortex Models for Use in Probabilistic Aviation Safety Analysis*. Proceedings of the 25th International System Safety Conference. Baltimore, MD. System Safety Society, 581-589.

Shortle, J., & Jeddi, B.G. (2007). *Probabilistic Analysis of Wake Vortex Hazards for Landing Aircraft Using Multilateration Data*. Transportation Research Record. 2007. 10.3141/2007-11.

Shortle, J., Sherry, L., Yousefi, A. & Xie, R. (2012). *Safety and sensitivity analysis of the advanced airspace concept for NextGen.* Proceedings of the Integrated Communication, Navigation, and Surveillance Conference, Herndon, VA, O2-1 – O2-10.

Shortle, J. (2013). *Efficient Simulation of Blackout Probabilities Using Splitting*. Electrical Power and Energy Systems 44:743–751.

Smith, P. J., Shafi, M., & Gao, H. (1997). *Quick simulation: A review of importance sampling techniques in communications systems*. IEEE Journal on Selected Areas in Communications, 15:4, 597-613.

Sridhar, B., Grabbe, S., Sheth, K. & Bilimoria, K. (2006). *Initial Study of Tube Networks for Flexible Airspace Utilization.* AIAA Guidance, Navigation, and Control Conference and Exhibit, Keystone, Colorado.

Thompson, S. D. (1997). *Terminal Area Separation Standards: Historical Development, Current Standards, and Processes for Change.* Massachusetts Institute of Technology Lincoln Laboratory, Project Report ATC-258, January 16,1997.

Wang, Z., & Shortle, J. (2012). *Sensitivity Analysis of Potential Wake Encounters to Stochastic Flight-Track Parameters*. In Proceedings of the International Conference on Research in Air Transportation, Berkeley, CA, 1–8.

Wing, D. J., Smith, J. C. & Ballin, M. G. (2008). *Analysis of a Dynamic Multi-Track Airway Concept for Air Traffic Management*. Tech. Rep. NASA/TP-2008-215323, Langley Research Center, Hampton, Virginia.

Xue, M. & Kopardekar, P. (2009). *High-Capacity Tube Network Design using the Hough Transform.* Journal of Guidance, Control, and Dynamics, Vol. 32, No. 3, pp. 788–795

Ye, B., Hu M. & Shortle J. (2014). *Collision risk-capacity tradeoff analysis of an en-route corridor model*. Chinese Journal of Aeronautics, Vol. 27 pp 124-135.

Yousefi, A. & Donohue, G. (2004). *Temporal and Spatial Distribution of Airspace Complexity for Air Traffic Controller Workload-Based Sectorization.* In AIAA 4th Aviation Technology, Integration and Operations (ATIO) Forum, Chicago, Illinois, Sep. 20-22, 2004.

Yousefi, A., Donohue, G. & Sherry, L. (2004). *High-Volume Tube-Shape Sectors (HTS): A Network of High Capacity Ribbons Connecting Congested City Pairs.* Proceedings of the 23rd Digital Avionics Systems Conference, Salt Lake City, CT.

Zhang, Y. (2014). *Methodology for Collision Risk Assessment of an Airspace Flow Corridor Concept (Doctoral Dissertation).* George Mason University, Fairfax, Virginia, USA.

BIOGRAPHY

Azin Zare Noghabi received her Bachelor of Science in Industrial Engineering from Sharif University of Technology, Tehran, Iran, in 2010. She received her Master of Science in Industrial Engineering from Sharif University of Technology in 2013.